Characterization of *Listeria* Bacteriophages and mutant *Listeria monocytogenes* for the study of resistance mechanisms

A Dissertation Presented for the

Doctor of Philosophy

Degree

The University of Tennessee, Knoxville

Yaxiong Song

December 2022

ACKNOWLEDGEMENTS

First, I would like to express great gratitude to my supervisor, Dr. Thomas Denes, for his mentoring and guidance throughout my studies. When I had a hard time with my research, his advice and encouragement could give me the confidence and energy to continue my experiment.

I am highly thankful to all my committee members, Dr. Tao Wu, Dr. Jun Lin, and Dr. Mark Radosevich. I appreciate their helpful suggestions and professional comments from the committee meeting, which I benefited greatly.

Also, I would like to thank all my colleagues in our lab. Many thanks to Tracey L. Peters and Danielle M Trudelle, who provided me with a lot of help when I first came to the United States. My special thanks to Daniel W. Bryan, who taught me a lot of experimental knowledge and contributed to my experiment. Many thanks to Lauren K. Hudson, who helped me in bioinformatics. I want to express my gratitude to my other colleagues for the enjoyable moments we have spent together.

Finally, I want to express my sincere thanks to my parents. Without their support, encouragement, and love, I could not reach this far.

ABSTRACT

Listeria monocytogenes (*L. monocytogenes*) is a foodborne pathogen widely detected in contaminated food, threatening food safety. Consumption of food that contains *L. monocytogenes* may lead to fatal listeriosis. In all thirteen serotypes of *L. monocytogenes*, serotype 1/2a is responsible for the most food contamination cases, and serotype 4b accounts for the most clinic disease. With the widespread emergence of antibiotic resistant bacteria, using bacteriophages (phages) to biocontrol pathogens in food and the food processing environment becomes a promising way to protect food from contamination in the food industry. However, the effect of *Listeria* phages is limited by the appearance of phage resistant mutants. The purpose of this study is to study the interplay between *Listeria monocytogenes* and *Listeria* phages, especially the resistance mechanisms developed by resistant mutant strains.

Rhamnose is an essential receptor for many phages which infect *L. monocytogenes*, and rhamnose deficient mutants can avoid infection from most *Listeria* phages except for LP-018 from a collection of 120 phages. The characteristics of LP-018 were studied, and a resistance mechanism independent of adsorption inhibition was identified. To increase the diversity of characterized phages, wild phages that target serotype 4b strains were also identified and characterized. Co-evolution experiments between bacteriophages and *Listeria monocytogenes* serotype 1/2a and 4b were also conducted to develop a diversity of mutant strains to study resistance mechanisms.

TABLE OF CONTENTS

LIST OF TABLES

LIST OF FIGURES

1 CHAPTER I

LITERATURE REVIEW

1.1 Introduction

Listeria monocytogenes (*L. monocytogenes*) is a well-known foodborne pathogen that infects both humans and animals, severe infections and huge economic losses are caused by *L. monocytogenes* outbreaks (Gray et al., 2018; J. Pizarro-Cerda & P. Cossart, 2018). Among 13 serotypes, serotype 1/2a strains are responsible for most food contamination, and serotype 4b strains are responsible for most clinical cases (Aarnisalo et al., 2003; Hasebe et al., 2017; Leong, Alvarez-Ordóñez, & Jordan, 2014). As a result, strict food safety regulations are applied to *L. monocytogenes* contamination, and *L. monocytogenes* is not allowed to be detected in ready-to-eat foods in the United States (Kraiss & Fotin, 2008). However, *L. monocytogenes* is considered a challenging pathogen to control in the food industry, as it can survive in various extreme environments (Kramarenko et al., 2013; Todd & Notermans, 2011).

Bacteriophages (phages) are viruses that are parasites of bacteria, which have been used to biocontrol pathogens for over one hundred years (Moye, Woolston, & Sulakvelidze, 2018). Due to the discovery of antibiotics, phage research did not get a large amount of attention until the widespread emergence of antibiotic-resistant pathogens (Smith & Huggins, 1983). Bacteriophages have some unique advantages as a natural antimicrobial reagent, such as high specificity, self-replication capability, etc., which make bacteriophages a promising strategy for the biocontrol of pathogens (R. M. Carlton, 1999). However, bacteria develop various resistance mechanisms to avoid phage infection, limiting the application of phages (Dy, Richter, Salmond, & Fineran, 2014).

Listeria phages have been used to biocontrol *L. monocytogenes* since 2006. N-acetylglucosamine (GlcNAc) and rhamnose (Rha) are two known receptors for *Listeria* phage binding (Denes, den Bakker, Tokman, Guldimann, & Wiedmann, 2015; Tracey Lee Peters, Song, Bryan, Hudson, & Denes, 2020). Loss of receptors can avoid phage infection, leading to phage-resistant mutants. In the previous research in our lab, Rha deficient mutants are able to resist most of the phages, except LP-018 (Trudelle, Bryan, Hudson, & Denes, 2019). A better understanding of phage resistance mechanisms could help to overcome this limitation of phage treatment.

Co-culture of bacteriophages and bacteria leads to the co-evolution between bacteriophages and bacteria, providing phage-resistant mutant strains and pre-adapting phages (Koskella & Brockhurst, 2014; Scanlan, 2017). Mutant strains and pre-adapting phages could provide information to explain the anti-phage mechanisms and the counter mechanisms of the phages.

This dissertation work aims to study the interplay between *Listeria monocytogenes* and *Listeria* phages, including i) characterize phage LP-018, study the infection kinetics of LP-018, and identify the infection mechanism of LP-018 with a rhamnose deficient mutant; ii) select and characterize wild *Listeria* phages that are able to infect and lyse the model serotype 4b strain F2365, and to assess the inhibition effect of the selected phages on the serotype 4b strain; iii) observe the dynamics of co-evolution between *Listeria monocytogenes* and *Listeria* phages, isolate mutant strains and phages, and analyze the genetics of the isolated phage-resistant mutants.

The aim of this review chapter is to provide a detailed introduction to *L. monocytogenes*, bacteriophages, phage resistance mechanisms, and co-evolution between bacteria and phages. Additionally, specific background for this dissertation and the significance of studies were also included.

1.2 *Listeria monocytogenes*

1.2.1 General introduction

The genus *Listeria* are Gram-positive, facultative anaerobic bacteria with low G+C content, including 28 published species to date (Hain et al., 2007; "LPSN - List of Prokaryotic names with Standing in Nomenclature. *Genus Listeria*,"). *L. monocytogenes* and *L.ivanovii* are two known species that show pathogenicity (Hain et al., 2007; Milillo et al., 2012). *L.ivanovii* is only responsible for infections in animals, but *L. monocytogenes* accounts for listeriosis in both humans and animals (Hain et al., 2007).

L. monocytogenes was first described as pathogenic to humans in 1926, but was first recognized as a foodborne pathogen in 1983 (Milillo et al., 2012; Nyfeldt, 1929; Schlech III et al., 1983). *L. monocytogenes* can survive and propagate in a variety of natural environments and food processing environments, due to its high tolerance to acidic environments, high and low temperatures, and high salt concentrations (Fenlon, 1985; Grau & Vanderlinde, 1990; Jordan & McAuliffe, 2018; Sauders et al., 2012; Vivant, Garmyn, & Piveteau, 2013).

1.2.2 Classification of L. monocytogenes

Teichoic acids (TA) are one of the main constituents of the *L. monocytogenes* cell wall (Sumrall, Keller, Shen, & Loessner, 2020). Polymeric TA that are anchored to the peptidoglycan are known as Wall teichoic acids (WTA) (Sumrall et al., 2020). Two types of WTA with different repeating units have been described, classified as type I and type II WTA. Various decorations composed of different sugar molecules in type I and type II WTAs lead to a more detailed classification (Sumrall et al., 2020). Based on the variation of somatic and flagellar antigens, *L. monocytogenes* can be classified into at least 13 serotypes, 1/2a, 1/2b, 1/2c, 3a, 3b, 3c, 4a, 4ab, 4b, 4c, 4d, 4e, 7 (Karthikeyan, Gayathri, Gunasekaran, Jagannadham, & Rajendhran, 2019). Among all serotypes, 1/2a and 4b are mainly responsible for food contamination and clinical cases, respectively (Borucki & Call, 2003; Y. Huang et al., 2018). Bacteriophages infect *L. monocytogenes* by recognizing and binding the receptors in WTA, making bacteriophages a novel subtyping technology (Bielmann et al., 2015; Guerrero‐Ferreira et al., 2019).

Besides the structure of WTA, *L. monocytogenes* can also be classified into different subtypes by other serological and molecular methods, including phage typing, multilocus enzyme electrophoresis (MLEE), esterase typing, pulse field gel electrophoresis (PFGE), ribotyping and PCR based methods (Shamloo et al., 2019). According to the results of subtyping studies, all *L. monocytogenes* are divided into at least four different groups with different evolutionary lineages (Orsi, den Bakker, & Wiedmann, 2011). Lineages I and II are predominantly types that are mainly responsible for clinical cases and food contamination, first identified by MLEE typing in 1989 (Orsi et al., 2011; Piffaretti et al.,

1989). However, Lineages III and IV are rare types that are mainly isolated from ruminants. Lineage I group includes serotypes 1/2b, 3b, 3c, and 4b, and the Lineage II group consists of serotypes 1/2a, 1/2c, and 3a (Orsi et al., 2011; Vines, Reeves, Hunter, & Swaminathan, 1992). Serotypes 4a, 4b, and 4c are detected in both lineage III and lineage IV (Orsi et al., 2011).

1.2.3 L. monocytogenes in the food industry

The consumption of food, especially ready-to-eat (RTE) meats and dairy products that were contaminated by *L. monocytogenes* results in listeriosis outbreaks (Rodríguez-López, Rodríguez-Herrera, Vázquez-Sánchez, & Lopez Cabo, 2018). It is estimated that there are 23,150 listeriosis cases with a 26% mortality rate in the world annually (de Noordhout et al., 2014). According to the estimation of the United States Department of Agriculture (USDA), there are 2,518 listeriosis cases with a 20% mortality rate in the United States annually (Mead et al., 1999; Scallan et al., 2011), and the economic losses associated with listeriosis were more than $3.1 billion in 2018 ("Cost Estimates of Foodborne Illnesses," 2021). During 2017-2018, the current largest listeriosis outbreaks were reported in South Africa, with 1060 clinical cases and 216 deaths, leading to a recall of $52.9 million worth of polony (Olanya et al., 2019).

The risk groups of *L. monocytogenes* include infants, the aged, pregnant woman, and the immunocompromised. *L. monocytogenes* infection in healthy adults leads to gastroenteritis, but *L. monocytogenes* infection in at-risk groups can develop into more severe symptoms, including meningitis, sepsis, stillbirths, and abortions in pregnant individuals (Lee, 2020).

Due to the high hospitalization rate and high mortality rate of listeriosis, the regulations of *L. monocytogenes* contamination are some of the strictest in the world (Rodríguez-López et al., 2018). In the United States, a "zero tolerance" policy is adopted by USDA and the Food and Drug Administration (FDA) for RTE food (Kraiss & Fotin, 2008). In Europe, the concentration of *L. monocytogenes* should not be higher than 100 CFU/g in RTE food within the shelf life, but *L. monocytogenes* should not be detected in 25g of products for infants or specific medical purposes (Rodríguez-López et al., 2018). Canada, Australia, and New Zealand share a similar regulation with Europe (Jordan & McAuliffe, 2018; Rodríguez-López et al., 2018).

In the food industry, *L. monocytogenes* shows resistance to various technologies during food processing and preservation (Bucur, Grigore-Gurgu, Crauwels, Riedel, & Nicolau, 2018). Thermal treatments are largely used for the storage of food and to avoid contamination, including mild thermal treatment and low temperature treatment (Bucur et al., 2018). However, *L. monocytogenes* is able to tolerate temperatures from -0.4 to 45°C, which weakens the effect of thermal treatment (Y. C. Chan & Wiedmann, 2008). *L. monocytogenes* shows stronger resistance to heat when challenged by heat stress, and is able to maintain normal metabolism when challenged by cold stress (Y. C. Chan & Wiedmann, 2008; Shen et al., 2014). Acidification is another method that has been used for food storage for centuries (Hill et al., 2017). *L. monocytogenes* adopts several acidity response mechanisms to maintain its internal pH, including the F0F1-ATPase complex, the glutamate decarboxylase (GAD) system, arginine deiminase (ADI), and the Acid tolerance response (ATR) (Bucur et al., 2018; Matereke & Okoh, 2020; Poimenidou,

Chatzithoma, Nychas, & Skandamis, 2016). Osmotic stress is used to improve the shelf life of food by disrupting the osmotic balance between bacteria and the environment (Bae et al., 2012). *L. monocytogenes* reduce the osmotic stress by osmolyte accumulation or adapted gene (*lmo1078* and *lmo2085*) expression levels (Chassaing & Auvray, 2007; Dmitrieva, Cai, & Burg, 2004; Duché, Trémoulet, Glaser, & Labadie, 2002; Utratna, Shaw, Starr, & O'Byrne, 2011). Bacteriocins are ribosomally-synthesized, natural antimicrobial peptides that used as a preserving additive in food (Cotter, Ross, & Hill, 2013). However, *L. monocytogenes* are able to develop resistance to bacteriocins by DNA mutations or alterations in the phosphotransferase system (PTSs) (Macwana & Muriana, 2012). High pressure processing (HPP) is another technology that is used for food preservation, and different *L. monocytogenes* shows different survivability to HPP (Bucur et al., 2018; H.-W. Huang, Lung, Yang, & Wang, 2014). UV-light can eliminate pathogens on the surface of food by damaging DNA, which is used for decontamination (Gomez-Lopez, Ragaert, Debevere, & Devlieghere, 2007). Compared with other pathogens, *L. monocytogenes* shows a stronger ability to resist UV-light by unknown mechanisms (Gayán, Serrano, Pagán, Álvarez, & Condón, 2015). Pulsed electric fields (PEF) are mainly used to kill unwanted microorganisms in liquid food by electric fields (Góngora-Nieto, Sepúlveda, Pedrow, Barbosa-Cánovas, & Swanson, 2002). However, PEF proved to be an inefficient decontamination method for *L. monocytogenes*, due to the thick cell wall of gram-positive bacteria (Lado & Yousef, 2002). A high concentration of oxygen can cause lethal oxidative damage to bacteria, known as oxidative stress (Suo et al., 2014). Enzymes that are activated by reactive oxygen (ROS)

or reactive chlorine species (RCS) or the formation of biofilms can help *L. monocytogenes* endure oxidative stress (Archambaud, Nahori, Pizarro-Cerda, Cossart, & Dussurget, 2006; Suo, Huang, Liu, Shi, & Shi, 2012). What's more, *L. monocytogenes* shows stress adaptations to the sanitizers used for the decontamination in the food industry environment, owing to biofilm formation or mutated cell structure (Bansal, Nannapaneni, Sharma, & Kiess, 2018; Rodríguez-López et al., 2018).

1.2.4 Antibiotic-resistance of L. monocytogenes

In the clinical context, human listeriosis is usually treated by antibiotics, such as penicillin or a combination of ampicillin and aminoglycosides (Shamloo et al., 2019; Swaminathan & Gerner-Smidt, 2007). However, since antibiotic-resistant *L. monocytogenes* was first reported in 1988, more and more antibiotic-resistant *L. monocytogenes* have been identified in the world (Letchumanan et al., 2018). Horizontal gene transfer, biofilm formation, and efflux pumps are the main mechanisms responsible for the emergence of antibiotic-resistant strains (Shamloo et al., 2019). What is worse, the misuse of antibiotics accelerates the emergence of antibiotic-resistant *L. monocytogenes*, leading to the prohibition of use antibiotics in animal feed since 2006 in the European Union (Castanon, 2007; Shamloo et al., 2019). Facing the increasing resistance to antibiotics, novel strategies such as bacteriophages or combined treatments may be promising solutions to *L. monocytogenes* contamination (Rodríguez-López et al., 2018).

1.3 Bacteriophages

1.3.1 General introduction of bacteriophages

Bacteriophages (phages) are natural hunters of bacteria, which can infect and lyse specific strains for reproduction (Hagens & Loessner, 2007). Phages were first observed in 1896 by Hankin, due to the antibacterial effect of Indian river water (Hankin, 1896). In the early 1900s, bacteriophages were described by Frederick Twort and Felix d'Hérelle independently (d'Herelle, 1961; Twort, 1961). Due to the development of antibiotics, the research on phages and their applications stalled in western countries, and active research into phage applications predominantly remained in the Soviet Union and its successor states in Eastern Europe (Cof fey, Mills, Coffey, McAuliffe, & Ross, 2010; Lasagabaster, Jiménez, Lehnherr, Miranda-Cadena, & Lehnherr, 2020). The emergence of antibiotic-resistance, has revitalized the research on phages in the west as an alternative to antibiotics (B. K. Chan, Abedon, & Loc-Carrillo, 2013).

As the most abundant biological entity on earth, the abundance of phage is estimated to be approximately more than 10^{31} , showing extreme diversity (Kawacka, Olejnik-Schmidt, Schmidt, & Sip, 2020). Based on genomic composition, phages can be divided into double-stranded (ds) DNA phages, single-stranded (ss) DNA phages, dsRNA phages, and ssRNA phages (Hans-W Ackermann, 2006). Based on their life cycle, phages can be classified into lytic phages and temperate phages (Lasagabaster et al., 2020). In the process of the lytic cycle, phages take over the host's metabolic system to produce next-generation phages, including steps of absorption, penetration, biosynthesis, assembly, and release (Batinovic et al., 2019). In the step of absorption, phages require specialized

receptors on the surface of their target bacteria for binding, including proteins, oligosaccharides, and lipopolysacchrides (Guttman, Raya, & Kutter, 2005). For many phages, Mg^{2+} and Ca^{2+} are essential cofactors for binding (Guttman et al., 2005). After absorption, the phage genome enters into the host cell through the tail in the step of penetration (Guttman et al., 2005). Then, in the step of biosynthesis, most biosyntheses of the host cell would be inactivated or terminated, and the host metabolism would be taken over for the synthesis of the next generation of phages (Guttman et al., 2005). Following biosynthesis, the phage DNA is packaged into the protein shell in the assembly step (Guttman et al., 2005). Finally, the host cell would be lysed by *lysin* and *holin*, and the next-generation phages would be released in the step of release (Guttman et al., 2005). In the temperate cycle, phages integrate their genetic material into the host's chromosome instead of immediately taking over host metabolism leading to the lysis of the bacteria (Batinovic et al., 2019). Lytic phages can only utilize the lytic cycle, and temperate phages are able to switch between the lytic cycle and temperate cycle as the environment changes (Lasagabaster et al., 2020). Most isolated phages are dsDNA phages with an icosahedral capsid and a tail, belonging to the order of the *Caudovirales* (Lasagabaster et al., 2020; Sharma et al., 2017). Based on the morphology of the tail, phages can be classified into *Myoviridae* (contractile tail), *Podovirdae* (short, non-contractile tail), and *Siphovirdae* (long, non-contractile tail) (D. Turner, Kropinski, & Adriaenssens, 2021). In addition, phages also may be classified by their host ranges (Mihara et al., 2016; Pons et al., 2021).

1.3.2 Advantages and disadvantages of bacteriophage applications

Compared with antibiotics, bacteriophages have advantages as a natural antibacterial agent:

i) High specificity. Bacteriophages will only attach to and lyse its host strains and have no direct influence on the other microorganisms in the environment (R. M. Carlton, 1999; Chernomordik, 1989). As a result, food quality would not be affected by phage treatment, including taste, sight, and smell (Perera, Abuladze, Li, Woolston, & Sulakvelidze, 2015).

ii) Self-propagation ability. In every lytic cycle, bacteriophages will release next-generation phages that can infect surviving hosts and initiate another lytic cycle in target strains. As a result, phage concentration will rise exponentially under ideal conditions (R. M. Carlton, 1999).

iii) High safety. Phages cannot survive independently from the host, and as the bacterial host is eliminated, the phage will also be slowly degraded. Bacteriophages are eventually degraded into amino acid and nucleic acid fragments, which will enter the normal metabolic process of the body (R. Carlton, Noordman, Biswas, De Meester, & Loessner, 2005; Monk, Rees, Barrow, Hagens, & Harper, 2010). All available evidence suggests that phages cause no direct harm to humans, including oral administration (Bruttin & Brüssow, 2005; R. Carlton et al., 2005; Hagens & Loessner, 2007).

iv) High abundance. Bacteriophages are widely co-existing with their host strains in all natural environments, providing abundant natural phage resources (Batinovic et al., 2019; Kawacka et al., 2020). For example, the concentration of phages in water is about

10^8 particles per milliliter (Ashelford, Day, & Fry, 2003), and the abundance of phages in human feces is more than 10^{12} particles per gram (Barr, 2017).

v) Self-evolving ability. When phage resistant mutants develop, phages are able to adapt to the resistance, due to their ability to evolve (Koskella & Brockhurst, 2014; Safari et al., 2020).

However, phages have limitations for application:

i) Transfer of harmful genes. Temperate phages can integrate their genome into the host's chromosome via the temperate life cycle, which may lead to the transduction of virulence factors or other undesirable host genes (Moye et al., 2018). Therefore, bacteriophages are required to be strictly lytic for application (Kawacka et al., 2020).

ii) Emergence of phage resistance. Under the selective pressure of phage infection, the emergence of resistant mutants reduces the effect of the phage treatment (Moye et al., 2018). A cocktail that contains mixed phages with different host ranges can minimize the chances of the emergence of phage resistance (Kawacka et al., 2020).

iii) Narrow host range. Although the narrow host range of phages avoids interfering in the normal activity of other microorganisms, it also limits the range and effect of the application. Cocktail therapy utilizing multiple phages can expand the host range of the treatment (Loc-Carrillo & Abedon, 2011).

iv) Sensitivity to storage condition. The activity of phages is affected by various environmental factors, such as temperature, pH, etc. For example, phages need to be stored at a refrigerated temperature to maintain their activity (Moye et al., 2018).

1.3.3 Bacteriophage applications in the food industry

Due to their high specificity, bacteriophages can be used to detect pathogens in the food industry (Hagens & Loessner, 2007). Phages may identify specific surface-associated molecules to distinguish different serotypes, known as phage typing (Hagens & Loessner, 2007). Bacteriophage-based detection systems adopt various strategies: i) In the process of the lysis induced by phage, the release of adenosine triphosphate (ATP), adenylate kinase (AK), and other cytoplasmic markers, or the changes of impedance or conductivity can be detected; ii) phages can act as a signal-amplifier by the phage amplification assay; iii) Modifying natural phages into reporter phages by introducing reporter genes; iv) Using phage or phage components as affinity molecules; v) Biosensor technology for detection, which can transfer the interaction between phages and pathogens into an electrical signal, allowing for rapid and accurate detection. These systems mainly consist of five components, including a sensor surface, transduction platform, signal amplifier, signal detector and signal display (Aliakbar Ahovan, Hashemi, De Plano, Gholipourmalekabadi, & Seifalian, 2020; Schmelcher & Loessner, 2014).

As an alternative to antibiotics, phages can be used as sanitation method to biocontrol pathogens in food, equipment, and the environment during industrial food processing (Sillankorva, Oliveira, & Azeredo, 2012). Phages are viewed as one of the most environment-friendly antimicrobial agents, and phage biocontrol is increasingly accepted in the food industry by the public (Moye et al., 2018). In 2006, the first commercial phage product, ListShield^{TM}, was approved by the USDA (Moye et al., 2018; Perera et al., 2015). Besides the United States, commercial phage products are also

approved and successfully applied in other countries, including the European Union, Canada, and Switzerland (Vengarai Jagannathan, Kitchens, Vijayakumar, Price, & Morgan, 2020).

Phage can also act as a natural food preservative in the food industry by reducing the growth of spoilage bacteria. By inhibiting the growth of *Brocothrix thermosphacta*, the shelf life of pork adipose tissue can be increased from 4 days to 8 days by phages (Strauch, Hammerl, & Hertwig, 2007). However, the application of phages as a food preservative is still at an experimental stage, which is not ready for commercial conditions (Strauch et al., 2007).

However, there are more specific limitations that need to be solved for biocontrol applications in the food industry, i) High doses of phage preparations are required to control pathogens in food with the desired effect; ii) The low density of pathogens on food make the phage binding difficult; iii) The traditional disinfection methods used in the industry are not tolerated well by phage preparations, and novel technologies which phages tolerate better are needed; iv) All phage preparations should be recognized and approved by the local government before their application (López-Cuevas, Medrano-Félix, Castro-Del Campo, & Chaidez, 2021).

1.3.4 Listeria phages

Listeria phages, which infect and lyse *L. monocytogenes*, were first reported in the 1940s (Klumpp & Loessner, 2013; Schultz, 1945). Most isolated *Listeria* phages are dsDNA phages, belonging to the *Siphoviridae* family or *Myoviridae* family, in the order of *Caudovirales* (Klumpp & Loessner, 2013). For the genomics of all *Listeria* phages to

date, the genome sizes of most *Listeria* phages are between 30 to 65 kb with the exception of some myoviruses with broad host ranges which have a larger genome size (125-140 kb) (Klumpp & Loessner, 2013). *Listeria* phages can not be used for therapy, as *L. monocytogenes* is an intracellular pathogen that can avoid infection from phages (Kawacka et al., 2020).

Bacteriophage biocontrol, as one of the most natural and environmentally-friendly technologies, is increasingly accepted by the public (Moye et al., 2018). In the food industry, there are already two approved commercial phage preparation products to biocontrol *L. monocytogenes* contamination, ListShield™, and Listex™. ListShield™, produced by Intralytix Inc, is a phage cocktail with a combination of six *Listeria* phages, aiming to avoid the contamination of *L. monocytogenes* on food surfaces ("U.S. Food & Drug Administration GRAS Notice No. 528,"). ListShield™ could provide up to 10^8 PFU/g on food surfaces with a year of shelf life (Lasagabaster et al., 2020). Listex™, produced by Micreos Food Safety, contains *Listeria* phage P100 with a broad host range (R. Carlton et al., 2005; Kawacka et al., 2020). Listex™ could reduce the concentration of *L. monocytogenes* on food surfaces by 1.5~2 log CFU/cm^2 (Chibeu et al., 2013). The biofilms of *L. monocytogenes* formed on stainless steel could be reduced by Listex™, with a 5-log reduction (Gray et al., 2018; Montañez-Izquierdo, Salas-Vázquez, & Rodríguez-Jerez, 2012; Soni & Nannapaneni, 2010).

According to research, more than 76% of *Listeria* species are able to encode lytic proteins with a phage tail structure, known as monocins (Lee, 2020; R Zink, Loessner, Glas, & Scherer, 1994; Ralf Zink, Loessner, & Scherer, 1995). Monocins are considered

as defective prophages without the ability to reproduce, and demonstrate the ability to inhibit the growth of other *Listeria* (Klumpp & Loessner, 2013). Prophages are phage genomes that integrated into the host chromosome in the process of the lysogenic cycle, which were first reported in 1953 (Canchaya, Proux, Fournous, Bruttin, & Brüssow, 2003; Jacob & Wollman, 1953). Monocins were first discovered in the 1960s, acting as a tool for phage typing (Hamon & Peron, 1963; Lee, 2020). Due to its growth-inhibiting effect, monocins can be used for pathogen biocontrol (Klumpp & Loessner, 2013; Scholl et al., 2009).

1.4 Phage resistance mechanisms and the phage counter mechanisms

Although bacteriophages offer unique advantages as an alternative to antibiotics, the emergence of phage-resistant mutants is one of the major challenges for application (B. K. Chan et al., 2013). Bacteria utilize several antiphage systems to interfere or prevent the process of adsorption and penetration (Dy et al., 2014; Hampton, Watson, & Fineran, 2020; Samson, Magadán, Sabri, & Moineau, 2013). However, phages are able to overcome the resistance mechanisms, due to their self-evolution ability (Samson et al., 2013).

In the process of adsorption, the receptor-binding protein (RBP) of phages recognizes and attaches to the bacterial surface receptors. The known bacterial receptors mainly include lipopolysaccharide (LPS), membrane proteins, pili, and flagella (Samson et al., 2013). By altering or blocking receptors, bacteria can prevent the attachment of phages (Dy et al., 2014).

For receptor blocking, i) bacteria can avoid phage binding by masking the cellular receptors; ii) the production of extracellular polymers which form a physical barrier against phage infection; iii) the production of small molecules which attach to the active site of receptors and interfere with phage attachment (Dy et al., 2014). For receptor alteration, bacteria use phase variation, leading to mutated or deleted receptors (Dy et al., 2014). To overcome the adsorption-inhibiting defenses, i) phages can modify its RBP to adapt to mutated receptors or bind to a new receptor; ii) phages can degrade the blocking barrier with hydrolases or lyases (Labrie, Samson, & Moineau, 2010; Stummeyer et al., 2006; Sutherland, 1999; Sutherland, Hughes, Skillman, & Tait, 2004).

In the process of penetration, the phage injects its DNA into the cell. The process of penetration can be blocked by the degradation of phage DNA and cell suicide (Labrie et al., 2010). Restriction-modification (RM) systems and CRISPR-Cas systems are responsible for the degradation of phage DNA, and Abortive Infection (Abi) and Toxin-Antitoxin (TA) Systems can lead to cell suicide (Dy et al., 2014).

RM systems are widely spread, existing in most bacterial genomes (Oliveira, Touchon, & Rocha, 2014). RM systems modify phage DNA with a methyltransferase (MTase) and cleave the modified DNA with a restriction endonuclease (REase) (Tock & Dryden, 2005). Depending on the difference in subunits, recognition site, co-factor requirement, and cleavage position, RM systems can be divided into four groups (Tock & Dryden, 2005). Type I RM system is made up of three different subunits, including two REase subunits, two Mtase subunits, and one specificity subunit (Dryden, Murray, & Rao, 2001); Recognition sequence is asymmetric and bipartite, and the cleavage site is variable

(Powell, Dryden, Willcock, Pain, & Murray, 1993); The co-factor for DNA methylation is S-adenosyl methionine (SAM), and co-factors for DNA cleavage are SAM, ATP and Mg^{2+} (Kan, Lautenberger, Edgell, & Hutchison III, 1979); The type I RM system is mainly described in prokaryotes, limiting the reproduction of phages (Webb, King, Ternent, Titheradge, & Murray, 1996). The type II RM system is made up of separate Mtase and REase in general (Pingoud & Jeltsch, 2001; Tock & Dryden, 2005); The recognition sequence is usually symmetrical, and the cleavage site is a fixed location; SAM is required for methylation, and Mg^{2+} is required for cleavage. The type III RM system contains two different subunits, a "mod" subunit for substrate recognition and modification, and a restriction subunit; The recognition sequence is asymmetric, and the cleavage site is fixed location (Halford & Marko, 2004); SAM is required for methylation, and Mg^{2+} and ATP are required for cleavage (Halford & Marko, 2004; R. J. Roberts et al., 2003); The type III system is mainly identified in phages or Gram-negative bacteria (Bickle & Krüger, 1993). The type IV RM system consists of two different subunits, McrBC and McrC (Stewart, Panne, Bickle, & Raleigh, 2000); Recognition sequence is bipartite and methylated, and the cleavage site is between methylated bases (Tock & Dryden, 2005); Mg^{2+} and GTP are required for cleavage (Pieper, Brinkmann, Krüger, Noyer-Weidner, & Pingoud, 1997). In response to the possibility of the degradation of phage DNA, phages have evolved various strategies (Tock & Dryden, 2005). The recognition process could be prevented by DNA alterations or phage DNA modification to block binding proteins (Iida, Streiff, Bickle, & Arber, 1987; Krüger & Bickle, 1983). DNA methylation and DNA cleavage could be reduced by the depletion of the required

co-factors (Studier & Movva, 1976). Additionally, phages can encode proteins to block the RM system by inhibiting the enzymes involved in the process (Bandyopadhyay, Studier, Hamilton, & Yuan, 1985; Krüger, Schroeder, Santibanez-Koref, & Reuter, 1989).

CRISPR stands for clustered, regularly interspaced short palindromic repeats, and CRISPR-associated (Cas) protein can recognize and cleave phage DNA by adaptation, CRISPR RNA (crRNA) biogenesis, and interference (Dy et al., 2014; Makarova et al., 2011). In the process of adaptation, new spacers, which are short pieces of phage-specific DNA, are integrated into the CRISPR array (Barrangou et al., 2007; Makarova et al., 2011); During the crRNA biogenesis stage, short crRNAs are achieved by cleaving the primary CRISPR transcript (pre-crRNA) (Makarova et al., 2011); Interference is the last step in which phage DNA is recognized and cleaved with the guidance of crRNA (Garneau et al., 2010; Makarova et al., 2011).CRISPR-Cas was first reported in 1987 and can be divided into two classes with six types, as well as more than 30 subtypes (Jansen, Embden, Gaastra, & Schouls, 2002; Makarova et al., 2011; Safari et al., 2020). Class 1 systems are made up of multi-subunit complexes, including types I, III, and IV (Hampton et al., 2020). Class 2 systems consist of single-subunit, including type II, V, and VI (Hampton et al., 2020). Cas1 and Cas2 are two highly conserved subsystems that exist in all CRISPR–Cas systems, which are necessary in the adaptation stage (Makarova et al., 2011). The type I CRISPR–Cas system encodes Cas3 that shows helicase and DNase activities (Makarova et al., 2011; Sinkunas et al., 2011). The type II CRISPR–Cas system encodes Cas9 for DNA cleavage, adopting a unique mechanism in the crRNA biogenesis stage associated with duplex formation (Makarova et al., 2011). The type III CRISPR–

Cas system is made up of polymerase and Repeat-Associated Mysterious Protein (RAMP), which can be divided into several subtypes (Makarova et al., 2011). Type IV CRISPR–Cas system is similar to type I, but its resistance mechanism still needs to be studied further (Hampton et al., 2020; Taylor et al., 2019). The type V CRISPR–Cas system encodes Cas12 for DNA cleavage with few related studies (Hampton et al., 2020; Zetsche et al., 2015). The type VI CRISPR–Cas system adopts Cas13 to cleave phage DNA and phage RNAs (Abudayyeh et al., 2016; Hampton et al., 2020; Meeske, Nakandakari-Higa, & Marraffini, 2019). Under the selective pressure from the CRISPR-Cas system, phages have developed various strategies (Samson et al., 2013), i) Phages could evade the CRISPR-Cas system by DNA mutations or deletions (Deveau et al., 2008); ii) Phages could encode anti-CRISPR proteins to inactivate the CRISPR-Cas system (Bondy-Denomy, Pawluk, Maxwell, & Davidson, 2013); iii) Phages could encode antibacterial CRISPR-Cas system to counteract the host's CRISPR-Cas system (Seed, Lazinski, Calderwood, & Camilli, 2013).

Abortive infection (Abi) systems prevent the propagation of phages by inhibiting essential metabolic activity at the sacrifice of the infected host (Dy et al., 2014). After DNA injection, dormant proteins would be activated by phages and the essential metabolic process would be inhibited, the other bacteria are protected by avoiding the release of the new generation of phages (Dy et al., 2014). RexAB is the first discovered Abi system and is activated by a phage protein–DNA complex, leading to cell death by forming an ion channel to depolarize the bacterial membrane (Dy et al., 2014; Parma et al., 1992). Lit and PrrC are two other known Abi systems, targeting the translation

process (Bingham, Ekunwe, Falk, Snyder, & Kleanthous, 2000; Dy et al., 2014; Levitz et al., 1990). Abi systems are widely discovered in *Lactococcus lactis* (*L. lactis*) with 23 known lactococcal Abis, such as AbiD1, AbiA, AbiK and AbiZ (Anba, Bidnenko, Hillier, Ehrlich, & Chopin, 1995; Durmaz & Klaenhammer, 2007; Dy et al., 2014; Emond et al., 1997). Phages can evade the Abi system by specific mutations in phage DNA (Hampton et al., 2020; Samson et al., 2013; Stummeyer et al., 2006; Sutherland et al., 2004).

Toxin-Antitoxin (TA) Systems is a subgroup of Abi system that were classified into six types, depending on the different toxin repression modes (Cook et al., 2013; Safari et al., 2020). TA systems encode toxin molecules and antitoxin molecules, which keep a balance in the bacteria. The toxins will lead to cell death unless neutralized by the antitoxin. In the type I TA systems, toxins are mRNAs that are downregulated by antitoxin sRNAs; In the type II TA system, toxin proteins are neutralized by antitoxin proteins; In the type III TA systems, toxin proteins are inactivated by RNA antitoxins; In the type IV TA systems, antitoxin proteins play an interfering role in the process of the binding of the toxin protein; In the type V TA system, antitoxin proteins act as RNases to cleave the toxin mRNAs; In the type VI TA system, antitoxin proteins degrade toxins (Safari et al., 2020). It was hypothesized that the infection of phages limits the TA synthesis and breaks the balance between toxins and antitoxins, inducing cell death (Fineran et al., 2009; Pecota & Wood, 1996). Phages can encode antitoxin molecules to prevent cell death before the completion of the phage life cycle (Blower, Evans, Przybilski, Fineran, & Salmond, 2012; Otsuka & Yonesaki, 2012).

1.5 Co-evolution between bacteria and phages

Antagonistic co-evolution (AC) between bacteria and phages plays a crucial role in maintaining the diversity of both bacteria and phages (Koskella, 2014; Scanlan, 2017). In the process of AC, bacteria that are able to resist phage infection with various strategies, and phages that are able to evade bacterial resistance mechanisms with counter mechanisms would be selected as they attempt to coexist (Dy et al., 2014; Koskella & Brockhurst, 2014; Safari et al., 2020). Co-evolution experiments can generate a diversity of bacteria and phages to study resistance mechanisms (De Sordi, Lourenço, & Debarbieux, 2019). Under the pressure of phage infection, bacteria show a 10-1000-fold higher mutation rate compared with wild-type bacteria (Matic et al., 1997). Pre-adapting phages can be adopted to decrease the likelihood of resistance, improving the effect of phage treatment (Borin, Avrani, Barrick, Petrie, & Meyer, 2021; Scanlan, Buckling, & Hall, 2015; Torres-Barcelo, 2018). The dynamics of AC can be classified into two main types, arms race dynamics (ARD) and fluctuating selection dynamics (FSD) (Buckling & Brockhurst, 2012; CUI & JI, 2020; Oechslin, 2018). ARD is driven by directional selection and generates increasingly resistant bacterial populations and broad host range phages, which mainly happens in the initial stages of co-evolution (Betts, Kaltz, & Hochberg, 2014). FSD is not driven by directional selection and keeps a stable diversity of bacteria and phages, which mainly happens at later stages (Betts et al., 2014; S. Frank, 1992; S. A. Frank, 1993).

1.6 Specific background for this research

LP-048 and LP-125 are two well-studied *Listeria* phages that are able to form plaques on *L. monocytogenes* serotype 1/2a, belonging to the genus *Pecentumvirus* (Thomas Denes et al., 2014; Vongkamjan, Switt, den Bakker, Fortes, & Wiedmann, 2012). N-acetylglucosamine (GlcNAc) and rhamnose (Rha) are two essential receptors on the WTA for phage binding (Denes et al., 2015; Tracey Lee Peters et al., 2020). GlcNAc deficient mutants can evade infection from LP-125, and Rha deficient mutants show broad phage resistance (Trudelle et al., 2019). LP-018 is the only phage that shows strong lytic activity on the Rha deficient mutant from a collection of 120 phages (Trudelle et al., 2019; Vongkamjan et al., 2012). Co-evolution experiments between *L. monocytogenes* 10403S and *Pecentumvirus* phages (LP-048, LP-125, and a mixture of LP-048 and LP-125) were conducted for 60 hours. Most isolated bacterial survivors were resistant against the phages used in the experiment, most isolated phages showed an expanded host range, and two recombinant phages of LP-048 and LP-125 were identified (Tracey Lee Peters et al., 2020).

1.7 Significance of studies

L. monocytogenes is a worldwide foodborne pathogen that infects both animals and humans, threatening food safety. As a result, various technologies are adopted to control *L. monocytogenes* contamination in the food industry. Bacteriophages, as a natural antibacterial agent, are used for food storage and sterilization by controlling *L. monocytogene*s. Bacteriophages are considered a promising method with some unique

advantages, such as high specificity and self-replication ability. However, the emergence of phage resistance mutants is the main challenge for phage application.

In the process of phage binding, Rha is one of the important receptors in the cell wall. Loss of Rha makes *L. monocytogenes* able to resist infection by most phages, and LP-018 is the only phage that is able to form plaques on a Rha deficient mutant from a diverse collection of 120 phages. Characterization of LP-018 can provide a better understanding of phage resistance mechanisms. A comprehensive understanding of all possible resistance mechanisms can reduce the emergence of phage-resistant mutants for phage application.

Serotype 4b *L. monocytogenes* is responsible for most isolates from clinical cases and is also widely detected in food processing environments. Controlling serotype 1/2a strains and serotype 4b strains are both important to food safety. To increase the diversity of characterized phages, phages that target serotype 4b *L. monocytogenes* were screened and characterized, which may be useful for biocontrol settings.

In the co-evolution experiment, bacteria would develop mutations to avoid the infection of phages, and bacteriophages would evolve to adapt to the resistance mechanisms of the bacteria. The isolation and characterization of mutant strains provide predictions of bacterial mutations that may occur during phage application in industry. What's more, pre-adapting phages that are able to overcome resistance mechanisms could be used over wild-type phages in biocontrol applications, reducing the emergence of resistance.

2 CHAPTER II

HOMBURGVIRUS LP-018 HAS A UNIQUE ABILITY TO INFECT PHAGE-RESISTANT *LISTERIA MONOCYTOGENES*

A version of this chapter was originally published by Yaxiong Song, Tracey L. Peters, Daniel W. Bryan, Lauren K. Hudson and Thomas G. Denes:

Song Y, Peters T L, Bryan D W, et al. Homburgvirus LP-018 has a unique ability to infect phage-resistant *Listeria monocytogenes*[J]. Viruses, 2019, 11(12): 1166.

2.1 Abstract

Listeria phage LP-018 is the only phage from a diverse collection of 120 phages able to form plaques on a phage-resistant *Listeria monocytogenes* strain lacking rhamnose in its cell wall teichoic acids. The aim of this study was to characterize phage LP-018 and to identify what types of mutations can confer resistance to LP-018. Whole genome sequencing and transmission electron microscopy revealed LP-018 to be a member of the *Homburgvirus* genus. One-step growth curve analysis of LP-018 revealed an eclipse period of ~60–90 min and a burst size of ~2 PFU per infected cell. Despite slow growth and small burst size, LP-018 can inhibit the growth of *Listeria monocytogenes* at a high multiplicity of infection. Ten distinct LP-018-resistant mutants were isolated from infected *Listeria monocytogenes* 10403S and characterized by whole genome sequencing. In each mutant, a single mutation was identified in either the LMRG_00278 or LMRG_01613 encoding genes. Interesting, LP-018 was able to bind to a representative phage-resistant mutant with a mutation in each gene, suggesting these mutations confer resistance through a mechanism independent of adsorption inhibition. Despite forming plaques on the rhamnose deficient 10403S mutant, LP-018 showed

reduced binding efficiency, and we did not observe inhibition of the strain under the conditions tested. Two mutants of LP-018 were also isolated and characterized, one with a single SNP in a gene encoding a BppU domain protein that likely alters its host range. LP-018 is shown to be a unique *Listeria* phage that, with additional evaluation, may be useful in biocontrol applications that aim to reduce the emergence of phage resistance.

2.2 Introduction

Listeria monocytogenes is a Gram-positive, opportunistic, foodborne pathogen that has the capacity to cause the potentially fatal disease listeriosis (Gray et al., 2018; Javier Pizarro-Cerda & Pascale Cossart, 2018). *Listeria monocytogenes* is ubiquitous in the environment, where it can survive and grow over a wide range of environmental conditions (Fenlon, 1985; Sauders et al., 2012; Vivant et al., 2013). This makes it a particularly problematic pathogen to control in the food and food processing environment as it can grow in refrigeration temperatures, and under low pH and high salt conditions (Kramarenko et al., 2013; Todd & Notermans, 2011). It is estimated that there are ~1600 cases of human listeriosis per year in the United States, with a ~19% mortality rate (Hoffman, Maculloch, & Batz, 2015). Costs associated with these cases are estimated to exceed $2.8 billion in economic losses (Hoffman et al., 2015). Due to the high mortality rate and large financial burden caused by listeriosis, a “zero tolerance” policy was adopted in 1985 by the U.S. Food and Drug Administration for the detection of *L. monocytogenes* in ready-to-eat foods (Kraiss & Fotin, 2008). Listeriosis is also a global problem, with an estimated total of 23,150 cases in 2010 (de Noordhout et al., 2014). In 2017, South Africa recalled $52.9 million worth of polony (processed meat product) due

to the largest confirmed listeriosis outbreak to date. There was a total of 1,060 confirmed cases and 216 known deaths associated with the outbreak (Olanya et al., 2019).

Bacteriophages, or "phages," have been in use in biocontrol products targeting *Listeria monocytogenes* for over a decade (Moye et al., 2018). A couple of the key advantages of using phages to control *L. monocytogenes* are that they are highly host-specific and can self-replicate wherever contamination by the host bacteria is encountered (R. M. Carlton, 1999; Chernomordik, 1989). However, one of the key challenges limiting the potential long-term efficacy of phage-based biocontrols is the emergence of phage resistance in the treated environment. One study showed that phage-resistant mutants of *L. monocytogenes* were selected from 95 out of 110 phage-infected cultures (Denes et al., 2015). Another study showed that phage-resistant strains were isolated from specific Austrian dairies only after phage biocontrol products were used in the dairies (Fister et al., 2016). Previously characterized phage-resistant mutants have been shown to confer resistance through adsorption inhibition due to loss of phage receptor sugar moieties associated with the cell wall teichoic acids (Denes et al., 2015; Eugster et al., 2015; Sumrall et al., 2019; Trudelle et al., 2019). Recently, Trudelle et al. showed that phage resistance in serotype 1/2a strains, caused by loss of rhamnose in the wall teichoic acids, demonstrated resistance against 119/120 phages from a diverse phage collection. The authors of this study concluded that this type of mutation may represent a serious challenge for phage-based biocontrol (Trudelle et al., 2019). In this study we characterize *Listeria* phage LP-018, the only phage capable of forming plaques on the

phage-resistant mutant lacking rhamnose in its cell wall teichoic acids, and the phage-resistant mutants that are selected by this unique phage.

2.3 Materials and Methods

2.3.1 Bacterial Strains and Bacteriophages.

L. monocytogenes strain MACK was used for phage enumeration and amplification (Table 2.1, Table S2. 1). *L. monocytogenes* strain 10403S and 10403S-derived mutants were the model strains used in the reported experiments. FSL D4-0014, referred to here as "10403S (GlcNAc$^-$)" and FSL D4-0119, referred to here as "10403S (Rha$^-$)" are previously characterized phage-resistant mutants of 10403S (Denes et al., 2015). UTK S1-0004 and UTK S1-0010 are 10403S-derived mutants isolated in this study that resist LP-018 infection (Table 2.1**)**, referred to in this paper as "10403S (m_acid-resistance)" and "10403S (m_foldase)" respectively. All the *Listeria monocytogenes* strains were stored at -80°C in Brain Heart Infusion (BHI) with 15%(wt/vol) glycerol and grown at 37°C on 1.5% (wt/vol) BHI agar plates. Liquid cultures of *L. monocytogenes* were started by inoculating BHI broth with a single colony from a streak plate and incubating at 37°C with shaking at 160 RPM.

Listeria phages LP-048 and LP-125 are well-studied phages in the *Pecentumvirus* genus that are not able to infect mutant strains of *Listeria monocytogenes* lacking rhamnose in their cell wall teichoic acids (Denes et al., 2015; Trudelle et al., 2019). *Listeria* phage LP-018 was the only phage found to form visible plaques on 10403S (Rha$^-$) (Trudelle et al., 2019). Phage titers were enumerated on

Table 2.1 *Listeria monocytogenes* strains and bacteriophages used in this study

Strain or phage	Description	Reference or original
Listeria monocytogenes		
strains		
MACK	Lineage II, Serotype 1/2a	(Hodgson, 2000)
10403S	Lineage II, Serotype 1/2a	(Bishop & Hinrichs, 1987)
FSL D4-0014	10403S mutant; nonsense mutation in *LMRG_00541*; N-acetyl glucosamine deficient mutant	(Denes et al., 2015)
FSL D4-0119	10403S mutant; nonsense mutation in *LMRG_00542*; Rhamnose deficient mutant	(Denes et al., 2015)
UTK S1-0004	10403S mutant; nonsense mutation in *LMRG_00278*; HdeD family acid-resistance protein deficient mutant	This study
UTK S1-0010	10403S mutant; nonsense mutation in *LMRG_01613*; Foldase protein PrsA precursor deficient mutant	This study
***Listeria* phages**		
LP-018	*Homburgvirus*	(Vongkamjan et al., 2012)
LP-026	*Homburgvirus*	(Vongkamjan et al., 2012)
LP-037	*Homburgvirus*	(Vongkamjan et al., 2012)
LP-110	*Homburgvirus*	(Vongkamjan et al., 2012)

Table 2.1 Continued

Strain or phage	Description	Reference or original
***Listeria* phages**		
LP-114	*Homburgvirus*	(Vongkamjan et al., 2012)
LP-048	*Pecentumvirus*	(T. Denes et al., 2014; Vongkamjan et al., 2012)
LP-125	*Pecentumvirus*	(T. Denes et al., 2014; Vongkamjan et al., 2012)

lysogeny broth morpholino-propane sulfonic acid (LB-MOPS) agar supplemented with 0.1% glucose, 1mM $CaCl_2$ and 1 mM $MgCl_2$ by top agar double layer overlay and were incubated at 25°C overnight (16±2h).

2.3.2 Morphological Observation of LP-018 by transmission electronic microscopy

High titer stocks of LP-018 were centrifuged at 21,000× *g* for 60 min, and the pellet was washed with 0.1 M ammonium acetate solution (pH 7). The washing step was repeated twice, then LP-018 samples were applied to 200-mesh carbon-coated copper grids and stained with 1% phosphotungstic acid (PTA; pH adjusted to 7.4 with NaOH). After staining, the samples of LP-018 were imaged on a JEOL JEM-1400 TEM (JEOL, Inc., Peabody, MA, USA) at 80kV. Morphological characterization was performed with the Gatan Microscopy Suite Software (version 3; Gatan, Pleasanton, CA, USA) and analyzed with ImageJ (version 2.0.0-rc-69/1.52).

2.3.3 Isolation of Phage-Resistant Mutants

To isolate *Listeria monocytogenes* 10403S mutants resistant to LP-018, two different methods were used. The first method was to combine 100 μL of a high titer stock (3.3×10^{10} PFU/mL) with 30 μL of an overnight culture of 10403S and 3 mL of molten LB-MOPS top agar, gently vortexed, then poured onto LB-MOPS plates. The second method was to pipette 100 μL of a high titer LP-018 stock (3.3×10^{10} PFU/mL) on to a top agar lawn of 10403S and gently spread the phage with a sterile cell spreader to evenly distribute the phage. All plates for both methods were incubated at 25 °C overnight, and

individual colonies were selected as mutants resistant to phage LP-018. All isolated resistant mutants were tested with LP-018 by spot assay to confirm phage resistance.

2.3.4 DNA Extraction and Genomic Analysis

An adapted version of the Extraction of Bacteriophage λ DNA from Large-scale Cultures Using Formamide protocol by Sambrook and Russel was used (Sambrook & Russell, 2006). High titer phage stocks (>5 × 10^{10} PFU/mL) were pretreated with 2 mM $CaCl_2$, 5 μg/mL DNase I (Promega BioScience, Madision, WI, USA), 30 μg/mL RNase A (Sigma-Aldrich, St. Louis, MO, USA), and incubated at room temperature for 30 min to remove exogenous genomic material. Samples were incubated at 65 °C for 10 min to inactive enzymes before adding 2 mg/mL Proteinase K, following the rest of the Sambrook and Russel protocol. Gel phase-lock tubes (light gel, QuantaBio cat# 10847-800) were used for phase separation. DNA pellets were resuspended in 10 mM Tris-buffer (pH 8.0). The concentration and quality of the extracted DNA were measured on a Nanodrop One spectrophotometer (ThermoFisher Scientific Inc., Waltham, MA, USA). DNA of LP-018-resistant *Listeria* was extracted with the Qiagen DNA Easy mini kit (Qiagen GmbH, Hilden, Germany) with modifications to the manufacturer protocol, as previously described (Denes et al., 2015).

Sequencing libraries were prepared using NexteraXT library kits (Illumina, San Diego, CA, USA), and sequenced using an Illumina MiSeq v.3 instrument, with 300 paired-end read chemistry and 275 cycles, or an Oxford Nanopore Technologies MinION. Raw Illumina reads were trimmed using Trimmomatic V0.35 (Bolger, Lohse, & Usadel, 2014), and checked for quality using FastQC v0.11.7 (Andrews, 2010). For variant

analysis of LP-018-resistant bacterial mutants, trimmed reads were run in McCortex v.0.0.3 against the 10403S RefSeq assembly (RefSeq ID 376088) with joint calling and kmer size of 57 (I. Turner, Garimella, Iqbal, & McVean, 2018). VCF output files were annotated using SnpEff v4.3t (Cingolani et al., 2012). For phage genome assemblies, reads were assembled into single contigs using the hybrid assembler, Unicycler (Wick, Judd, Gorrie, & Holt, 2017), or SPAdes v3.12.0 (Bankevich et al., 2012). Assembly statistics were generated using BBMap v38.08 (Bushnell, 2018), SAMtools v0.1.8 (H. Li et al., 2009) and Quast v4.6.3 (Gurevich, Saveliev, Vyahhi, & Tesler, 2013). The LP-018 genome was annotated using RASTtk using the customized pipeline ("annotate-proteins-phage" moved above "annotate-proteins-kmer-v2") (Brettin et al., 2015). The annotation was manually inspected and updated using InterProScan (Philip Jones et al., 2014). JSpeciesWS was used to analysis the relatedness of LP-018 with other P70-like (*Homburgvirus*) phages using the average nucleotide identity MUMer (ANIm) method (Richter, Rosselló-Móra, Oliver Glöckner, & Peplies, 2015). Sequencing data can be accessed from NCBI bioproject accessions PRJNA544490 and PRJNA544516.

2.3.5 One-Step Growth Experiment

To determine the growth characteristics of LP-018 in liquid media, a one-step growth experiment was performed using an adapted version of the protocol described in Denes et al.(Denes et al., 2015). We added 500 µL of the overnight culture of *Listeria monocytogenes* 10403S into 50 mL LB-MOPS with 0.1% glucose, 1 mM $CaCl_2$, and 1 mM $MgCl_2$ in a 250 mL flask. The culture was incubated in a shaking water bath at 25 °C and 160 RPM. When the optical density at 600 nm (OD_{600}) grew to 0.1, 1×10^9 PFU of

LP-018 was added to the culture (multiplicity of infection (MOI) of ~0.1). For each time point, two samples were taken. To measure infected host cells and unabsorbed viable phages, one sample was immediately diluted with phosphate-buffered saline (PBS) and enumerated by the double-layered agar method. To measure the total concentration of viable phages, the other sample was transferred into a dilution tube with 50 μL chloroform and gently mixed, then after at least 15 min, the aqueous phase was diluted and enumerated by the double-layered agar method. To prevent the lysis of infected cells due to shear forces from micropipetting during sample collection and dilution, 60 min after infection, the infected culture was portioned and diluted in 15 mL centrifuge tubes with 9 mL of fresh media using serological pipettes to three concentrations appropriate for plating without additional dilution. This dilution also served to limit further adsorption of LP-018, which would impact the synchronicity of the infection. After being portioned and diluted, samples were plated directly from the diluted tubes using 1 mL micropipettes. After plating, 5 mL of each diluted infection was transferred to a 250 mL flask containing 45 mL of fresh media. These flasks were then incubated at 25 °C with shaking at 160 RPM. All further samples were plated directly from these flasks using 1 mL micropipettes.

2.3.6 Growth Inhibition Assay of Listeria monocytogenes by LP-018

Experimental cultures were started by inoculating 5 mL LB-MOPS supplemented with 0.1% glucose, 1 mM $CaCl_2$, and 1 mM $MgCl_2$ with 50 μL of overnight culture. The experimental cultures were then incubated at 25 °C with shaking at 160 RPM. At an OD_{600} of 0.1, each culture was diluted 100-fold in fresh supplemented LB-MOPS, and

each bacterial strain was transferred into one 15 mL tube for each experimental condition tested. Each tube was then infected with LP-018 at the target MOI or with SM buffer (control). The OD_{600} of each infection was measured every 0.5 h for 12 h. The experiment was replicated three times for each experimental condition.

2.3.7 Phage Adsorption Assay

L. monocytogenes cultures were grown to an OD_{600} of 0.1. Each culture was then portioned into three 1 mL aliquots and infected with 20 µL of LP-018, LP-048, or LP-125 at 1×10^9 PFU/mL. The infected aliquots were incubated at 25 °C with shaking at 160 RPM. After 15 min for the aliquots containing LP-048 or LP-125, and after 80 min for the aliquot containing LP-018, the tubes were centrifuged for 1 min at 17,000× *g* and 4 °C. The supernatant was then immediately diluted in PBS and enumerated by the double-layer agar method. The experiment was replicated three times and values reported for each experiment were the average of two duplicate samples (technical replicates). Percent binding values were analyzed using JMP Pro (Version 14.0.0; SAS Institute Inc., Cary, NC, USA). A linear model was constructed using the factors *L. monocytogenes* strain, phage, *L. monocytogenes* strain*phage (cross), and biological replicate (random factor), with percent binding as the model response. Pairwise comparisons were made using Tukey's honestly significant difference (HSD) test. The significance level was set at $p < 0.05$.

2.4. Results and Discussion

2.4.1 Characterization of LP-018

2.4.1.1 LP-018 Shares Morphology with Phages of the Genus *Homburgvirus*

Based on the observed morphological characteristics (Figure 2.1**),** LP-018 was identified as a likely member of the genus *Homburgvirus,* belonging to the family *Siphoviridae* in the order of *Caudovirales*. LP-018 had an elongated capsid (63.2 ± 4.67 nm × 132.2 ± 3.68 nm, n = 33) with a non-contractile tail (168.02 ± 9.15 nm in length). This morphology is nearly identical to other homburgviruses (T. Denes et al., 2014; Hudson, Peters, Song, & Denes, 2019; Schmuki, Erne, Loessner, & Klumpp, 2012). Interestingly, the morphology is also shared by *Enterococcus* phage VD13 (Hans-W Ackermann, Caprioli, & Kasatiya, 1975), which was previously shown to cluster by genomic analysis with sequenced homburgviruses (T. Denes et al., 2014).

2.4.1.2 Whole Genome Sequencing Confirms LP-018 is a *Homburgvirus*

The *Listeria* phage LP-018 genome assembled into a single contig of 65.3 Kbp that had an average read coverage of 823. The G + C content of the genome was 36.4%. It contained 112 predicted coding sequences, of which 85 were annotated as hypothetical proteins or phage proteins without known specific functions (Figure 2.2). The genome contained no tRNAs. As the morphological characteristics of LP-018 match the features of homburgviruses, the LP-018 genome nucleotide identity was compared with all other sequenced homburgviruses. The results show that LP-018 was most closely related to LP-037, with an ANIm of 97.71% across 96.74% of its aligned nucleotide sequence (Table 2.2). As the genome sequence identity between LP-018 and LP-037 is 94.52% which is

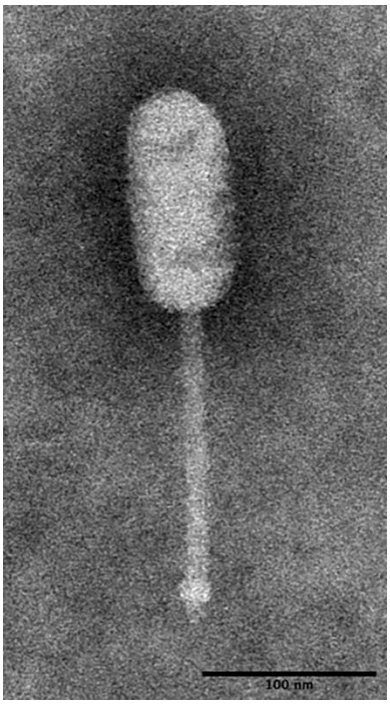

Figure 2.1 Transmission electron micrograph of phage LP-018. The sample was stained with 1% phosphotungstic acid (PTA) at pH 7.4 and imaged at 80 kv with a final magnification of 41,000×.

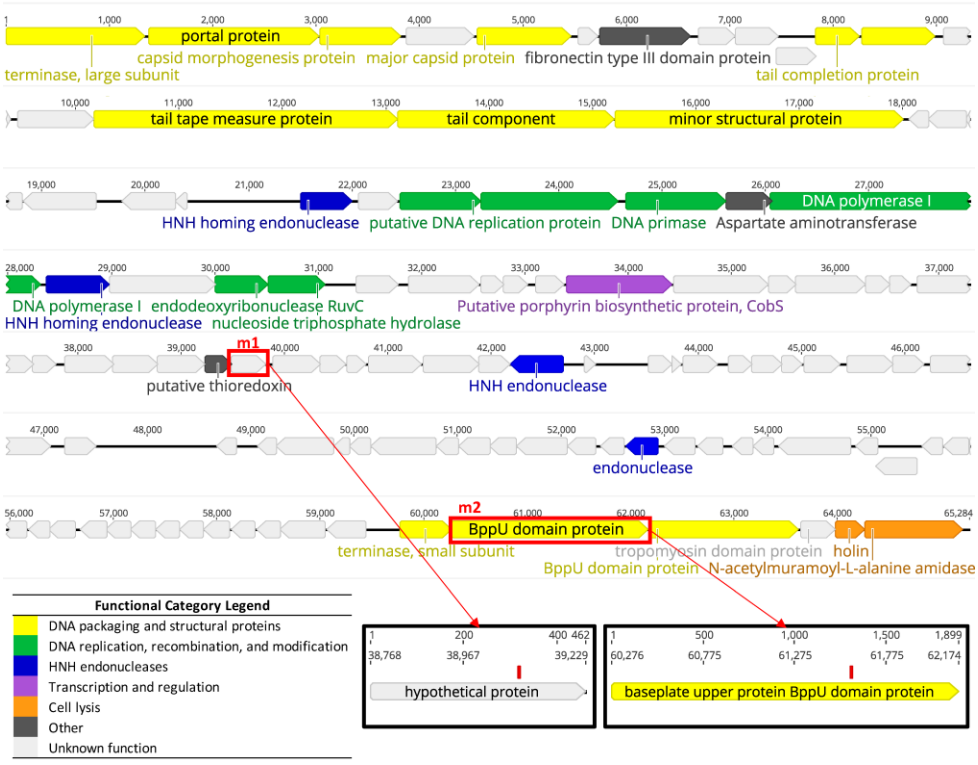

Figure 2.2 Genome map of LP-018 showing predicted coding sequences. Gene colors correspond to functional category: DNA packaging and structural proteins are yellow; DNA replication, recombination, and modification are green; His-Asn-His (HNH) endonucleases are blue; transcription and regulation are purple; cell lysis are orange; others are dark gray; and unknown (including hypothetical proteins and phage proteins (annotations not shown)) are light gray. Coding sequences containing mutations identified in this study are in red boxes. The figure was made with Geneious Prime (v. 2019.1.1).

Table 2.2 Average nucleotide identity [across aligned nucleotide percentage] for LP-018 and other *homburgviruses* as calculated by JSpeciesWS MUMer (ANIm).

	LP-026	**LP-037**	**LP-110**	**LP-114**	**P70***	**LP-018**
LP-026	*	97.60 [93.40]	96.63 [93.26]	96.38 [93.62]	96.29 [91.95]	97.59 [93.72]
LP-037	97.60 [96.74]	*	96.83 [96.56]	97.49 [95.52]	96.29 [95.73]	97.71 [97.50]
LP-110	96.63 [95.96]	96.83 [95.92]	*	97.34 [93.17]	96.68 [95.42]	97.45 [95.62]
LP-114	96.38 [94.17]	97.49 [92.89]	97.34 [91.08]	*	96.31 [93.88]	97.41 [92.41]
P70*	96.29 [92.05]	96.29 [92.46]	96.68 [92.75]	96.31 [93.11]	*	96.31 [91.47]
LP-018	97.59 [96.21]	97.71 [96.74]	97.45 [95.37]	97.41 [94.31]	96.33 [93.90]	*

*****Type species of *Homburgvirus* genus

lower than 95%, we propose that LP-018 be classified as a new species belonging to *Homburgvirus* (Adriaenssens & Brister, 2017).

2.4.2 Growth Characteristics of LP-018

2.4.2.1 One-Step Growth Experiment

LP-018 was found to have a significantly longer adsorption time and a much smaller burst size than either LP-048 and LP-125; the only other *Listeria* phages we know to have published one-step growth curve data (Denes et al., 2015). At 60 min post-infection, 85.1% (5.63% standard deviation) of LP-018 had adsorbed to *L. monocytogenes* 10403S (Figure 2.3). As a comparison, 78.2% of LP-048 and 99% of LP-125 adsorbed to 10403S in 20 min (Denes et al., 2015). The latent period of LP-018 could not be determined, as infected cells without viable internal phages were below the limit of detection. A possible explanation for this is that cells newly infected by LP-018 could be extremely fragile and are thus lysed during the dilution or plating of the unchloroformed samples. In a typical one-step growth experiment, we would have expected the unchloroformed samples to remain stable at the beginning of the experiment (T. Denes et al., 2014). The eclipse period of LP-018 was between 60 min and 90 min, which is much longer than the *Pecentumvirus* phages previously tested; the eclipse period of LP-048 and LP-125 were only 40–50 min and 35–40 min, respectively (T. Denes et al., 2014). The eclipse period of LP-018 was between 60 min and 90 min, which is much longer than the Pecentumvirus phages previously tested, the eclipse period of LP-048 and LP-125 were only 40~50 min and 35~40 min, respectively (Denes et al., 2015). The calculated burst size of LP-018 was approximately 2 PFU/cell, which was much lower than LP-048 (13.6)

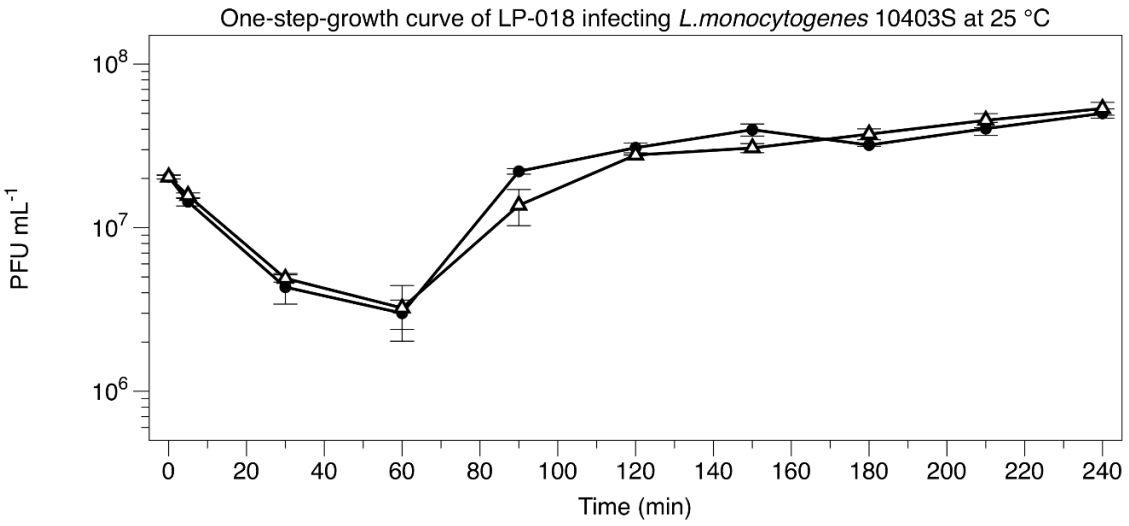

Figure 2.3 Low multiplicity of infection of 10403S with LP-018 at 25 °C. Closed circles represent the phage titer in chloroform treated samples; open triangles represent the phage titer in untreated samples. Data are mean values of three biological replicates, and error bars represent standard error.

and LP-125 (21.3); however, the slow adsorption rate made calculating a burst size that represents the true burst size extremely challenging. Interestingly, LP-018 appears to perform differently in liquid media and solid media. LP-018 appears to produce clear, well-defined plaques on solid media, but in liquid media (under the conditions tested) shows unexpectedly slow binding and small bursts after a relatively long infection period.

2.4.2.2 Growth inhibition of *Listeria* by LP-018

The growth of 10403S treated with different concentrations of LP-018 was determined (Figure 2.4). The results showed that LP-018 was not capable of inhibiting the growth of 10403S at a multiplicity of infection (MOI) of one or lower. However, at higher MOI's (10 and 100), LP-018 could notedly keep the OD_{600} of *L. monocytogenes* 10403S under 0.1 for 12 h. Lower concentrations of LP-018 (MOI's ≤ 1) had no observable effect on the growth of 10403S, possibly due to its slow adsorption rate and small burst size.

2.4.3 Isolation and Characterization of LP-018-Resistant Mutants

2.4.3.1 Isolation of new LP-018-resistant mutants

Characterization of phage-resistant mutants can be a useful tool for identifying potential phage receptors (Bishop-Lilly et al., 2012; Denes et al., 2015). It is also an important step in designing cocktails specifically to reduce the frequency of phage resistance selection. In this study, we were able to isolate 10 distinct phage-resistant mutants of 10403S by LP-018. We selected one mutant from each of the 10 selection experiments (i.e., we successfully isolated a phage-resistant mutant from each attempt). All isolated mutants were confirmed to be resistant to LP-018 infection by spot assay.

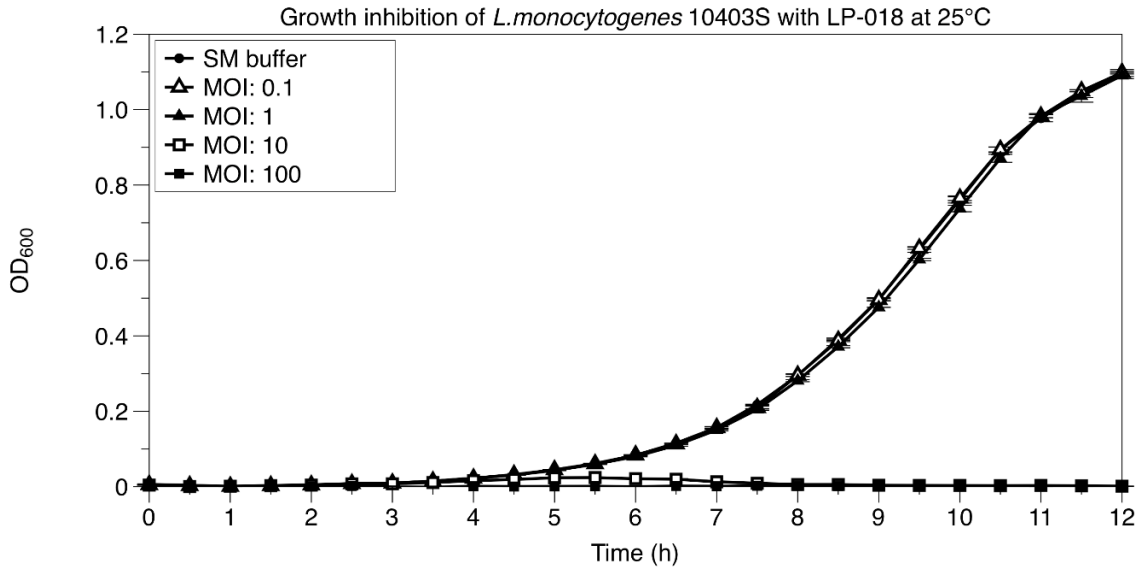

Figure 2.4 Bacterial growth of 10403S treated with different concentrations of LP-018. Closed circles represent the uninfected control (SM buffer), open triangles represent the infection condition at a multiplicity of infection (MOI) of 0.1, closed triangles represent the infection condition at a MOI of one, open squares represent the infection condition at a MOI of 10, closed squares represent the infection condition at an MOI of 100. The SM Buffer control and infection conditions at MOI of ≤1 were indistinguishable. Data are mean values of three biological replicates, and error bars represent standard error.

2.4.3.2 Genetic Characterization of LP-018-Resistant Mutants

Whole-genome sequencing of LP-018-resistant mutants revealed that all identified mutations mapped to three genes on the 10403S chromosome. Of the phage-resistant mutants, nine were found to contain only a single mutation. Three of these mutations were found in LMRG_00278, which was annotated as an HdeD family acid-resistance protein, and six of these mutations were found in LMRG_01613, which was annotated as a precursor to the foldase protein PrsA2 (Figure 2.5). Expression of *LMRG_00278*, which encodes the putative HdeD family acid-resistance protein, an uncharacterized membrane protein, is known to be regulated by the general stress response alternative sigma factor B (Y. Liu et al., 2019; Tiensuu, Andersson, Rydén, & Johansson, 2013). If LP-018 infection depends on the expression of *LMRG_00278*, further work should be conducted to determine if LP-018 shows improved lytic activity against *L. monocytogenes* under σB active conditions (Denes & Wiedmann, 2014). Interestingly, PrsA2 is a post-translocation chaperone that contributes to the virulence of *L. monocytogenes* by stabilizing and promoting the activity of secreted virulence factors (Alonzo & Freitag, 2010; Alonzo, Port, Cao, & Freitag, 2009; Zemansky et al., 2009). This suggests that LP-018 may select for phage-resistant mutants that are less virulent than the parental strain. Identifying mutants in these genes was a surprising result as all previously characterized phage-resistant mutants have been identified in genes affecting cell wall teichoic acids, and were found to confer resistance by inhibiting adsorption (Denes et al., 2015; Eugster et al., 2015; Sumrall et al., 2019; Trudelle et al., 2019). One of the ten phage-resistant mutants was found to have two mutations: one nonsense mutation in *LMRG_00278* (total of four

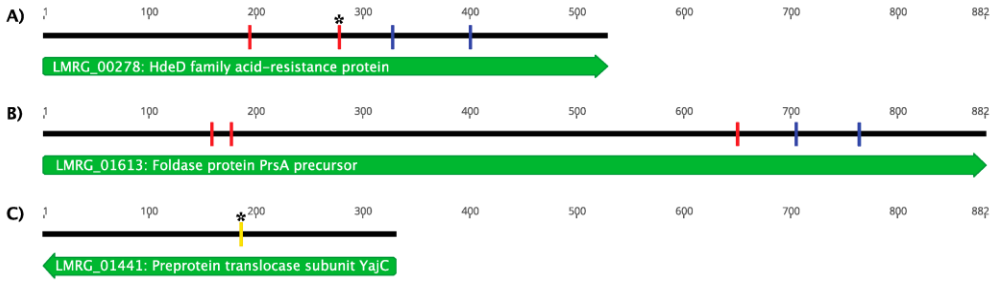

Figure 2.5 Map of mutations identified in mutant 10403S strains resistant to LP-018. Mutations were identified in (A) LMRG_00278, an HdeD family acid-resistance protein, (B) LMRG_01613, a foldase protein PrsA precursor, and in (C) LMRG_01441, a preprotein translocase subunit YajC. In nine of the ten phage-resistant mutants, only one mutation was present, while one phage-resistant mutant had two mutations in two different genes (designated by asterisks). The numbers in the figure represent the nucleotide position of the coding sequence in each gene. Nonsense mutations are designated by red marks, frameshift mutations are designated by blue marks, and missense mutations are designated by yellow marks.

phage-resistant mutants had an identified mutation in this gene) and a missense mutation in *LMRG_01441*, which was annotated as encoding a preprotein translocase subunit of YajC. The missense mutation in *LMRG_01441* resulted in one amino acid change from aglycine to a cysteine with no other notable predicted effects on the protein product. For this reason, and because all other mutations occurred in genes *LMRG_00278* and *LMRG_01613*, the characterization of this gene was not investigated further. We selected a representative phage-resistant strain with a mutation in either gene *LMRG_00278* or *LMRG_01613* for further characterization. We selected the representative mutants based on our prediction of which mutants would be expected to have the greatest effect on the function of the target gene. UTK S1-0010, referred to throughout the remainder of this article as 10403S (m_acid-resistance), was selected as it was the mutant strain with a nonsense mutation at nucleotide position 160/882, and was predicted to result in the expression of a truncated protein (54 /294 amino acids). UTK S1-004, referred to throughout the remainder of this article as 10403S (m_foldase), was selected as it is the mutant strain with a nonsense mutation at nucleotide position 65/176 and is predicted to result in the expression of a truncated protein (194/ 528 amino acids).

2.4.3.3 Adsorption Assay with Phage-Resistant Mutants

The mutations identified in the LP-018-resistant mutants were found in genes without any obvious effect on the cell's outer surface. We thus performed adsorption assays to see if we could identify the first phage-resistant mutants in *Listeria* that resist infection through a mechanism independent of adsorption inhibition. Adsorption assays revealed that the mutations in 10403S (m_acid resistance) and 10403S (m_foldase) had

no significant impact on adsorption of LP-018 (Figure 2.6). Interestingly, LP-018 showed significantly reduced binding to the 10403S mutant lacking rhamnose in its cell wall teichoic acids (Rha^-) and the 10403S mutant lacking N-acetylglucosamine in its cell wall teichoic acids ($GlcNAc^-$); although there was significantly higher binding to the 10403S (Rha^-) strain than the 10403S ($GlcNAc^-$) strain. This was expected, as LP-018 could form clear, distinct plaques on the Rha^- strain, which would require some degree of binding capacity for LP-018. This data suggests that (i) N-acetylglucosamine and rhamnose are involved in the adsorption of LP-018 to its host and (ii) resistance conferred by mutations in the acid resistance and foldase genes, *LMRG_00278* and *LMRG_01613*, respectively, is likely through a mechanism independent of phage adsorption inhibition. However, we cannot rule out the possibility that these mutations impact a secondary adsorption step that is dependent on initial adsorption to cell wall teichoic acids.

As *LMRG_00278* and *LMRG_01613* encode a putative membrane protein and a secreted foldase, respectively, the mutations observed most likely impact the cellular inner wall zone (Beveridge & Matias, 2006). Such an effect could potentially block the penetration or translocation steps of phage infection (Fernandes & São-José, 2018). Growth curves of all *LMRG_00278* and *LMRG_01613* mutants were also performed; no growth defects were observed that could indicate an indirect cause of phage resistance (Figure S2. 1)

2.4.4 Growth Inhibition of Phage-Resistant Mutants by LP-018

Due to LP-018's significantly reduced adsorption efficiency against 10403S (Rha^-), we performed growth inhibition assays in liquid culture of the 10403S (Rha^-) and 10403S ($GlcNAc^-$) strains. Interestingly, no observable differences were seen between

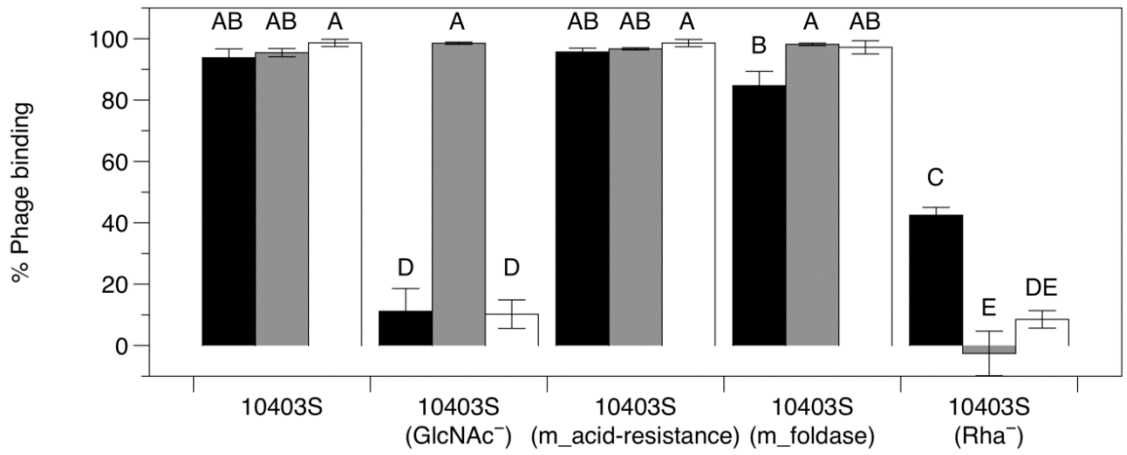

Figure 2.6 Phage binding of LP-018, LP-048, and LP-125 to 10403s and phage-resistant 10403S mutants. Black bars represent LP-018, grey bars LP-048, and white bars LP-125. LP-018 binding was measured after 80 min, and LP-048 and LP-125 binding were measured after 15 min; comparisons between phages should consider these differences. Values are the mean of three biological replicates, and error bars represent standard error. Bars that share the same letter are not significantly different (e.g., bars marked AB are not significantly different from bars marked A or B).

the LP-018 treated and untreated mutant samples (Figure 2.7a). This suggests that LP-018 is likely not as effective at inhibiting rhamnose deficient phage-resistant mutants in liquid conditions as it is in solid conditions, as was shown by Trudelle et al. (Trudelle et al., 2019). Growth inhibition of the LP-018-resistant mutants 10403S (m_acid resistance) and 10403S (m_foldase) was also tested (Figure 2.7b). As expected, LP-018 showed no inhibitory effect against these phage-resistant mutants.

2.4.5 Isolation and Characterization of LP-018 Mutants with Different Host Ranges

It was previously observed that LP-018 showed a low level of activity against 10403S (GlcNAc$^-$) (Trudelle et al., 2019). A possible explanation for this was that LP-018 had a low-level mutant population responsible for that activity. To test this hypothesis, we plaque purified LP-018 on 10403S (Rha−) and 10403S (GlcNAc−).The efficiency of plaquing experiments revealed that LP-018_m1 (isolated on the Rha$^-$ strain) showed no activity against 10403S (GlcNAc$^-$), and LP-018_m2 (isolated on the GlcNAc$^-$ strain) showed no activity against 10403S (Rha$^-$) (Table 2.3). This confirmed our hypothesis that there was a subpopulation of LP-018 mutants in the LP-018 stocks. Further, the data suggests that LP-018_m1 requires GlcNAc in the cell wall teichoic acids for binding, and LP-018_m2 requires rhamnose in the cell wall teichoic acids for binding. As expected, LP-018 and LP-018_m1 formed plaques on 10403S (Rha$^-$), although at reduced efficiency. The pecentumviruses LP-048 and LP-125 were both able to infect the 10403S (m_acid-resistance) and 10403S (m_foldase) mutants.

Whole genome sequencing of LP-018_m1 and LP-018_m2 was conducted to

Figure 2.7 (a): Effect of LP-018 on the growth of 10403S (GlcNAc−) and 10403S (Rha−) at 25 °C. Open circles represent 10403S buffer control, open triangles 10403S infected at MOI five, closed triangles 10403S infected at a MOI of 10, open squares 10403S (GlcNAc−) buffer control, closed squares 10403S (GlcNAc−) infected at MOI five, open diamonds 10403S (GlcNAc−) infected at MOI 10, closed diamonds 10403S (Rha−) buffer control, open inverted triangles 10403S (Rha−) infected at MOI 5, and closed inverted triangles 10403S (Rha−) infected at MOI 10. (b): Effect of LP-018 on growth of 10403S (m_acid-resistance) and 10403S (m_foldase). Open circles represent 10403S buffer control, open triangles 10403S infected at MOI five, closed triangles 10403S infected at MOI 10, open squares 10403S (m_acid-resistance) buffer control, closed squares 10403S (m_acid-resistance) infected at MOI five, open diamonds 10403S (m_acid-resistance) infected at MOI 10, closed diamonds 10403S (m_foldase) buffer control, open inverted triangles 10403S (m_foldase) infected at MOI five, and closed inverted triangles 10403S (m_foldaseb) infected at MOI 10. Values are the mean of three biological replicates, and error bars represent standard error.

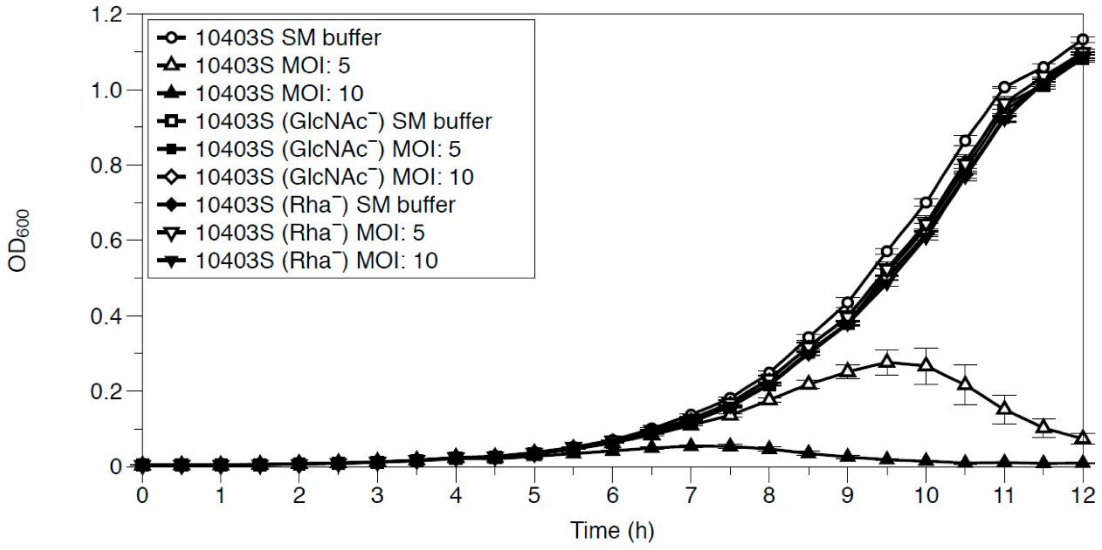
10403S SM buffer
10403S MOI: 5
10403S MOI: 10
10403S (GlcNAc⁻) SM buffer
10403S (GlcNAc⁻) MOI: 5
10403S (GlcNAc⁻) MOI: 10
10403S (Rha⁻) SM buffer
10403S (Rha⁻) MOI: 5
10403S (Rha⁻) MOI: 10
OD600
Time (h)

(a)

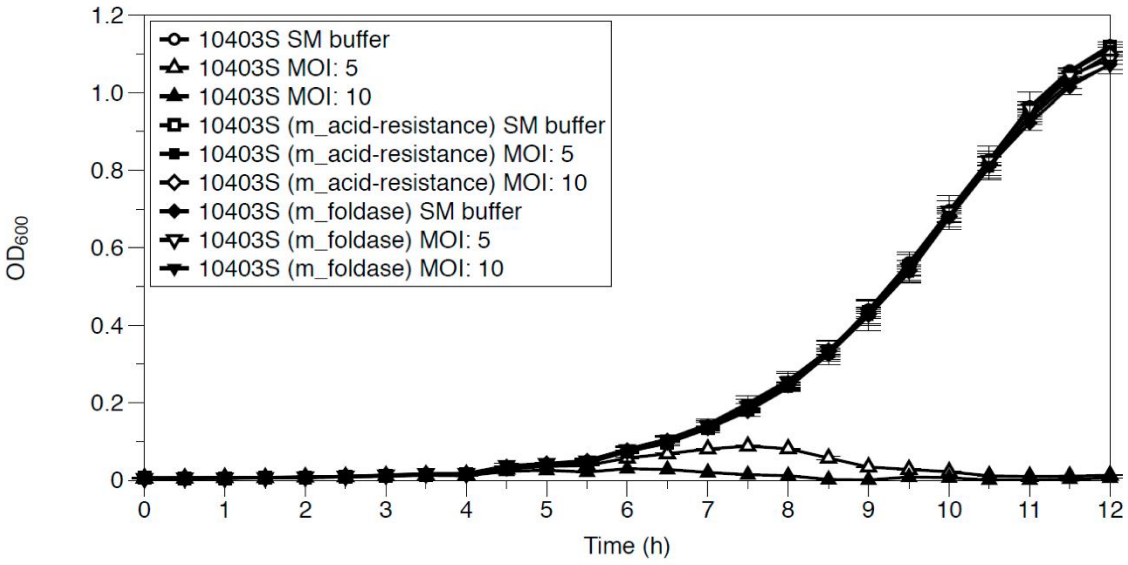
10403S SM buffer
10403S MOI: 5
10403S MOI: 10
10403S (m_acid-resistance) SM buffer
10403S (m_acid-resistance) MOI: 5
10403S (m_acid-resistance) MOI: 10
10403S (m_foldase) SM buffer
10403S (m_foldase) MOI: 5
10403S (m_foldase) MOI: 10
OD600
Time (h)

(b)

Table 2.3 Mean efficiencies of plaquing of *Listeria* phages against phage-resistant mutants. Values represent the mean titer (n = 3) of each phage on each bacterial strain compared to the titer on the propagation host (*L. monocytogenes* strain MACK). Standard deviations are shown in parentheses.

Phages*	*Listeria monocytogenes* Strains				
	10403S	**FSL D4-0014** 10403S (GlcNAc-)	**FSL D4-0119** 10403S (Rha-)	**UTK-S1-0004** 10403S (m_acid-resistance)	**UTK-S1-0010** 10403S (m_foldase)
LP-018	1.3 (0.36)	0.0016 (0.0013)	0.061 (0.018)	0	0
LP-018_m1	1.5 (0.64)	0	0.13 (0.064)	0	0
LP-018_m2	0.91 (0.19)	0.49 (0.13)	0	0	0
LP-048	0.70 (0.11)	0.55 (0.21)	0	0.35 (0.091)	0.35 (0.24)
LP-125	0.80 (0.34)	0	0	0.76 (0.52)	0.78 (0.45)

identify potential mutations. Two were identified (Figure 2.2). A mutation was present in LP-018_m1 in a gene annotated as a hypothetical protein, and would result in a nonsense mutation leading to a truncated protein product (the stop codon is located at amino acid position 107 of 153). This mutation was located at nucleotide position 39,086 and caused a codon change of GAA to TAA. This mutation was not detected in the sequenced LP-018 sample, and 116/116 reads confirmed the mutation in the LP-018_m1 sample. This suggests the mutation likely occurred in the plaque purification and amplification steps. The host range data collected from this phage mutant does not suggest any change in host range from the dominant phage strain present in the LP-018 stock. The other mutation was present in LP-018_m2 in a gene annotated as a hypothetical protein containing a conserved BppU-family domain and would result in a radical nonsynonymous substitution (the polar and acidic amino acid, aspartic acid would be substituted with the nonpolar valine (Veesler et al., 2012). This mutation was located at nucleotide position 61,585 and caused a codon change of GAT to GTT. This radical nonsynonymous mutation was detected in the original LP-018 sample at very low levels (1 out of 396 reads supported this variant) and was confirmed to be present in the LP-018_m2 sample by 969/970 of the reads. BppU is a baseplate protein that is part of the host adsorption machinery in Gram-positive-infecting phages (X. Li et al., 2016; Veesler et al., 2012). This supports the EOP data, suggesting that the mutation was present at very low levels in a subpopulation of LP-018. Further, this data suggests the mutation identified in LP-018_m2 is affects the host range by altering the function of a baseplate protein involved in the adsorption to the host.

2.4.6 Effciency of Plaquing of Homburgviruses Against LP-018-Resistant Mutants

To test whether the phage-resistant mutants selected for by LP-018 was just specific to LP-018 or to homburgviruses in general, an EOP experiment was performed with four other homburgviruses (*Listeria* phages LP-026, LP-037, LP-110, and LP-114) against 10403S (m_acid-resistance) and 10403S (m_foldase). All four homburgviruses showed no activity against 10403S (m_foldase). Interestingly, *Listeria* phage LP-114 plaqued 89% (18% standard deviation) as efficiently on 10403S (m_acid-resistance) as on 10403S, and LP-026 plaqued 11% (9% standard deviation) as efficiently on 10403S (m_acid-resistance) as on 10403S. This data suggests that these resistance types do broadly effect homburgviruses, but LP-110, and LP-026 to a lesser degree, are able to overcome the resistance caused by a nonsense mutation in the putative acid-resistance protein encoded by *LMRG_00278*.

2.5 Conclusions

LP-018 is a *Homburgvirus* with the unique ability to infect phage-resistant mutants that have lost rhamnose in their cell wall teichoic acids (Trudelle et al., 2019). Sequencing of LP-018 revealed that if genome length is accounted for, it may meet the criteria for qualifying as a new species (Adriaenssens & Brister, 2017). Although we did not observe levels of growth that would be characteristic of a potent lytic phage, it is possible that the conditions selected in this study were not ideal for determining the full potential of LP-018. It is known that environmental conditions can have a strong impact on phage infection (Denes & Wiedmann, 2014). For example, Tokman et al. previously showed that growth temperature had a particularly large effect on the plaquing

efficiencies of homburgviruses (Tokman, Kent, Wiedmann, & Denes, 2016). Future work will be needed to explore if other conditions in liquid media provide more favorable growth of LP-018, and if LP-018 is effective at reducing *L. monocytogenes* concentrations in food matrices.

Most notably, this study identified and characterized the first phage-resistant mutants of *Listeria* that resist phage infection through a mechanism independent of adsorption inhibition. Interestingly, these mutations appear to affect phages in the *Homburgvirus* genus specifically. Further work will need to be conducted to determine the mechanism of resistance conferred through these newly identified mutations. We have also identified a gene in LP-018 that is likely involved in host range determination. Current phage-based products targeting *L. monocytogenes* have all relied on the pecentumviruses of *Listeria* (Moye et al., 2018). The work reported here provides knowledge of a unique member of a genus of *Listeria* phage that has not been explored for potential use in food safety applications. Such knowledge of new and diverse phages may be essential for reaching the full potential of phage-based biocontrol while maintain long-term efficacy.

.

3 CHAPTER III

CHARACTERIZATION OF A NOVEL GROUP OF *LISTERIA* PHAGES THAT TARGET SEROTYPE 4B *LISTERIA MONOCYTOGENES*

A version of this chapter was originally published by Yaxiong Song, Tracey L. Peters, Daniel W. Bryan, Lauren K. Hudson and Thomas G. Denes:

Song Y, Peters T L, Bryan D W, et al. Characterization of a Novel Group of *Listeria* Phages That Target Serotype 4b *Listeria monocytogenes*[J]. Viruses, 2021, 13(4): 671.

3.1 Abstract

Listeria monocytogenes serotype 4b strains are the most prevalent clinical isolates and are widely found in food processing environments. Bacteriophages are natural viral predators of bacteria and are a promising biocontrol agent for *L. monocytogenes*. The aims of this study were to characterize phages that specifically infect serotype 4b strains and to assess their ability to inhibit the growth of serotype 4b strains. Out of 120 wild *Listeria* phages, nine phages were selected based on their strong lytic activity against the model serotype 4b strain F2365. These nine phages can be divided into two groups based on their morphological characteristics and host range. Comparison to previously characterized phage genomes revealed one of these groups qualifies to be defined as a novel species. Phages LP-020, LP-027, and LP-094 were selected as representatives for these two groups of phages for further characterization through one-step growth curve and inhibition of serotype 4b *L. monocytogenes* experiments. *Listeria* phages that target serotype 4b showed an inhibitory effect on the growth of F2365 and other serotype 4 strains and may be useful for biocontrol of *L. monocytogenes* in food processing environments.

3.2 Introduction

Listeria monocytogenes is a Gram-positive foodborne pathogen that infects humans and animals (Karthikeyan et al., 2019). *L. monocytogenes* is widely isolated from soil, agriculture environments, and urban environments, and is able to tolerate high salt concentrations and a broad range of temperatures and pH levels (Fenlon, 1985; D. Liu, Lawrence, Ainsworth, & Austin, 2005; Sauders et al., 2012; Vivant et al., 2013). Contamination of the food processing environment with *L. monocytogenes* can lead to consumers ingesting the pathogen, which can cause the potentially fatal invasive disease listeriosis (Malakar, Borah, Das, & Kumar). The global burden of listeriosis cases has been estimated at 23,150 annually, with a mortality rate of 26% (de Noordhout et al., 2014). Within the United States alone, there is an estimated 2518 annual cases, with a 20% mortality rate (Mead et al., 1999; Scallan et al., 2011), and economic losses caused by listeriosis were more than $3.1 billion in 2018 ("Cost Estimates of Foodborne Illnesses," 2021).

Bacteriophages are natural viral predators of bacteria, which infect and lyse specific host strains (R. Carlton et al., 2005). High specificity, self-replication capability, and tolerance of a wide range of temperatures and pHs (Jurczak-Kurek et al., 2016) make bacteriophages a promising candidate for biocontrol of *L. monocytogenes* in the food processing environment (Sillankorva et al., 2012). *Listeria* phage biocontrol products have been approved for use by the United States Food and Drug Administration since 2006. These products are marketed to control *L. monocytogenes* contamination on food and in food processing plants. Currently used *Listeria* phages have been characterized as

belonging to the genus *Pecentumvirus* (Chibeu et al., 2013). *Pecentumvirus* phages have been shown to utilize rhamnose and N-acetylglucosamine of wall teichoic acids as binding receptors during the adsorption step of infection (Denes et al., 2015). Presence or absence of these sugars corresponds to the various serotypes of *L. monocytogenes* (Sumrall et al., 2020); thus, *Listeria* phages show some level of serotype specificity (Vongkamjan et al., 2012).

Based on cell surface antigenic determinants, *L. monocytogenes* can be divided into at least 13 serotypes. Serotype 4b strains account for most clinal isolates from humans, causing about 50% of illnesses; serotype 1/2a ranks second and is associated with 27% of cases (Aarnisalo et al., 2003; Hasebe et al., 2017; D. Liu, 2008; Pontello et al., 2012). Serotype 1/2a and 4b are the most frequently recovered from food and environmental samples (Aarnisalo et al., 2003; Y. Huang et al., 2018; Leong et al., 2014; Nucera et al., 2010). Previous phage host-range studies employing efficiency of plaquing assays showed three *Pecentumvirus* phages, LP-048, LP-125, and A511, that effectively form plaques against serotype 1/2 strains and serotype 4b strain F2365 (Tracey Lee Peters et al., 2020); however, *Homburgvirus* LP-018, which also shows some potential use in biocontrol applications (Song, Peters, Bryan, Hudson, & Denes, 2019), was not able to infect this model strain (Tracey Lee Peters et al., 2020). In order to increase the diversity of characterized phages available for use against serotype 4 strains, we screened and characterized nine *Listeria* phages that show strong infectivity against the serotype 4b *L. monocytogenes* strain F2365.

3.3 Materials and Methods

3.3.1 Bacterial Strains and Bacteriophages

All bacterial strains in this study are listed in Table 3.1. *L. monocytogenes* MACK was used for phage titering and phage propagation of *Listeria* phages A511, LP-048, and LP-125. *L. monocytogenes* F2365 is the *L. monocytogenes* serotype 4b standard strain that was used for phage titering and phage propagation of the remaining *Listeria* phages (LP-020, LP-021, LP-024, LP-027, LP-053, LP-054, LP-057, LP-085, and LP-094). *L. monocytogenes* 10403S is a *L. monocytogenes* serotype 1/2a model strain. FSL D4-0014 and FSL D4-0119 are mutants of *L. monocytogenes* 10403S that lack N-acetyl glucosamine and rhamnose in their wall teichoic acid, respectively. All the strains were stored at -80 °C in Brain Heart Infusion (BHI) supplemented with 15% (*w*/*v*) glycerol and grown on 1.5% (*w*/*v*) BHI agar plates at 37 °C. Overnight cultures for each strain were inoculated with a single colony from a streak plate into BHI broth and grown at 37 °C in a shaking water bath at 160 RPM.

All *Listeria* phages in this study are listed in Table 3.2. *Listeria* phages LP-048 and LP-125 were well-studied phages that are able to infect serotype 1/2a strains. *Listeria* phage A511 is a broad range phage that is able to infect both serotype 1/2a strains and 4b strains (Kim & Kathariou, 2009; Tokman et al., 2016). The other *Listeria* phages (LP-020, LP-021, LP-024, LP-027, LP-053, LP-054, LP-057, LP-085, and LP-094) were included in the study due to their ability to show strong lytic activity against *L. monocytogenes* F2365. All phages were titered on lysogeny broth morpholino-propane sulfonic acid (LB-MOPS) agar supplemented with 0.1% glucose, 1 mM $CaCl_2$, and 1 mM $MgCl_2$ by 10 µL

Table 3.1 *Listeria monocytogenes* strains.

Strain	Serotype	Reference or Original
10403S	1/2a	(Bishop & Hinrichs, 1987)
MACK	1/2a	(Hodgson, 2000)
F2365	4b	(Nelson et al., 2004)
FSL J1-175	1/2b	(Bergholz, den Bakker, Fortes, Boor, & Wiedmann, 2010)
FSL J1-208	4a	(A. Roberts et al., 2006)
FSL C1-115	3a	(Fugett, Fortes, Nnoka, & Wiedmann, 2006)
FSL J1-094	1/2c	(Fugett et al., 2006)
FSL F2-695	4a	(A. Roberts et al., 2006)
FSL F2-501	4b	(A. Roberts et al., 2006)
FSL J2-071	4c	(A. Roberts et al., 2006)
FSL W1-110	4b	(De Jesus & Whiting, 2003)
FSL J1-158	4b	(De Jesus & Whiting, 2003)
FSL J1-169	3b	(Fugett et al., 2006)
FSL J1-049	3c	(Fugett et al., 2006)
FSL D4-0014	1/2a	(Denes et al., 2015)
FSL D4-0119	3	(Denes et al., 2015)
FSL R9-0915	7	(Denes et al., 2015)

Table 3.2 *Listeria monocytogenes* phages.

Phages	Description	Reference or Original
A511		(Klumpp et al., 2008; Loessner & Busse, 1990)
LP-020		(Vongkamjan et al., 2012)
LP-021		(Vongkamjan et al., 2012)
LP-024		(Vongkamjan et al., 2012)
LP-027		(Vongkamjan et al., 2012)
LP-048	P100-like phage	(T. Denes et al., 2014; Vongkamjan et al., 2012)
LP-053		(Vongkamjan et al., 2012)
LP-054		(Vongkamjan et al., 2012)
LP-057		(Vongkamjan et al., 2012)
LP-085		(Vongkamjan et al., 2012)
LP-094		(Vongkamjan et al., 2012)
LP-125	P100-like phage	(T. Denes et al., 2014; Vongkamjan et al., 2012)

spot assay and were incubated at 25 °C overnight (16 ± 2 h). Phage stocks were prepared by liquid amplification. A culture of the host strain was grown to an OD_{600nm} of 0.2, infected with the phage at a multiplicity of infection (MOI) of 0.1; after 3 h of incubation at 25 °C in a shaking water bath, the infected culture was filtered with a 0.45 µm SCFA sterile filter, and then centrifuged at 12,000× *g* at 4 °C for 2 h. The supernatant was then removed, and the pellet was resuspended in SM buffer (0.1% *v*/*v* gelatin, 0.05 M Tris-Cl pH 7.5, 0.58% *w*/*v* NaCl, 0.2% *w*/*v* $MgSO_4 \cdot 7H_2O$) by static incubation at 4 °C for 24 h, then filtered with a 0.20 µm SCFA sterile filter and transferred to a sterile tube as new phage stock. All phage stocks were stored at 4 °C in SM buffer. Storage at 4 °C in liquid media with structurally similar phages has been demonstrated to maintain stable titers for months to years with minimal degradation of stock viability (Hans-Wolfgang Ackermann, Tremblay, & Moineau, 2004; Clark, 1962; Cooper, Denyer, & Maillard, 2014).

3.3.2 Transmission Electron Microscopy

A purified, high titer phage sample (~1×10^{10} PFU/mL) was prepared for transmission electron microscopy (TEM) as previously described with modifications (Song et al., 2019). One milliliter of each phage sample was washed using a 0.1 M ammonium acetate solution (pH 7) and centrifuged at 21,000× *g* with a microcentrifuge (Thermo Fischer Scientific, Waltham, MA, USA). One drop of the phage sample was deposited onto a 150–200 mesh carbon-coated Formvar film copper grid (Electron Microscopy Sciences, Hatfield, PA, USA) and stained using 1% phosphotungstic acid (PTA; pH 7.4). Samples were imaged using a JEOL 1400 Flash transmission electron microscope at 120 kV. Images were analyzed using Fiji 3 v.2.0.0-rc-69/1.52p.

3.3.3 DNA Extraction and Genomic Analysis

Phage DNA were extracted by the phenol-chloroform method as previously described (Song et al., 2019).

Libraries were prepared using a Nextera kit (Illumina, San Diego, CA, USA) and sequenced with an Illumina NextSeq 550 using 150 bp paired-end read chemistry. LP-027 was additionally long-read sequenced; the library was prepared using a Rapid Barcoding Kit (SQK-RBK0004; Oxford Nanopore Technologies, Oxford, UK) and sequenced with a MinIon. Illumina reads were trimmed using Trimmomatic (v0.35) (Bolger et al., 2014) and read quality statistics were generated using FastQC (v0.11.7). Reads were mapped to the *L. monocytogenes* propagation host strain (F2365) genome in order to filter out host contamination reads. Assemblies were generated using SPAdes (v3.12.0) (Bankevich et al., 2012) and a hybrid assembly was generated with Unicycler (v0.4.8-beta) (Wick et al., 2017) for LP-027 using both Illumina and Nanopore reads. For some genomes, reads were subsampled to obtain better assemblies. Final assemblies were re-oriented to start at the large terminase subunit and annotated using RASTtk (Brettin et al., 2015), with the pipeline modified to run "annotate-proteins-phage" before "annotate-proteins-kmer-v2." Assembly statistics were generated using Quast (v4.6.3) (Gurevich et al., 2013), BBMap (v38.08) (Bushnell, 2018), and SAMtools (v1.8) (H. Li et al., 2009). Average nucleotide identity (ANI) values between phages from this study and those described previously by Denes et al. (T. Denes et al., 2014) were calculated using BLAST with JSpeciesWS (Richter et al., 2015). Genome similarity maps of the representative phages and most similar previously described phages were created using

EasyFig (v2.2.2) (Sullivan, Petty, & Beatson, 2011) with similarity calculated using both BLASTn and tBLASTx (v2.11.0+) (Altschul, Gish, Miller, Myers, & Lipman, 1990). The phage lifestyles were classified using PHACTS (McNair, Bailey, & Edwards, 2012) and were additionally assessed by manually inspecting the genomes for genes related to lifestyle (e.g., integrases) and the phage genomes were used as queries to BLAST against the nr/nt database limited to *L. monocytogenes* (txid: 1639). Sequencing data and assemblies are available on NCBI under BioProject PRJNA688926.

3.3.4 Efficiencies of Plaquing and Relative Phage Activity

All twelve *Listeria* phages and sixteen *L. monocytogenes* strains (except MACK) listed in Table 3.1 were used to conduct efficiency of plaquing (EOP) and relative phage activity (RPA) assays as previously described (Tracey Lee Peters et al., 2020; Trudelle et al., 2019). In brief, bacterial lawns were prepared with the double agar overly method and allowed to solidify. All the phages were amplified from the original phage stock and diluted to 1×10^7 PFU/mL as a working stock. Serial dilutions were made from each working stock and spotted onto bacterial lawns. The EOP of each phage was determined from the highest dilution with countable plaques against the strain in question compared to the number of plaques against the phage propagation host strain. Similarly, the RPA of each phage was determined from the highest dilution with observable inhibitory activity against the strain in question compared to the phage propagation host strain. Inhibitory activity is defined as an observable inhibition of the growth of the bacterial lawn where the phage dilution was spotted without the formation of any phage plaques. Three

biological replicates were performed. EOP and RPA clustered heatmaps were generated using *pheatmap* in R (Kolde, 2019).

3.3.5 One-Step Growth Curve

An exponential-phase culture of F2365 was infected with LP-020, LP-027, or LP-094 at a multiplicity of infection (MOI) of 0.1. The infected culture was incubated at 25 ℃ and 160 RPM for 3 h. To measure infected host cells and unabsorbed viable phages, two samples were taken at each time point. One sample was serially diluted and enumerated by the spot assay method immediately after collection, the other sample was treated with 5%(*v*/*v*) chloroform for 15 min and then serially diluted and enumerated by the spot assay method, and the plates were incubated at 25 ℃ for 12 h. Three biological replicates were performed.

3.3.6 Inhibition Growth Curve of Listeria Monocytogenes F2365 by LP-020, LP-027, and LP-094

A measure of 2 mL of *L. monocytogenes* F2365 overnight culture was added into 100 mL LB-MOPS with 0.1% glucose, 1 mM $CaCl_2$, and 1 mM $MgCl_2$. The culture was incubated at 25 ℃ and 160 rpm until the OD_{600nm} grew to ~0.1. The culture was then diluted 10-fold with fresh supplemented LB-MOPS. A measure of 7 mL of the diluted culture was added to twelve sterile 15 mL glass culture tubes. Each tube was infected with LP-020, LP-027, or LP-094 at MOI = 0.1, 1, 10 with SM buffer as a negative control and incubated at 25 ℃ and 160 RPM for 15 h. The OD_{600nm} of each tube was measured every half an hour for 15 h on a Genesys 30 Visible spectrophotometer

(Thermo-Fisher Scientific, Waltham, MA, USA). Three biological replicates were performed.

3.3.7 Inhibition Growth Curve of Listeria Monocytogenes Cocktail by LP-020 and LP-094

Seven strains were used in this experiment: F2365 (4b), FSL J1-208 (4a), FSL F2-695 (4a), FSL F2-501 (4b), FSL J2-071 (4c), FSL W1-110 (4b), and FSL J1-148 (4b). Each strain was incubated in LB-MOPS supplemented with 0.1% glucose, 1 mM $CaCl_2$, and 1 mM $MgCl_2$ at 25 °C and 160 rpm until the OD_{600nm} grew to ~0.1. A *L. monocytogenes* cocktail was prepared by transferring 1 mL of each strain into one 15 mL sterile tube and mixing by vortex mixer. The cocktail was then diluted 10-fold with fresh supplemented LB-MOPS. A total of 7 mL of the diluted cocktail was added to eight sterile 15 mL glass culture tubes. Each tube was infected with LP-020 or LP-094 with MOI =0.1, 1, 10 or SM buffer as a negative control, grown at 25 °C, and shaken at 160 RPM for 15 h. The OD_{600nm} of each tube was measured every half an hour for 15 h. Three biological replicates were performed.

3.4 Results and Discussion

3.4.1 Transmission Electron Microscopy Imaging of Wild Type Listeria Phages Revealed Two Distinct Morphologies

Based on morphological characteristics, all phages were classified within the *Siphoviridae* family (Figure 3.1). One group that includes two phages, LP-024 and LP-027, were found to have icosahedral capsids with flexible, elongated tails (Table 3.3).

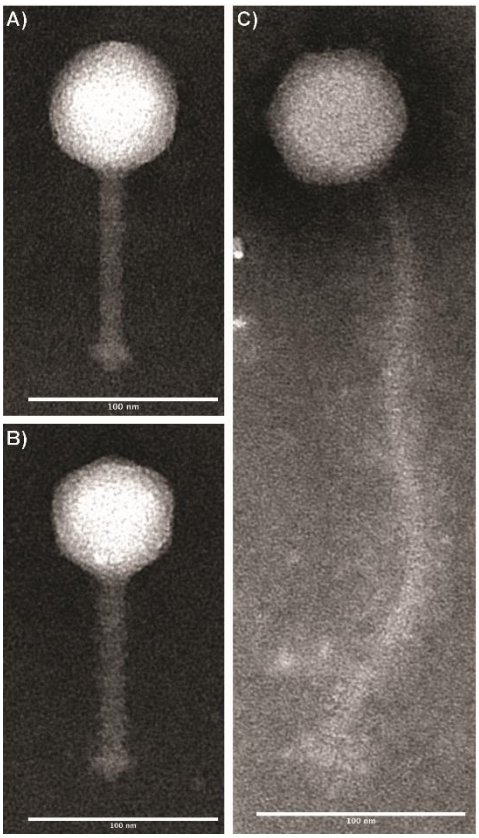

Figure 3.1 Transmission electron microscopy images of wild type *Listeria* phages representing two morphologies: (A) LP-020 and (B) LP-094, characterized by an icosahedral capsid and a flexible, non-contractile tail; (C) LP-027, characterized by an icosahedral capsid and a long, flexible, non-contractile tail. Phages were stained with 1% phosphotungstic acid (pH &) and imaged at a final magnification of × 69,700–83,600. Images were analyzed using FIJI 3 (v2.0.0-rc-69/1.52p).

Table 3.3 Morphology of *Listeria monocytogenes* phages.

Listeria monocytogenes Phages	Capsid Diameter (nm)	Tail Length (nm)	Tail Width (nm)
LP-020	73.40 ± 0.61	104.80 ± 1.45	11.54 ± 0.09
LP-021	69.92 ± 4.62	102.45 ± 2.32	11.01 ± 0.61
LP-024	66.10 ± 5.07	291.29 ± 18.56	8.25 ± 2.54
LP-027	70.35 ± 2.40	295.38 ± 10.42	7.95 ± 2.09
LP-053	68.03 ± 4.76	104.01 ± 3.00	11.88 ± 1.91
LP-054	73.70 ± 0.50	100.71 ± 3.55	11.43 ± 0.33
LP-057	73.60 ± 0.37	102.45 ± 1.62	13.46 ± 0.90
LP-085	72.22 ± 0.62	104.02 ± 3.19	12.61 ± 0.77
LP-094	71.75 ± 2.98	100.49 ± 2.87	12.81 ± 0.97

The second group also had icosahedral capsids; however, these phages were found to have short flexible tails (Table 3.3) .

3.4.2 Genomic Analysis

All phage reads assembled into complete, single-contig genomes; genome statistics are presented in Table 3.4. Based on genome statistics, two distinct groups were evident. LP-024 and LP-027 were 41.0–41.4 kb, with G+C contents of 36.5–36.6%, and each contained 74 coding sequences (CDS) and no RNAs. The other phage genomes were 35.6–36.0 kb, with G+C contents of 39.9–40.0%, and each contained 54–57 CDS and no RNAs. The two distinct groups were also supported by average nucleotide identity (ANI) values (Table 3.5, Table 3.6) and amino acid similarity (Figure S3. 1). LP-024 and LP-027 had an ANI of 100.00% over 95.51–96.63% of their genomes and were most similar to LP-030-3 (99.99–100.00% ANI over 95.92–96.63% of their genomes) (Table 3.5), a putative temperate phage. LP-030-3 was previously classified as an Orthocluster IV siphovirus (T. Denes et al., 2014), with a 41.2 kb genome containing 73 predicted genes. Electron micrographs show that LP-030-3 has a long and rigid tail (T. Denes et al., 2014) . Morphology and genome features of LP-030-3 are consistent with the LP-027-like phages and are likely putative temperate phage (T. Denes et al., 2014). These two phages are likely the same genus and species as LP-030-3, as they are above the 50% and 95% cutoffs for genus and species delineation. LP-030-3 is currently listed as a “unclassified Siphoviridae,” with no genus classification, on NCBI (NCBI:txid1458852) and is not included in the most recent ICTV Master Species List 2019.v1. The other phages had an ANIs of 97.66–100.00%, over 90.63–99.24% of their genomes, and were most similar to

Table 3.4 Assembly statistics for *Listeria* phages.

Phage	BioSample ID	Length (bp)	Avg. Illumina Read Coverage (X)	G+C (%)	No. CDS	No. RNAs
LP-020	SAMN17217625	35,609	326.6	40.0	54	0
LP-021	SAMN17217626	35,610	344.1	40.0	54	0
LP-024	SAMN17217627	40,964	153.7	36.5	74	0
LP-027	SAMN17217628	41,120	89.6	36.6	74	0
LP-053	SAMN17217629	35,951	143.5	40.0	57	0
LP-054	SAMN17217630	35,951	524.9	40.0	57	0
LP-057	SAMN17217631	35,608	1001.1	40.0	54	0
LP-085	SAMN17217632	35,951	650.4	39.9	57	0
LP-094	SAMN17217633	35,885	3397.6	40.0	56	0

Table 3.5 JSpecies results for LP-030-03-like *Listeria* phages.

	Average Nucleotide Identity (ANI; %) [aligned nucleotides (%)]					
Phage	**LP-024**	**LP-027**	**LP-030-3**	**A500**	**A118**	**A006**
LP-024	*	100.00 [96.63]	100.00 [96.63]	92.81 [63.99]	86.34 [52.10]	92.00 [6.82]
LP-027	100.00 [95.51]	*	100.00 [95.92]	92.77 [63.41]	86.10 [50.80]	91.76 [5.70]
LP-030-3	99.99 [96.21]	100.00 [96.57]	*	92.07 [62.93]	84.54 [47.14]	88.41 [6.80]
A500	92.74 [68.96]	92.74 [68.96]	92.74 [69.01]	*	84.52 [49.43]	89.93 [6.42]
A118	84.79 [53.25]	84.78 [53.48]	84.78 [53.51]	84.00 [47.63]	*	95.38 [23.01]
A006	89.85 [7.30]	89.54 [9.18]	89.54 [9.18]	84.93 [4.69]	94.91 [27.18]	*

Table 3.6 JSpecies results for P35-like *Listeria* phages.

	Average Nucleotide Identity (ANI; %) [aligned nucleotides (%)]								
Phage	**LP-020**	**LP-021**	**LP-053**	**LP-054**	**LP-057**	**LP-085**	**LP-094**	**P35**	**P40**
LP-020	*	99.99 [97.36]	97.68 [94.41]	97.68 [94.41]	98.71 [97.35]	97.86 [94.41]	97.66 [93.39]	79.51 [85.61]	61.76 [32.56]
LP-021	99.99 [97.36]	*	97.69 [94.41]	97.69 [94.41]	98.72 [97.34]	97.87 [94.41]	97.68 [93.39]	79.52 [85.63]	61.76 [32.55]
LP-053	97.77 [90.63]	97.78 [90.63]	*	100.00 [99.24]	99.15 [90.64]	99.74 [99.24]	99.98 [98.21]	79.85 [87.67]	61.47 [33.98]
LP-054	97.77 [90.63]	97.78 [90.63]	100.00 [99.24]	*	99.15 [90.64]	99.74 [99.24]	99.98 [98.21]	79.85 [87.67]	61.47 [33.98]
LP-057	98.71 [97.34]	98.72 [97.35]	98.97 [94.42]	98.97 [94.42]	*	99.02 [94.42]	98.96 [93.40]	79.62 [85.79]	61.80 [32.41]
LP-085	97.97 [90.63]	97.98 [90.63]	99.74 [99.24]	99.74 [99.24]	99.22 [90.64]	*	99.73 [98.21]	79.87 [87.67]	61.51 [33.94]
LP-094	97.75 [91.58]	97.76 [91.58]	99.98 [98.24]	99.98 [98.24]	99.08 [91.59]	99.73 [98.24]	*	79.98 [86.27]	61.54 [32.97]
P35	79.85 [83.06]	79.86 [83.07]	80.35 [84.12]	80.35 [84.12]	80.02 [83.03]	80.36 [84.12]	80.33 [84.12]	*	63.10 [23.90]
P40	61.52 [25.48]	61.81 [24.84]	62.26 [22.30]	62.26 [22.30]	62.37 [22.14]	62.36 [22.26]	62.29 [22.30]	62.80 [24.06]	*

P35 (79.51–80.36% ANI over only 83.03–87.67% of their genomes) (Table 3.6, Figure 3.2), a lytic phage (T. Denes et al., 2014). P35 was previously classified as an Orthocluster II siphovirus (T. Denes et al., 2014), with a 35.8 kb genome containing 56 predicted genes. Electron micrographs show that P35 has a short tail (T. Denes et al., 2014; Dorscht et al., 2009). Morphology and genome features of P35 are consistent with the LP-020-like phages and they are likely putative obligate lytic phages (T. Denes et al., 2014; Dorscht et al., 2009). Given the >50% nucleotide similarity to P35, this second group of phages likely belongs to the same genus(Adriaenssens & Brister, 2017). However, they clearly qualify as a novel species, as they are well below the 95% similarity cutoff to be considered the same species as P35. P35 is currently listed as a "unclassified *Siphoviridae*" with no genus classification, on NCBI (NCBI:txid330398) and is not included in the most recent ICTV Master Species List 2019.v1.

LP-024 and LP-027 were confidently predicted as having a temperate lifestyle by PHACTS (Table S3. 1) and both genomes contained a phage integrase gene. This was further confirmed through BLAST, which showed they have high similarity to *L. monocytogenes* genomes (up to 99.79% identity and 86% query coverage). LP-020 and LP-057 were non-confidently predicted as having a lytic lifestyle and LP-021, LP-053, LP-054, LP-085, and LP-094 were non-confidently predicted as having a temperate lifestyle (Table S3. 1). However, none of these genomes contained an integrase gene, and BLAST showed they did not have high similarity to any *L. monocytogenes* genomes (only up to 5% query coverage), indicating that they likely have a lytic lifestyle.

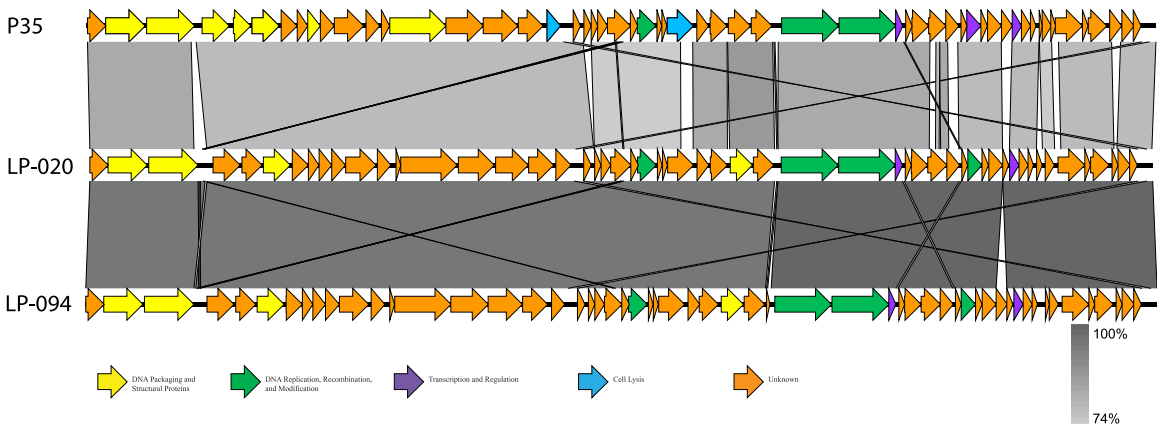

Figure 3.2 Linear BLASTn comparisons of representative P35-like *Listeria* phages. Genes are represented by arrows and are col-ored based on putative function (see key at bottom). The shaded region between genomes represents nucleotide sim-ilarity, with the darker gray representing higher similarity and lighter gray indicating lower similarity (see scale at bottom right).

3.4.3 Host Range Analysis

A511, which has been described as a broad host range phage (Kim & Kathariou, 2009), showed activity against 11 out of 17 *L. monocytogenes* (Figure 3.3A, Figure S3. 2), but only formed visible plaques on seven strains (Figure 3.3B, Figure S3. 2). Similarly, two previously characterized phages, LP-048 and LP-125, showed activity against a broad range of strains (thirteen and nine strains, respectively), compared to their ability to form plaques on the same strains (nine and four strains, respectively). All three of these *Pecentumvirus* phages were unable to infect all serotype 4b and 4a strains.

The phages selected for this study that showed strong activity against serotype 4b strain F2365 can be divided into two groups, and these groupings are consistent with those based on observed morphological characteristics. The first group, comprised of LP-024 and LP-027, showed a very narrow host range, forming plaques on F2365 (4b), FSL F2-501 (4b), and FSL J1-208 (4a). The second group, comprised of LP-020, LP-021, LP-053, LP-054, LP-057, LP-085, and LP-094, showed activity to all *L. monocytogenes* serotype 4 strains, and formed visible plaques on nearly all *L. monocytogenes* serotype 4 strains. Interestingly, LP-020 is the only phage in this group that was able to form plaques on non-serotype 4 strains.

FSL R9-0915 (7), FSL J1-049 (3c), and FSL D4-0119 (3) were the only three strains that were resistant to all phages in this study, although this is not surprising as these strains have consistently shown resistance to phage infection (Tracey Lee Peters et al., 2020; Vongkamjan et al., 2012).

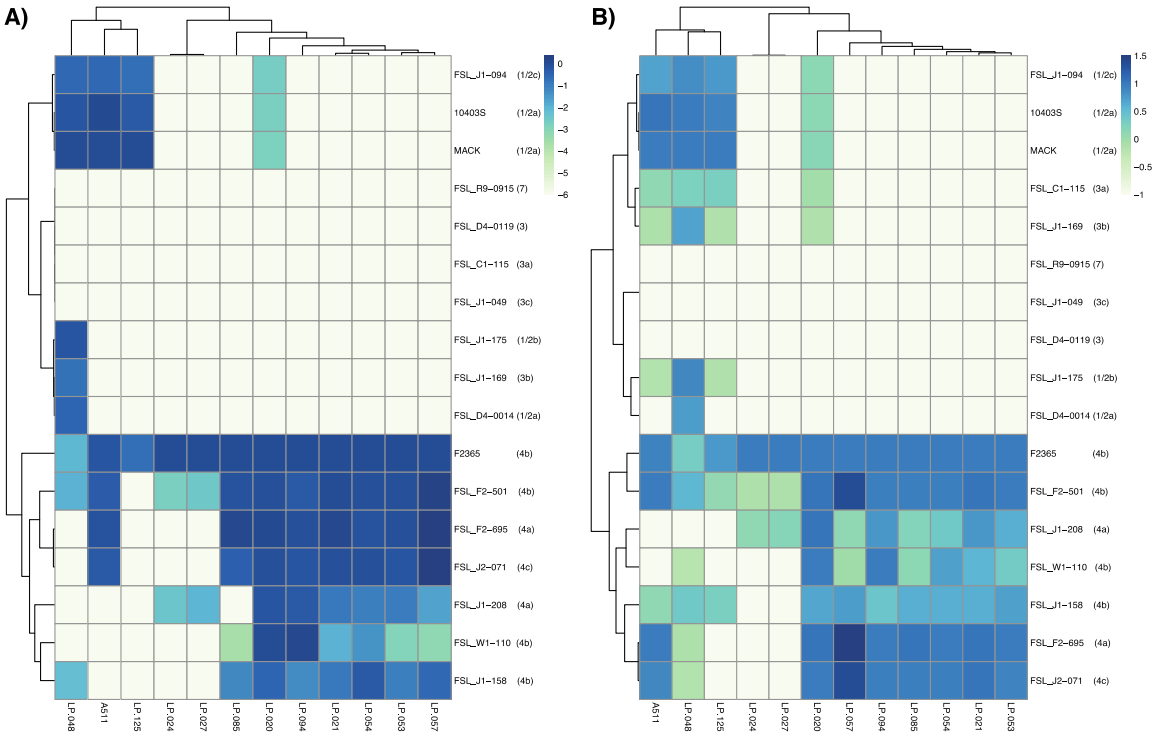

Figure 3.3 Host range analysis of *Listeria* phages against a panel of *Listeria monocytogenes* strains that represent different serotypes. Panel (A) represents efficiency of plaquing (EOP) results where values represent the log transformed efficiencies of plaquing of each phage against each bacterial strain compared to the phage propagation host strain. Panel (B) represents efficiency of activity (EOA) results where values represent the greatest dilution factor where phage activity was observed against each strain relative to the phage propagation host strain. Values are the mean of data from three biological replicates.

Based on the combination of their morphological characteristics and the results of their EOP and RPA, LP-020, LP-027, and LP-094 were selected as representative phages for further evaluation in this study.

3.4.4 One-Step Growth Curves

LP-020 was found to have a short adsorption time, in which 97.9% of LP-020 adsorbed to F2365 in 5 min. This is in contrast with LP-027 and LP-094, in which 30 min was required to attain adsorptions of 96.4% and 97.8%, respectively. One-step growth curve analysis of LP-020 showed a latent period of 60~90 min, an eclipse period of 5~15 min, and a burst size of ~9.7 (SE, 2.9) PFU/cell (Table 3.7, Figure 3.4A). One-step growth curve analysis of LP-027 showed a latent period of 45~60 min, an eclipse periods were 30~45 min, and a burst size of ~34.4 (SE, 5.8) PFU/cell (Table 3.7, Figure 3.4B). One-step growth curve analysis of LP-094 showed a latent period of 30~45 min, an eclipse period of 30~45 min, and a burst size of ~28.3 (SE, 4.1) PFU/cell (Table 3.7, Figure 3.4C).

However, the one-step growth curve of LP-020 showed a fluctuation in completed phage numbers between 5 min and 30 min (Figure 3.4A).

3.4.5 Inhibition Growth Curve of Listeria Monocytogenes F2365 by LP-020, LP-027, and LP-094

All the phages tested were able to inhibit the growth of F2365, at a range of different multiplicities of infection (MOIs). LP-020 showed high efficiency in inhibiting the growth of F2365. Even with the lowest concentration (MOI = 0.1), LP-020 can keep the

Table 3.7 Infection kinetics summary.

***Listeria monocytogenes* Phages**	LP-020	LP-027	LP-094
Adsorption Time(min)	5	30	30
Adsorption Rate(%)	97.9 ± 0.5	96.4 ± 2.3	97.8 ± 1.0
Latent Period(min)	60~90	45~60	30~45
Eclipse Period(min)	5~15	30~45	30~45
Burst Size(PFU/cell)	9.7 ± 2.9	34.4 ± 5.8	28.3 ± 4.1

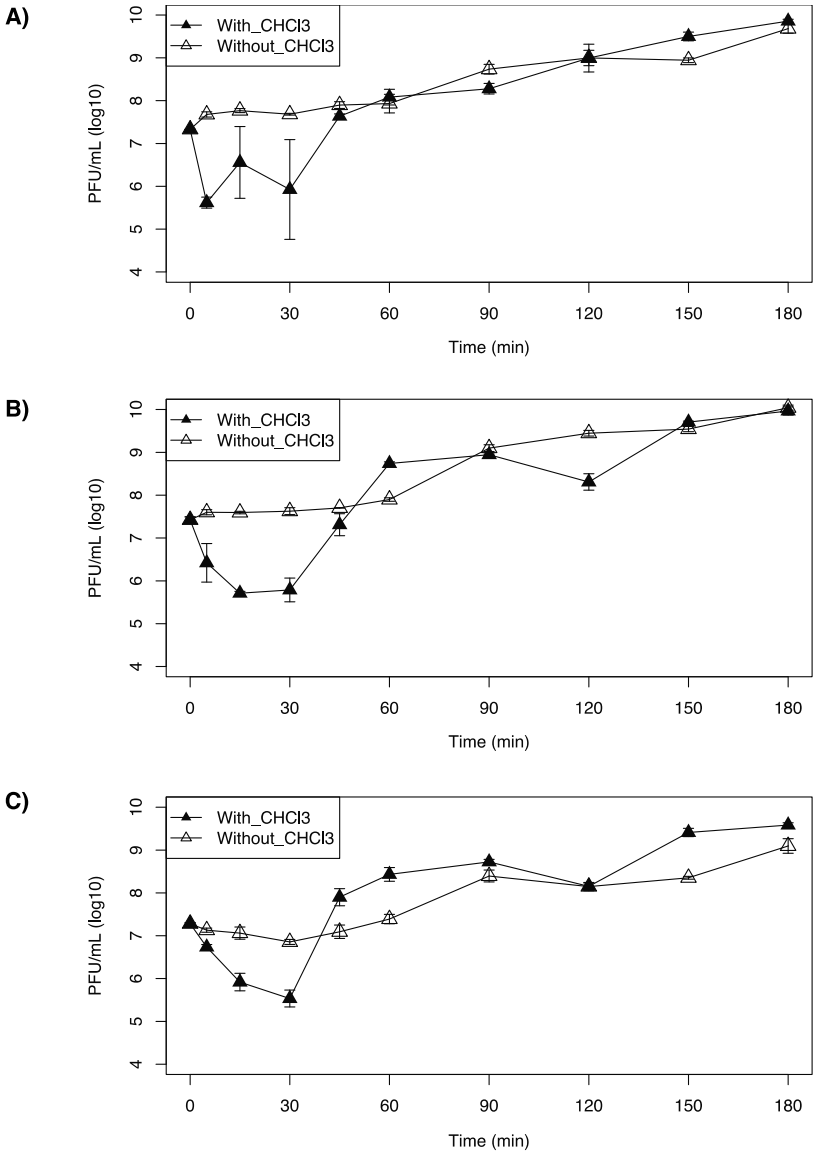

Figure 3.4 One-step growth curve of *Listeria monocytogenes* F2365 treated with (A) LP-20, (B) LP-0-27, or (C) LP-094 at a MOI = 0.1 at 25 °C. Filled triangles represent the phage titer in chloroform treated samples and unfilled triangles represent the phage titer in untreated samples. Data are mean values of three biological replicates and error bars represent standard error.

OD_{600nm} of F2365 under 0.03 for 15 h (Figure 3.5A). LP-027 could keep the OD_{600nm} of F2365 under 0.1 for 7 h with MOI = 0.1 and MOI = 1, and for 9 h with MOI = 10 (Figure 3.5B). LP-094 could keep the OD_{600nm} of the F2365 under 0.1 for 4 h and 4.5 h, with MOI = 0.1 and MOI = 1, respectively, and for 12 h with MOI = 10. Interestingly, after 12 h of incubation, the sample infected with LP-094 at MOI = 1 has a higher OD_{600nm} than the sample infected with LP-094 at MOI = 0.1, possibly due to the lower MOI (0.1) providing an opportunity for host to continue during early infection, leading to greater levels of phage production during later infection (Figure 3.5C).

3.4.6 Inhibition Growth Curve of Listeria Monocytogenes Cocktail by LP-020 and LP-094

LP-020 was able to inhibit the growth of a cocktail of *L. monocytogenes* serotype 4 at all tested MOIs, while LP-094 only showed an inhibitory effect with the highest MOI (Figure 3.6). For the first 8 h after LP-020 incubation, the growth curve of the cocktail showed no substantial difference. The growth curve of the cocktail treated with different dosages of LP-020 reached its peak at 11 h, 10 h, and 9 h, respectively. After reaching their peak, the bacterial cocktails treated with LP-020 showed a reduction in OD_{600nm}, with the 1 and 10 MOI infections reducing the OD_{600nm} to 0.06 and 0.08, respectively. Interestingly, the low MOI treatment group (MOI = 0.1) showed a large variation in OD_{600nm}, which may be due to the diversity of the host strains in the cocktail generating a more varied response to phage infection as the individual concentrations of each *L. monocytogenes* strain could vary from replicate to replicate due to complex growth interactions (Figure 3.6A). For the LP-094 infection, low MOI (MOI=0.1,1) showed no

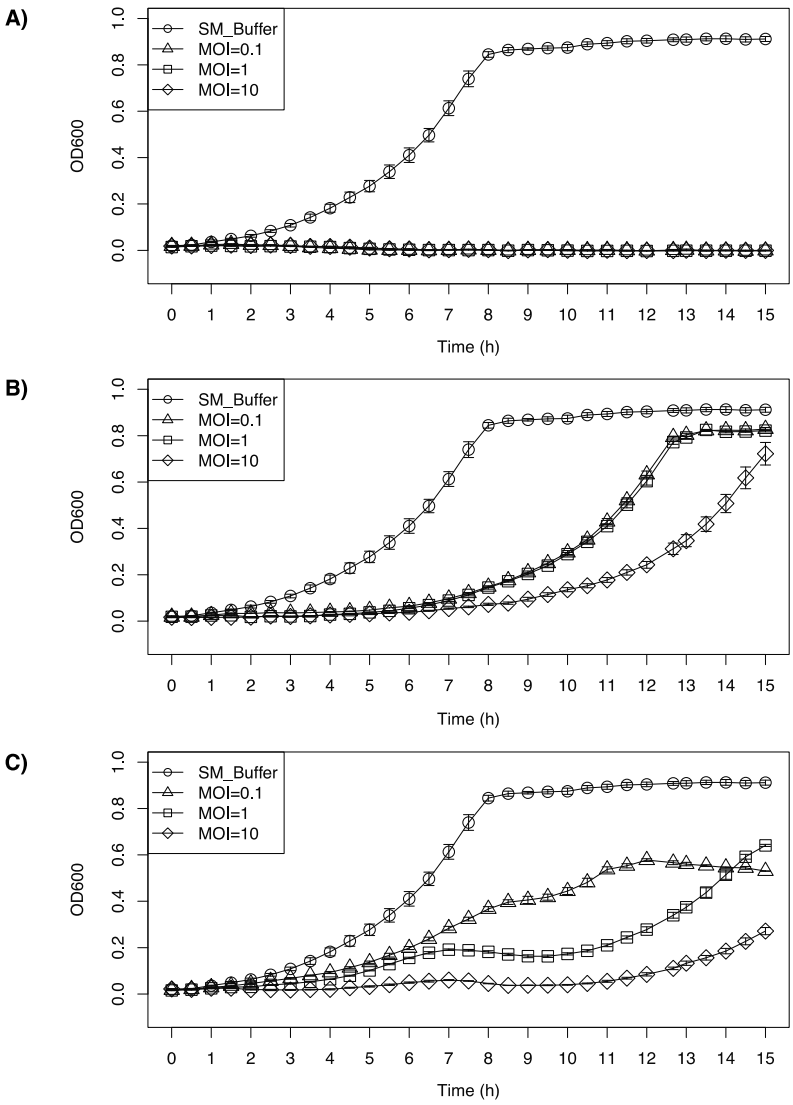

Figure 3.5 Inhibition growth curve of *Listeria monocytogenes* F2365 treated with (A) LP-020, (B) LP-027 or (C) LP-094 at different MOIs. Unfilled circles represent SM buffer control, unfilled triangles represent samples treated at an MOI of 0.1, unfilled squares represent samples treated at an MOI of 1, and diamonds represent samples treated at a MOI of 10. Data are mean values of three biological replicates and error bars represent the standard error.

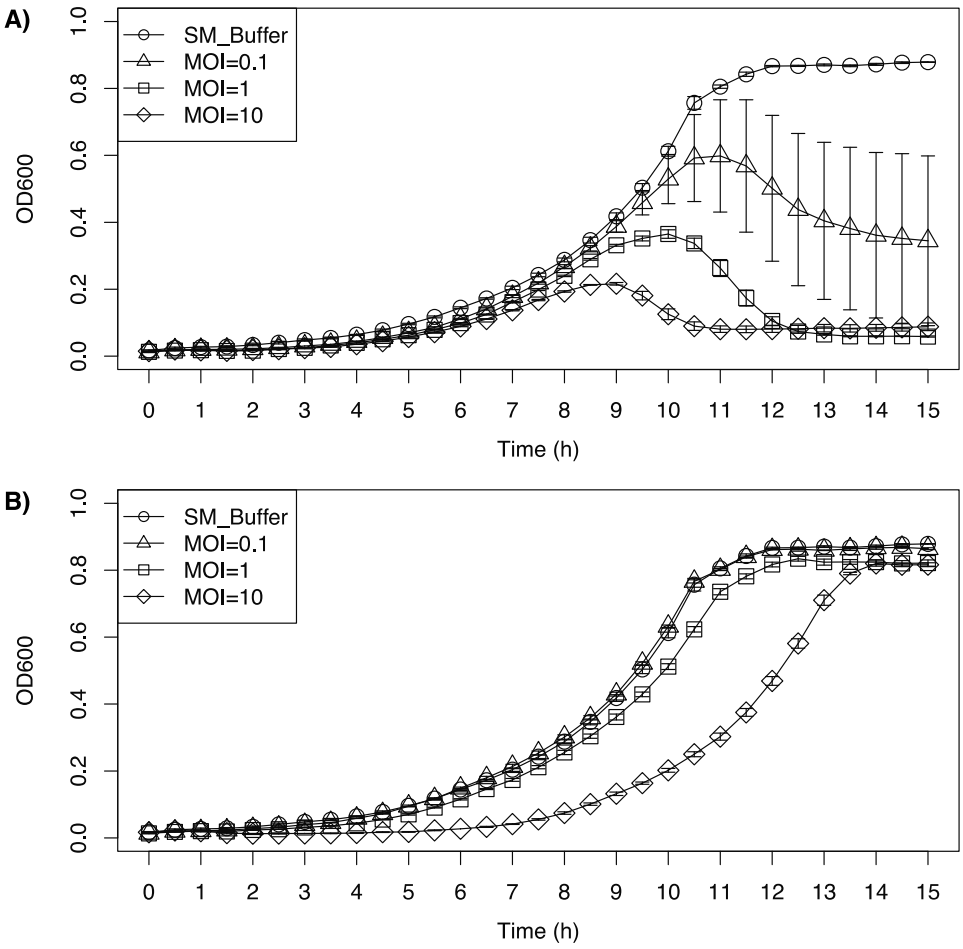

Figure 3.6 Inhibition growth curve of a cocktail of *Listeria monocytogenes* serotype 4 strains (F2365 (4b), FSL J1-208 (4a), FSL F2-695 (4a), FSL F2-501 (4b), FSL J2-071 (4c), FSL W1-110 (4b), and FSL J1-148 (4b)) treated with (A) LP-020 and (B) LP-094 at different MOIs. Unfilled circles represent SM buffer control, unfilled triangles represent samples treated at a MOI of 0.1, unfilled squares represent samples treated at a MOI of 1, and diamonds represent samples treated at a MOI of 10. Data are mean values of three biological replicates and error bars represent the standard error.

major influence of the growth curve of the cocktail. However, LP-094 can keep the OD_{600nm} of the cocktail under 0.1 for 8 h with a high dosage (MOI = 10) (Figure 3.6B). Compared with LP-094, LP-020′s ability to reduce the OD_{600nm} of a cocktail of serotype 4a, 4b, and 4c *Listeria* strains suggests it could be a promising phage for biocontrol applications in food processing environments.

3.5 Conclusions

In this study we describe two groups of *Listeria* phages that showed high levels of infectivity against serotype 4 strains of *L. monocytogenes*. One of these groups of phages, LP-020-like phages showed a level of nucleotide dissimilarity with previously sequenced phages that is well above the 5% cutoff for qualifying as a novel species. Inhibition assays of *L. monocytogenes* against a cocktail of serotype 4 strains (4a, 4b, and 4c) confirmed that EOP and RPA assays were predictive of a phage's inhibitory potential. We identified LP-020 as a phage that may be particularly useful in biocontrol settings. It shows strong activity against all serotype 4a, 4b, and 4c strains tested here. Given that some types of phage resistance is specific to a single species or closely related group of phages, such as CRISPR-Cas mediated resistance, it is critical to consider using diverse cocktails of phages. LP-020 may serve together with *Listeria* phages from other groups, such as *Pecentumviruses* (R. Carlton et al., 2005; Fernandes & São-José, 2018; Tracey L Peters, Hudson, Song, & Denes, 2019) and *Homburgviruses* (Hudson et al., 2019; Schmuki et al., 2012; Song et al., 2019), to increase both the diversity of *Listeria* phage cocktails and their infectivity against the problematic serotype 4 strains that are often associated with human illness. Further, the temperate phages described here, which are

similar to LP-030-3, may be useful as biocontrol agents if their integrases are knocked out, which has previously been shown for the temperate *Listeria* phage PSA (Kilcher, Studer, Muessner, Klumpp, & Loessner, 2018).

4 CHAPTER IV

CO-EVOLUTION DYNAMICS BETWEEN DISTINCT PHAGES AND SEROTYPE 1/2A AND 4B *LISTERIA MONOCYTOGENES*

4.1 Abstract

The co-evolutionary arms race between bacteriophages and their hosts is an important driver of population diversity. Better understanding of the interplay between new phage-resistant bacterial phenotypes and phage mutants which overcome this resistance will offer insight into the development of phage resistance in the environment, and mechanisms by which phages can overcome this resistance. The aims of this study were to observe the dynamics of co-evolution between *Listeria monocytogenes* and *Listeria* phages, the isolation of mutant *Listeria* and phages, and to identify mutations responsible for conferring phage resistance in the host and overcoming resistance in the phage. The dynamics of co-evolution between *Listeria* phages, representing two distinct groups (*pecentumvirus* and P35-like), and *L. monocytogenes* (serotype 1/2a and 4b) were observed through daily serial passage of phage and host coincubations over ten days. Phage lysates and surviving *L. monocytogenes* were recovered on day 5 and day 10. The resistance phenotype of recovered *L. monocytogenes* strains were tested by streak-spot assay (SSA) or spot assay, and the host range of phage lysates were tested with representative recovered *L. monocytogenes* by efficiency of plaquing assay. Genomic analysis of the recovered phage-resistant *L. monocytogenes* identified mutations repeatedly occurring in the same genes (i.e. *yfhO*,*rmlT*, *rmlA*), suggesting they are responsible for conferring phage resistance; different genes were implicated in different conditions. Besides genes that have no clear association with resistance mechanisms, all the remaining genes encode membrane proteins or are associated with wall teichoic acid

(WTA) synthesis, suggesting the mechanism of adsorption inhibition was the most common adaptation adopted by the mutants in the co-evolution experiment.

4.2 Introduction

Listeria monocytogenes is a ubiquitous foodborne pathogen that is widely detected in contaminated food (Lopes-Luz et al., 2021). *L. monocytogenes* infection is the cause of the serious disease listeriosis, which has a ~94.0% hospitalization rate and ~15.9% mortality rate in the United States in 2006 . According to the US Department of Agriculture (USDA)'s estimate, there were approximately1600 cases and 3.2 billion dollars in economic losses due to listeriosis in 2018 ((ERS), Cost Estimates of Foodborne Illnesses). *L. monocytogenes* can be classified into at least 13 subspecies, depending on cell surface antigenic determinants. Serotype 1/2a and serotype 4b strains are mainly responsible for food contamination and clinical infection, respectively (Aarnisalo et al., 2003; Hasebe et al., 2017; Y. Huang et al., 2018; Pontello et al., 2012).

Bacteriophages are natural predators of bacteria, which can only produce next-generation phages by infecting the appropriate host (R. Carlton et al., 2005; Tracey Lee Peters et al., 2020). Lytic phages that target foodborne pathogens offer a safe and efficient way to protect food from contamination because of their high specificity and self-replication ability (Jurczak-Kurek et al., 2016). Compared with antibiotics, another advantage of phages is the ability to evolve when phage-resistant mutants appear, leading to the co-evolution of bacteria and phages (Lopes-Luz et al., 2021; Safari et al., 2020). Wild phages isolated from the natural environment directly are the primary source of phages for phage-based applications. Co-evolution provides another way to isolate

phages that are able to overcome potential resistant mutants. In the process of co-evolution, host strains with mutations conferring phage resistance will be selected by the pressure of phages, and phages that are able to overcome the bacterial defense system will survive, leading to a diversity of both bacteria and phages (Koskella & Brockhurst, 2014; Safari et al., 2020).

In previous research in our lab, a 60 hour co-evolution experiment was conducted between *L. monocytogenes* 10403S and a number of *Pecentumvirus* phages. Most of the bacterial survivors isolated from this co-evolution experiment were unsusceptible to phage infection; Mutant phages with expanded host ranges were isolated, and recombination between two different phages infecting the same culture was confirmed to occur by genome sequencing and analysis (Tracey Lee Peters et al., 2020). The aims of this study are i) observe the dynamics of *Listeria*-phage co-evolution over 10 days and 10 passages; ii) recover phage lysates and isolate mutants of *L. monocytogenes* 10403S (model strain of serotype 1/2a) and *L. monocytogenes* H7858 (model strain of serotype 4b) from the co-evolution experiment; iii) identify the genes that are responsible for conferring phage resistance by genomic analysis.

4.3 Materials and Methods

4.3.1 Bacterial strains.

All the strains used in this experiment are shown in Table 4.1. *L. monocytogenes* MACK is a serotype 1/2a standard strain used for enumeration and propagation of *Listeria* phages A511, LP-048, and LP-Mix_6.2. *L. monocytogenes* F2365 is a serotype 4b standard strain used for enumeration and propagation of *Listeria* phages LP-020 and

Table 4.1 *Listeria monocytogenes* strains

Listeria monocytogenes strains	Lineage	Serotype	Reference or original
MACK	II	1/2a	(Hodgson, 2000)
10403S	II	1/2a	(Bishop & Hinrichs, 1987)
F2365	I	4b	(Nelson et al., 2004)
H7858	I	4b	(Nelson et al., 2004)
R9-0915	II	7	(Denes et al., 2015; Tracey Lee Peters et al., 2021)
FSL J1-175	I	1/2b	(Bergholz et al., 2010)
FSL J1-208	IV	4a	(A. Roberts et al., 2006)
FSL C1-115	II	3a	(Fugett et al., 2006)
FSL J1-094	II	1/2c	(Fugett et al., 2006)
FSL F2-695	IIIA	4a	(A. Roberts et al., 2006)
FSL D4-0014	II	1/2a	(Denes et al., 2015)
FSL D4-0119	II	3	(Denes et al., 2015)

LP-053. *L. monocytogenes* 10403S was the experimental strain representative of serotype 1/2a *L. monocytogenes. L. monocytogenes* H7858 was the experimental strain representative of serotype 4b *L. monocytogenes. L. monocytogenes* R9-0915 was the serotype 7 strain resistant to all the phages in this experiment which was used as the negative control. Other representative *L. monocytogenes* with different lineages and serotypes were also included in the efficiency of plaquing assays. All strains are stored in Brain Heart Infusion (BHI) media that contains 15% (vol/vol) glycerol at -80°C. BHI plates with 1.5% (wt/vol) agar were used for streak plates and were incubated at 37°C overnight before being stored at 4°C. Overnight cultures were prepared from a single colony on a BHI agar streak plate into BHI liquid media and were grown at 25°C shaking at 160 RPM.

4.3.2 Bacteriophages

All phages used in this experiment are shown in Table 4.2. *Listeria* phages A511 and LP-048 are well studied model phages, belonging to the family *Siphovirdae*. LP-020 and LP-053 are representative P35-*like* phages that are able to infect serotype 4b *Listeria* strains. LP-Mix_6.2 is a mutant *Listeria* phage that was identified as a recombinant of LP-048 and LP-125 (Tracey Lee Peters et al., 2020). Phage enumeration was carried out by the double-layer method. Briefly, diluted phages and the overnight culture of its propagation strain are mixed in molten top agar, and the mixture is poured onto a plate of LB-MOPS agar. Phages with suitable dilutions are able to form countable plaques after incubation. Depending on the amount of plaques, the dilutions of phages and the volume of phages mixed into the agar, the titer of the phage samples can be calculated. Lysogeny

Table 4.2 *Listeria monocytogenes* phages

***Listeria monocytogenes* phages**	**Description**	**Reference or original**
A511		(Klumpp et al., 2008; Loessner & Busse, 1990)
LP-048	P100-like phage	(T. Denes et al., 2014; Vongkamjan et al., 2012)
LP-Mix_6.2	Recombinant	(Tracey Lee Peters et al., 2020)
LP-020	P35-like phage	(Song, Peters, Bryan, Hudson, & Denes, 2021; Vongkamjan et al., 2012)
LP-053	P35-like phage	(Song et al., 2021; Vongkamjan et al., 2012)

broth morpholino-propane sulfonic acid (LB-MOPS) agar with 0.1% (wt/vol) glucose, 1mM $CaCl_2$, and $MgCl_2$ and 1.5% (wt/vol) agar was used as nutrient agar, and LB-MOPS with 0.1% (wt/vol) glucose, 10mM $CaCl_2$, and $MgCl_2$ and 0.7% (wt/vol) agar was used as top agar. The LB-MOPS plates were incubated at 25°C overnight for phage titering.

4.3.3 Co-evolution experiment

Three experimental groups were set up for the co-evolution experiment. Group 1, *L. monocytogenes* 10403S treated with A511, LP-048 or an even mixture of A511 and LP-048; Group 2, *L. monocytogenes* H7858 treated with A511, LP-Mix_6.2 or an even mixture of A511 and LP-Mix_6.2; Group 3, *L. monocytogenes* H7858 treated with LP-020, LP-053 or an even mixture of LP-020 and LP-053; SM buffer was added as the negative control. Each group had three biological replicates with individual bacterial colonies and plaque purified phage stocks used for each replicate. All data and sample collection was performed for each replicate.

50 μL of an overnight culture of the experimental strain was transferred into 4.95mL LB-MOPS liquid media, with 0.1% (wt/vol) glucose, 1mM $CaCl_2$ and $MgCl_2$, and was incubated in a shaking water bath at 25°C and 160 RPM. When the optical density at 600nm (OD_{600nm}) grew to ~0.1, each culture was treated with a single phage or an even mix of two phages at a total multiplicity of infection (MOI) of 0.1, SM buffer was added with the same volume as the negative control. After treatment, all samples were incubated at 25°C shaking at 160 RPM. 50 μL of each sample was transferred into fresh 4.95mL LB-MOPS liquid media every 24 hours for 10 days. The OD_{600nm} of each sample was measured before the transfer. On day 1, day 2, day 5 and day 10, the OD_{600nm} of each

sample was measured after transfer every hour for 8 hours. On day 5 and day 10, bacterial samples and phage samples were collected for further research. Modified Oxford (MOX) agar was used to identify potential contamination that occurred during the experiment. MOX agar is a selective medium for *Listeria, Listeria* colonies growing on MOX agar form a black precipitate surrounding the colonies. On day 5 and day 10, BHI plates were used for enumeration of bacteria in each sample and MOX agar was used for the enumeration of *L. monocytogenes* in each sample. By comparing the results from BHI agar and MOX agar plating, contamination could be detected.

For bacterial sample collection, each co-evolution culture was diluted and spread on BHI plates. For group 1, 33 colonies were taken from each sample and 12 of them were selected, depending on the result of the streak-spot assay (SSA). Each selected colony was streaked out on BHI plates and 5 uL working stock of LP-048 and A511 were spotted on each colony. SM buffer was used as negative control. The plates were incubated at 25°C. For group 2 and 3, 20 colonies were selected from each sample, and the phenotype of each bacterial sample was tested by spot assay in 6-well plates. Overnight cultures of each selected colony were mixed with 2mL of top agar and the mixture was poured into a well of a 6-well plate. 5 uL working stock of LP-048 and A511 were spotted on each lawn and SM buffer was used as negative control. The 6-well plates were incubated overnight at 25°C. All phage stocks used in this experiment were diluted to 1×10^8 PFU/mL as a working stock, and used for the SSA test and 6-well plate tests. Selected colonies representing a diversity of phenotypes were incubated in BHI media at

25°C shaking at 160 RPM and were stored in Brain Heart Infusion (BHI) media that contained 15% (vol/vol) glycerol at -80°C.

For phage sample collection, each sample was treated with chloroform by 1:200 after the transfer. After 15 min, 3.4 mL of each sample was transferred off the chloroform and evenly split into two 2 mL sterile centrifuge tubes and centrifuged at 5,000g, at 4°C for 10 minutes. After centrifugation, the supernatant was filtered with 0.2μm SCFA sterile filters and stored in sterile amber brown glass vials at 4°C.

4.3.4 Efficiency of plaquing assay

Based on the results of the SSA and 6-well plate assays, representative bacterial phenotypes from each sample were selected for the efficiency of plaquing (EOP) assay. *L. monocytogenes* R9-0915 was used as the negative control. The bacteria that were isolated on day 5 and day 10 from the samples treated with SM buffer were used as control. Wild type strains, including propagation strains and experimental strains were also included.

Phage lysates from the same condition with different replicates (A, B, C) were mixed 1:1:1 as a working stock. The original plaque purified stocks of the phages used for each biological replicate (A, B, C) were mixed 1:1:1 as a control. After the mixture, all working stocks were diluted to 10^{-1},10^{-2},10^{-3},$10^{-4,}$ and 10^{-5} with phosphate buffered saline (PBS) for the EOP experiment.

40 μL of overnight culture of each representative bacterial isolate was added into 4mL top agar, and the mixture was poured on LB-MOPS agar after briefly vortexing. When the top agar solidified, 5 μL of each dilution were spotted on the top agar. Then the plates were incubated at 25°C overnight. The highest dilution that phages showed activity

against the bacterial lawn was recorded as phage activity, and the titer was also recorded if the phage is able to form countable plaques on the selected bacterial lawn. Heatmaps of efficiency of plaquing (EOP) and efficiency of activity (EOA) were made in R (Kolde, 2019).

This test was performed with two biological replicates.

The results of the EOP experiment by spot assay showed that all phage mixtures are not able to form countable plaques on *L. monocytogenes* H7858, but most phage lysates can form countable plaques on the same host strain by double-layer method during the process of phage purification. To verify that the phage lysates isolated from co-evolution are unable to form countable plaques on *L. monocytogenes* H7858 due to limitations of the spot assay method, an EOP with purified phages on 6-well plates by double-layer method was performed. 5 mL LB-MOPS nutrient agar and 1mL LB-MOPS top with 10 uL of overnight culture and 40 uL of phage dilution in each well were used for tittering. The experimental strains and purified phages were selected due to the results of phage purification and the EOP experiment with purified phages (Figure S4. 1). EOA and EOP heatmaps were generated in R by using *pheatmap* (Kolde, 2019).

This test was performed with two biological replicates.

4.3.5 Temperature-dependent phage resistance test

In the EOP experiment, all phage mixtures have a lower activity on *L. monocytogenes* H7858 without forming countable plaques, compared with titers on *L. monocytogenes* F2365. The different EOP results may be due to a restriction-modification system in *L. monocytogenes* H7858 which is determined by the bacterial

growth temperature (Kim & Kathariou, 2009). To verify the influence of growth temperature and incubation temperature, wild phage A511 was selected as the experimental phage, and *L. monocytogenes* H7858 and *L. monocytogenes* F2365 were selected as experimental bacteria.

The overnight cultures were made following previously published methods (Kim & Kathariou, 2009), the overnight cultures of experimental bacteria were grown at 25°C and 37°C in BHI without shaking for different incubation times (25°C for 36 h and 37°C for 16 h). Titering by double-layer method on 6-well plates was used as the titering method, as it enables phages to form plaques on *L. monocytogenes* H7858, which provides a more accurate comparison. To be consistent with the titering method in this study, 5 mL LB-MOPS nutrient agar and 1mL LB-MOPS top were used for titering, adding 10 uL of overnight culture and 40 uL of phage dilution. In order to compare with the results of the previous research, 5 mL LB nutrient agar and 1mL LB top were used for titering, adding 80 uL of overnight culture and 40 uL of phage dilution. After titering, 25°C and 37°C were selected as incubation temperatures, testing the influence of incubation temperature on the phage titer.

This test was performed with three biological replicates.

4.3.6 Bacterial DNA extraction

All mutant bacteria that were used in the EOP experiment which represented the diversity of identified phenotypes were selected for DNA extraction, genome sequencing and analysis. As previously described, Qiagen DNA mini kits (Hilden, Germany) was used to extract the DNA of selected bacterial mutants (Song et al., 2019).

Raw reads were trimmed with Trimmomatic (v0.39) (Bolger et al., 2014) and read statistics were generated with FastQC (v0.11.9) (Andrews, 2010) and MultiQC (v1.11) (Ewels, Magnusson, Lundin, & Käller, 2016). For each strain group, the optimal kmer length was determined using KmerGenie (v1.7051) (Medvedev & Chikhi, 2013), variant calling was conducted with McCortex (v1.01.; with joint calling and using links) (I. Turner et al., 2018), and the resulting VCF files were annotated with SnpEff (v5.1) (Cingolani et al., 2012). For 10403S, the annotated reference genome was downloaded from NCBI RefSeq (GCF_000168695.2) and a kmer length of 99 was used. For H7858, the annotated reference genome was downloaded from NCBI (CP096157-CP096158) and a kmer length of 121 was used. Variants present at frequencies similar to the wild-type (<10% higher or lower) were filtered out. Missense substitutions were classified as radical or conservative based on amino acid charge and polarity (Hanada, Shiu, & Li, 2007).

4.4 Results

4.4.1 Listeria concentration is impacted by phage selection over multiple passages.

The concentration of *L. monocytogenes* was observed over the duration of coevolution experiments. *Listeria* phages and *L. monocytogenes* (serotype 1/2a and 4b) were observed by monitoring the optical density at 600nm (OD_{600nm}) of a serially passaged infection of host and phages every day for ten days.

All experimental phages impacted the *Listeria* concentration throughout 10 days of co-evolution, except for LP-053 (Figure 4. 1). All *Listeria* growth controls showed stable

Figure 4. 1 Dynamics of 10 day co-evolution experiment. The OD600nm of each sample was measured every 24 hours, before transferring the samples to fresh media. A) L. monocytogenes 10403S treated with A511, LP-048 or an even mixture of A511 and LP-048; B) L. monocytogenes H7858 treated with A511, LP-Mix_6.2 or an even mixture of A511 and LP-Mix_6.2; C) L. monocytogenes H7858 treated with LP-020, LP-053 or an even mixture of LP-020 and LP-053. Values are the mean of data from three biological replicates.

A)

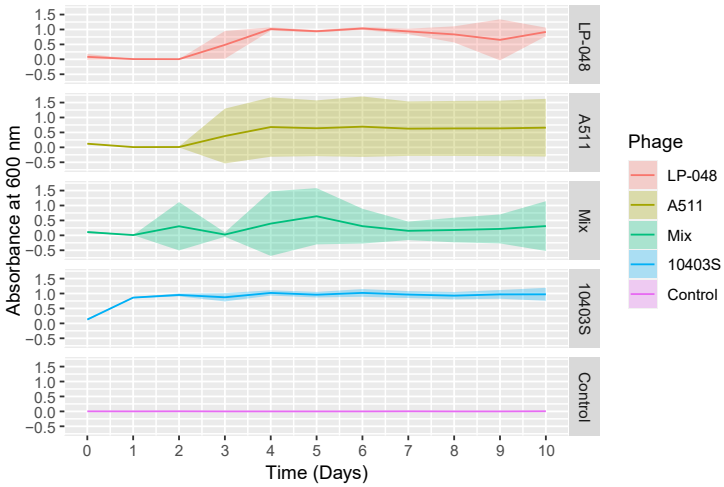
LP-048
A511
Mix
10403S
Control
Absorbance at 600 nm
Time (Days)
Phage
LP-048
A511
Mix
10403S
Control

B)

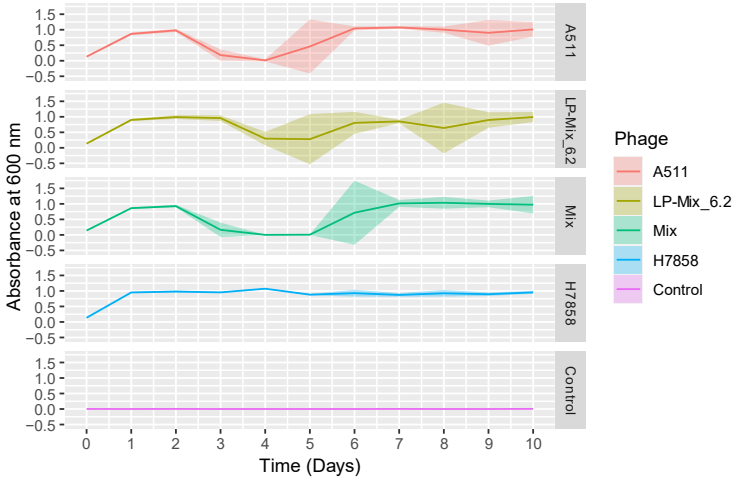
A511
LP-Mix_6.2
Mix
H7858
Control
Absorbance at 600 nm
Time (Days)
Phage
A511
LP-Mix_6.2
Mix
H7858
Control

C)

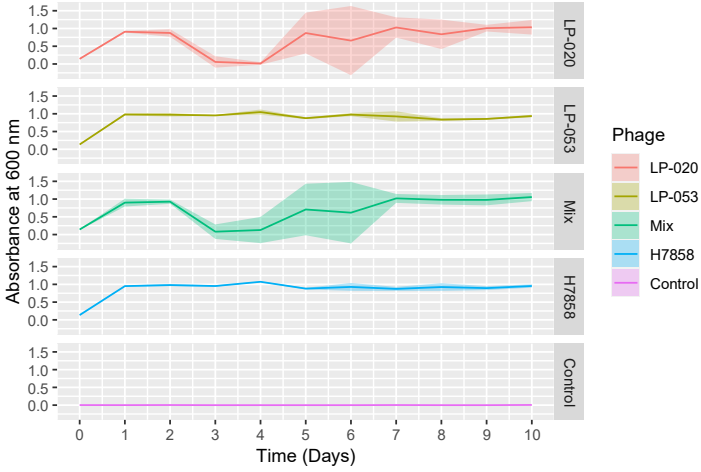
LP-020
LP-053
Mix
H7858
Control
Absorbance at 600 nm
Time (Days)
Phage
LP-020
LP-053
Mix
H7858
Control

OD_{600nm} readings of ~1.0 throughout the experiment and the uninoculated controls consistently showed OD_{600nm} readings of 0 (Figure 4. 1). The OD_{600nm} of serotype 1/2a strains was lower than 0.1 for first two days, and the re-growth of resistant mutants was observed on the third day when treated with LP-048 or A511 (Figure 4. 1A). The OD_{600nm} of serotype 4b strains experienced fluctuations over the ten days when treated with A511, LP-Mix_6.2 or LP-020 (Figure 4. 1B, Figure 4. 1C). LP-053 seems to have no influence on the growth of *L. monocytogenes* H7858, since the growth controls and LP-053 treatment shared a similar growth curve (Figure 4. 1C).

Pecentumvirus show different OD_{600nm} patterns on the serotype 1/2a and 4b strains. The OD_{600nm} of serotype 1/2a strains experienced an increase on day 2, and hold steady after reaching its peak on day 4 when treated with only LP-048 or LP-125 (Figure 4. 1A).The growth curve of serotype 1/2a strains showed a more complicated dynamic when treated a mixture of LP-048 and A511, experiencing fluctuations over the ten days (Figure 4. 1A). The growth curve of 4b strains infected with *pecentumvirus* shared a similar trend, experiencing a process of rising, holding steady, then falling again, holding steady, then rising before stabilizing again (Figure 4. 1B). The growth curves of 1/2a strains against *Pecentumvirus* shows variations after the emergence of re-growth, and the growth curves of 4b strains against *Pecentumvirus* show variations mainly between day 4 and day 7 (Figure 4. 1A, Figure 4. 1B).

Pecentumvirus and P35-like phages show different OD_{600nm} patterns on the serotype 4b strains. As LP-053 had no influence on the growth of 4b strains, LP-020 and a mixture of LP-020 and LP-053 had a similar impact on the host concentration of 4b strains, the

growth curve experienced a process of rising, holding steady, then falling, holding steady, then rising, holding steady, then rising before stabilizing again. The growth curves of 4b strains against P35-like phages show variations from day 3, which is earlier than the growth curves of 4b strains against *pecentumvirus* (Figure 4. 1B, Figure 4. 1C)

4.4.2 Phenotypic testing of mutant strains by streak-spot assay (SSA) and spot assay in 6-well plates

Bacterial survivors were isolated from each experimental condition on day 5 and day 10, and the phenotype of each mutant isolate was tested by SSA or spot assay in 6-well plates.

33 survivors derived from *L. monocytogenes* 10403S were isolated from each biological replicate (RepA, RepB and RepC) from the co-evolution with *pecentumvirus* on the fifth and tenth day. The phenotype was tested by SSA, each selected colony was streaked out on BHI plates and 5 uL of working stock from each experimental phage were spotted on each colony. On day 5, 198 of 225 isolated survivors showed resistance to LP-048 and A511, only the LP-048 treatment group had isolates which were sensitive to both phages or sensitive to just A511 in RepB or RepC (Figure 4. 2A). However on the tenth day, all isolated survivors showed resistance to LP-048 and A511 (Figure 4. 2B). No bacteria were isolated in RepB of the A511 treatment and RepC of the mixed phage treatment, indicating that no bacteria survived after the fifth day of co-evolution.

20 survivors derived from *L. monocytogenes* H7858 were isolated from each biological replication (RepA, RepB and RepC) from the co-evolution with *pecentumvirus* on the fifth and tenth day. The phenotype was tested by spot assay in 6-well plates

Figure 4. 2 Phenotypic testing of mutant strains by streak-spot assay (SSA) and spot assay in 6-well plates. A) and B) represent SSA result of L. monocytogenes 10403S treated with pecentumvirus on day 5 and day 10; C) and D) represent 6-well plates test of L. monocytogenes H7858 treated with pecentumvirus on day 5 and day 10; E) and F) represent 6-well plate tests of L. monocytogenes H7858 treated with P35-like phages on day 5 and day 10. Red color represents the mutant strains that show double negative results with experimental phages; green color represents the mutant strains that show double positive results with experimental phages; yellow and blue color represents the mutant strains which show one positive and one negative result with experimental phages.

A)

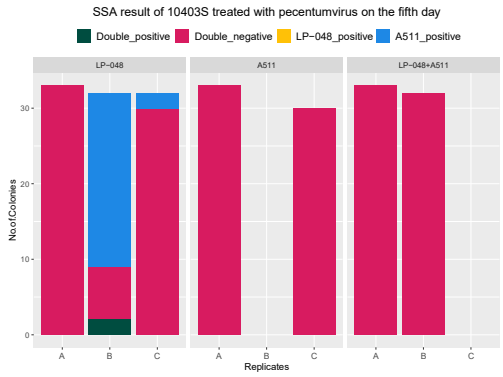
SSA result of 10403S treated with pecentumvirus on the fifth day
Double_positive
Double_negative
LP−048_positive
A511_positive
LP−048
A511
LP−048+A511
No.of Colonies
Replicates

B)

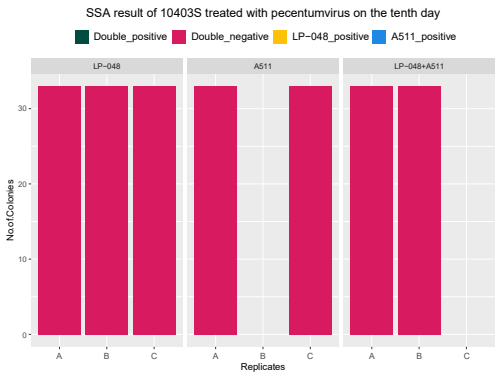
SSA result of 10403S treated with pecentumvirus on the tenth day
Double_positive
Double_negative
LP−048_positive
A511_positive
LP−048
A511
LP−048+A511
No.of Colonies
Replicates

C)

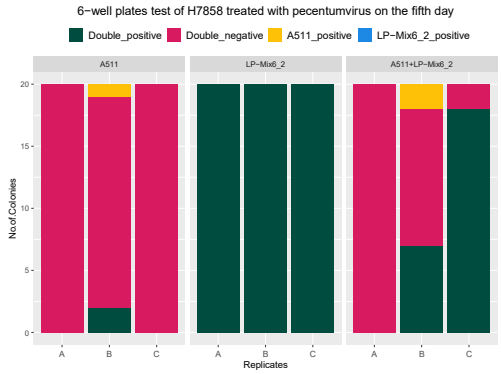
6−well plates test of H7858 treated with pecentumvirus on the fifth day
Double_positive
Double_negative
A511_positive
LP−Mix6_2_positive
A511
LP−Mix6_2
A511+LP−Mix6_2
No.of Colonies
Replicates

D)

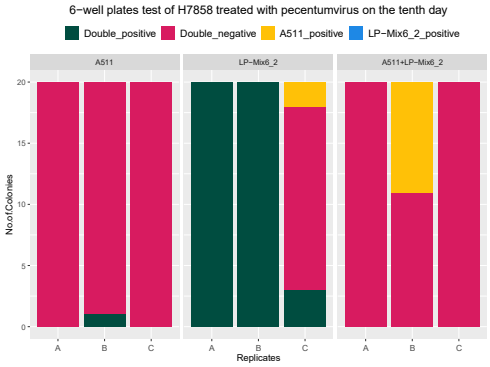
6−well plates test of H7858 treated with pecentumvirus on the tenth day
Double_positive
Double_negative
A511_positive
LP−Mix6_2_positive
A511
LP−Mix6_2
A511+LP−Mix6_2
No.of Colonies
Replicates

E)

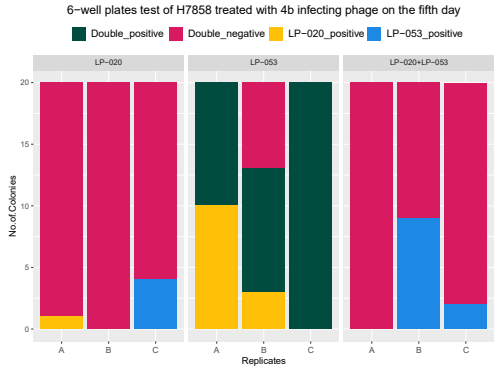
6−well plates test of H7858 treated with 4b infecting phage on the fifth day
Double_positive
Double_negative
LP−020_positive
LP−053_positive
LP−020
LP−053
LP−020+LP−053
No.of Colonies
Replicates

F)

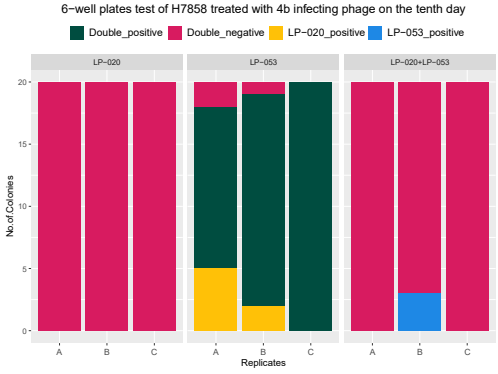
6−well plates test of H7858 treated with 4b infecting phage on the tenth day
Double_positive
Double_negative
LP−020_positive
LP−053_positive
LP−020
LP−053
LP−020+LP−053
No.of Colonies
Replicates

against both phages used in the experiment. On day 5, 57 of 60 mutants isolated from the A511 treatment showed double resistance, and only RepB had mutants which showed sensitivity to both phages or A511 sensitive phenotypes; all isolates from the LP-Mix_6.2 treatment group were sensitive to both phages; The phenotype of mutant strains isolated from the mixed phage treatment were sensitive to both phages, sensitive to A511 or resistant to both phages (Figure 4. 2C). Comparing day 5with day 10, the number of isolates sensitive to both phages decreased and the number of double resistant isolates increased under the same treatment conditions (Figure 4. 2D).

20 survivors derived from *L. monocytogenes* H7858 were isolated from each biological replication (RepA, RepB and RepC) from the co-evolution with P35-like phages on the fifth and tenth day. The phenotype was tested by spot assay in 6-well plates against both phages used in the experiment. For the LP-020 treatment group and mixed phages treatment group, most of the mutants showed resistance against both phages, and the number of double resistant isolates increased from day 5 to day 10 (Figure 4. 2E and Figure 4. 2F). Interestingly, the LP-053 treatment group is the only group that isolates sensitive to both phages increased from day 5 to day 10, maybe due to LP-053 not being able to replicate during the co-evolution process and being diluted out of the experiment over the daily transfers (Figure 4. 2E and Figure 4. 2F).

4.4.3 Efficiency of plaquing assay with phage lysates on representative mutant strains

Representative mutant strains were selected for the efficiency of plaquing experiment based on the phenotypic testing results. The crude phage lysates were

obtained from the co-evolution experiments on day 5 and day 10, and a working stock for each day was prepared by mixing each biological replicate (A, B, C) 1:1:1.

The *pecentumvirus* phage lysates obtained from the co-evolution against *L. monocytogenes* 10403S were tested against representative mutant strains by EOP assay (Figure 4. 3A, Figure 4. 3B). The lysates isolated from the mixed phage treatment on day 5 and day 10 have expanded host ranges when compared with controls and other lysates. The lysates from the A511 treatment on day 5 and day 10 only show activity and form plaques on *L. monocytogenes* MACK, the propagation host of the *pecentumvirus* used in these experiments, which is similar to the results with the uninfected control and may be due to the expression of a prophage which is in *L. monocytogenes* 10403S. 3B-01_D10 is the only strain that is resistant to all phages and lysates tested. 1B-01_D5,1B-05_D5, and 1C-04_D5 are susceptible to A511 but resist LP-048 infection, showing a rare phenotype that needs further research.

The *pecentumvirus* phage lysates obtained from the co-evolution against *L. monocytogenes* H7858 were tested against representative mutant strains by EOP assay (Figure 4. 3C, Figure 4. 3D). All phages and lysates used show either activity or plaquing on 14 of 35 mutant strains, and only show activity on most of the representative mutant strains. The lysates from the uninfected control shows activity on *L. monocytogenes* R9-0915 (Serotype 7), which may be due to the monocins from *L. monocytogenes* H7858. Based on the EOP heatmap, the lysates obtained from mixed phage treatment on day 10 have the broadest host spectrum.

Figure 4. 3 Efficiency of plaquing assay with phage lysates on representative mutant strains. Panel (A) and Panel (B) represent efficiency of activity (EOA) heatmap results and efficiency of plaquing (EOP) heatmap results with the phage lysates from the co-evolution between L. monocytogenes 10403S and pecentumvirus. Panel (C) and Panel (D) represent EOA heatmap results and EOP heatmap results with the phage lysates from the co-evolution between L. monocytogenes H7858 and pecentumvirus. Panel (E) and Panel (F) represent EOA heatmap results and EOP heatmap results with the phage lysates from the co-evolution between L. monocytogenes H7858 and P35-like phages. Experimental strains were selected based on the phenotypic testing results. Values are the mean of data from two biological replicates.

A)

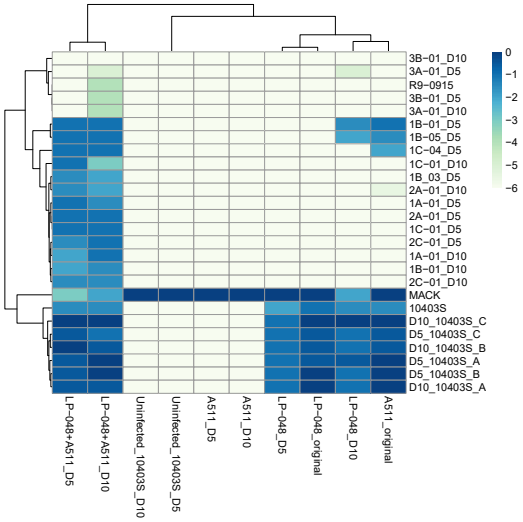
3B−01_D10
3A−01_D5
R9−0915
3B−01_D5
3A−01_D10
1B−01_D5
1B−05_D5
1C−04_D5
1C−01_D10
1B_03_D5
2A−01_D10
1A−01_D5
2A−01_D5
1C−01_D5
2C−01_D5
1A−01_D10
1B−01_D10
2C−01_D10
MACK
10403S
D10_10403S_C
D5_10403S_C
D10_10403S_B
D5_10403S_A
D5_10403S_B
D10_10403S_A
0
−1
−2
−3
−4
−5
−6
LP−048+A511_D5
LP−048+A511_D10
Uninfected_10403S_D10
Uninfected_10403S_D5
A511_D5
A511_D10
LP−048_D5
LP−048_original
LP−048_D10
A511_original

B)

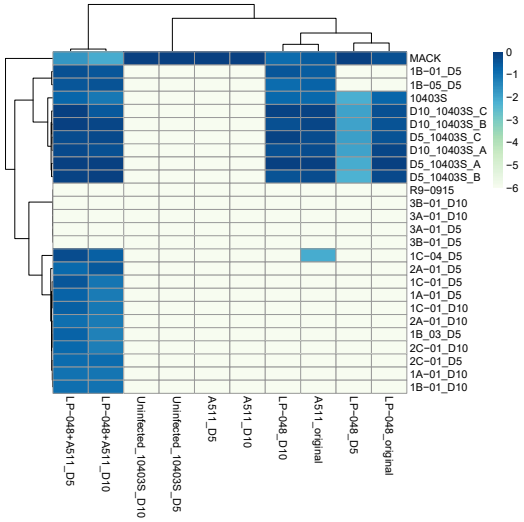
MACK
1B−01_D5
1B−05_D5
10403S
D10_10403S_C
D10_10403S_B
D5_10403S_C
D10_10403S_A
D5_10403S_A
D5_10403S_B
R9−0915
3B−01_D10
3A−01_D10
3A−01_D5
3B−01_D5
1C−04_D5
2A−01_D5
1C−01_D5
1A−01_D5
1C−01_D10
2A−01_D10
1B_03_D5
2C−01_D10
2C−01_D5
1A−01_D10
1B−01_D10
0
−1
−2
−3
−4
−5
−6
LP−048+A511_D5
LP−048+A511_D10
Uninfected_10403S_D10
Uninfected_10403S_D5
A511_D5
A511_D10
LP−048_D10
A511_original
LP−048_D5
LP−048_original

C)

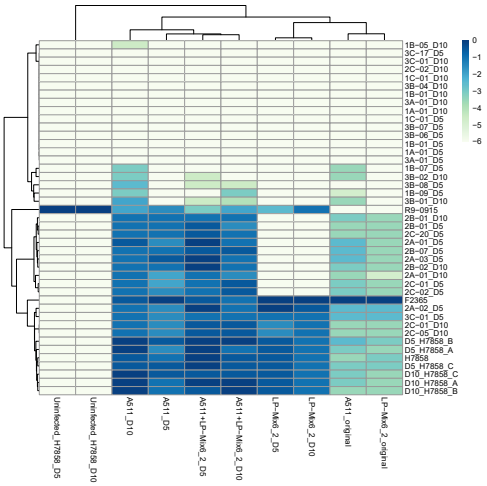
1B−05_D10
3C−17_D5
3C−01_D10
2C−02_D10
1C−01_D10
3B−04_D10
1B−01_D10
3A−01_D10
1A−01_D10
1C−01_D5
3B−07_D5
3B−06_D5
1B−01_D5
1A−01_D5
3A−01_D5
1B−07_D5
3B−02_D10
3B−08_D5
1B−09_D5
3B−01_D10
R9−0915
2B−01_D10
2B−01_D5
2C−20_D5
2A−01_D5
2B−07_D5
2A−03_D5
2B−02_D10
2A−01_D10
2C−01_D5
2C−02_D5
F2365
2A−02_D5
3C−01_D5
2C−01_D10
2C−05_D10
D5_H7858_B
D5_H7858_A
H7858
D5_H7858_C
D10_H7858_C
D10_H7858_A
D10_H7858_B
0
−1
−2
−3
−4
−5
−6
Uninfected_H7858_D5
Uninfected_H7858_D10
A511_D10
A511_D5
A511+LP−Mix6_2_D5
A511+LP−Mix6_2_D10
LP−Mix6_2_D5
LP−Mix6_2_D10
A511_original
LP−Mix6_2_original

D)

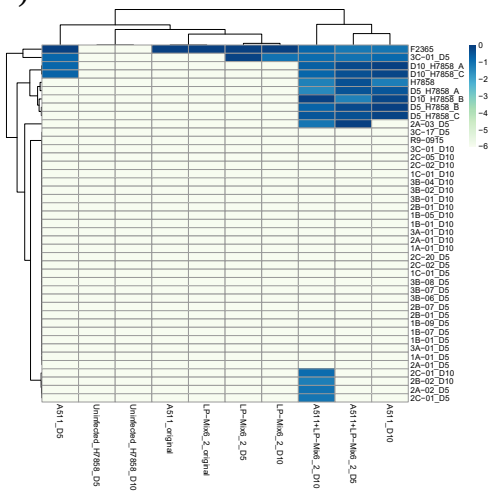
F2365
3C−01_D5
D10_H7858_A
D10_H7858_C
H7858
D5_H7858_A
D10_H7858_B
D5_H7858_B
D5_H7858_C
2A−03_D5
3C−17_D5
R9−0915
3C−01_D10
2C−05_D10
2C−02_D10
1C−01_D10
3B−04_D10
3B−02_D10
3B−01_D10
2B−01_D10
1B−05_D10
1B−01_D10
3A−01_D10
2A−01_D10
1A−01_D10
2C−20_D5
2C−02_D5
1C−01_D5
3B−09_D5
3B−06_D5
2B−07_D5
2B−01_D5
1B−09_D5
1B−07_D5
1B−01_D5
3A−01_D5
1A−01_D5
2A−01_D5
2C−01_D10
2B−02_D10
2A−02_D5
2C−01_D5
0
−1
−2
−3
−4
−5
−6
A511_D5
Uninfected_H7858_D5
Uninfected_H7858_D10
A511_original
LP−Mix6_2_D5
LP−Mix6_2_original
LP−Mix6_2_D10
A511+LP−Mix6_2_D10
A511+LP−Mix6_2_D5
A511_D10

E)

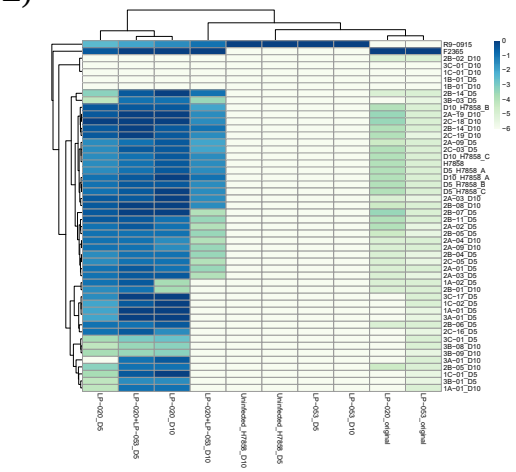
R9−0915
F2365
2B−02_D10
3C−01_D10
1C−01_D10
1B−01_D5
1B−01_D10
2B−14_D5
3B−03_D5
D10_H7858_B
2A−19_D10
2C−15_D10
2B−14_D10
2C−19_D10
2A−09_D5
2C−03_D5
D10_H7858_C
H7858
D5_H7858_A
D10_H7858_A
D5_H7858_B
D5_H7858_C
2A−03_D10
2B−08_D10
2B−07_D5
2B−11_D5
2A−02_D5
2B−05_D5
2A−04_D10
2A−09_D10
2B−04_D5
2C−05_D5
2A−01_D5
2A−03_D5
1A−02_D5
2B−01_D10
3C−17_D5
1C−02_D5
1A−01_D5
3A−01_D5
2B−06_D5
2C−16_D5
3C−01_D5
3B−08_D10
3B−09_D10
3A−01_D10
2B−05_D10
1C−01_D5
1B−01_D5
1A−01_D10
0
−1
−2
−3
−4
−5
−6
LP−020_D5
LP−020+LP−053_D5
LP−020_D10
LP−020+LP−053_D10
Uninfected_H7858_D10
Uninfected_H7858_D5
LP−053_D5
LP−053_D10
LP−020_original
LP−053_original

F)

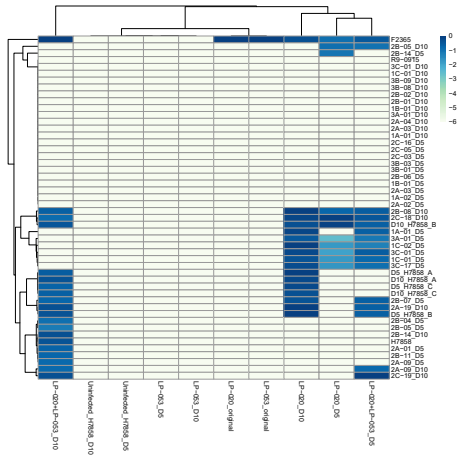
F2365
2B−05_D10
2B−14_D5
R9−0915
3C−01_D10
1C−01_D10
3B−09_D10
3B−08_D10
2B−02_D10
2B−01_D10
1B−01_D10
3A−01_D10
2A−04_D10
2A−02_D10
1A−01_D10
2C−16_D5
2C−05_D5
2C−03_D5
3B−03_D5
3B−01_D5
2B−06_D5
1B−01_D5
2A−03_D5
1A−02_D5
2A−02_D5
2B−08_D10
2C−18_D10
D10_H7858_B
1A−01_D5
3A−01_D5
1C−02_D5
3C−01_D5
1C−01_D5
3C−17_D5
D5_H7858_A
D10_H7858_A
D5_H7858_C
D10_H7858_C
2B−07_D5
2A−19_D10
D5_H7858_B
2B−04_D5
2B−05_D5
2B−14_D10
H7858
2A−11_D5
2B−11_D5
2A−06_D5
2A−09_D10
2C−19_D10
0
−1
−2
−3
−4
−5
−6
LP−020+LP−053_D10
Uninfected_H7858_D10
Uninfected_H7858_D5
LP−053_D5
LP−053_D10
LP−020_original
LP−053_original
LP−020_D10
LP−020_D5
LP−020+LP−053_D5

The P35-like phage lysates obtained from the co-evolution against *L. monocytogenes* H7858 were tested against representative mutant strains by EOP assay (Figure 4. 3E, Figure 4. 3F). LP-020 and LP-053 are able to show activity on most mutant strains but were not able to form countable plaques. The lysates isolated from the LP-020 treatment and mixed phages treatment showed higher activity in the EOA heatmap and had a broader host range in the EOP heatmap. The lysates obtained from the mixed phage treatment on day 10 showed the broadest host range. The lysates from the LP-053 treatment group only showed activity on R9-0915, likely due to the monocin from *L. monocytogenes* H7858, indicating LP-053 was not able to survive during the co-evolution process.

The isolated phage lysates and purified mutant phages from group 2 and group 3 are not able to form plaques on *L. monocytogenes* H7858 in the EOP experiment by spot assay. Interestingly, in the process of phage purification by *L. monocytogenes* H7858, 24 out of 36 phage lysates are able to form plaques on *L. monocytogenes* H7858 by double-layer method. To verify that the phages isolated from co-evolution are unable to form countable plaques on *L. monocytogenes* H7858 due to the limitation of the spot assay method, the EOP experiment with purified phages by double-layer method was performed on 6-well plates.

Fourteen purified phages were isolated from the crude phage lysates of *pecentumvirus* against *L. monocytogenes* H7858. All purified phages were used for the EOP experiment, the wild-type phages A511 and LP-Mix_6.2 were used as controls. *L. monocytogenes* F2365, *L. monocytogenes* H7858, FSL J1-208 and FSL F2-695 were

selected as experimental strains, as most of the purified phages show activity on these strains (Figure S4. 1A). The EOP heatmap is shown in Figure 4. 4A. All experimental phages are able to form countable plaques on *L. monocytogenes* H7858. Comparing the results of the EOP experiment with the purified phages by spot assay, the experimental phages share the same host range with the EOP heatmap for *L. monocytogenes* F2365, FSL J1-208 and FSL F2-695, but have the same host range as the EOA heatmap on *L. monocytogenes* H7858 by double-layer method with 6-well plates.

Ten purified phages were isolated from phage lysates of P35-like phages against *L. monocytogenes* H7858. All purified phages were used for the EOP, LP-020 and LP-053 were used as controls. Based on the results of the EOP with purified phages, *L. monocytogenes* F2365, *L. monocytogenes* H7858, FSL J1-175 and FSL F2-695 were selected as experimental strains, as most of purified phages show activity on these strains (Figure S4. 1C). The EOP heatmap is shown in Figure 4. 4B. All experimental phages are able to form countable plaques on *L. monocytogenes* H7858. Comparing the results of the EOP experiment using purified phages by spot assay with the results by double layer method in 6-well plates, the experimental phages share the same host range with the EOP heatmap results for *L. monocytogenes* F2365 and FSL F2-695 and have the same host range as the EOA heatmap for FSL J1-175. Interestingly, some experimental phages show no activity on *L. monocytogenes* H7858 in the EOA heatmap, but all experimental phages can form plaques on *L. monocytogenes* H7858 by double-layer method in 6-well plates.

A)

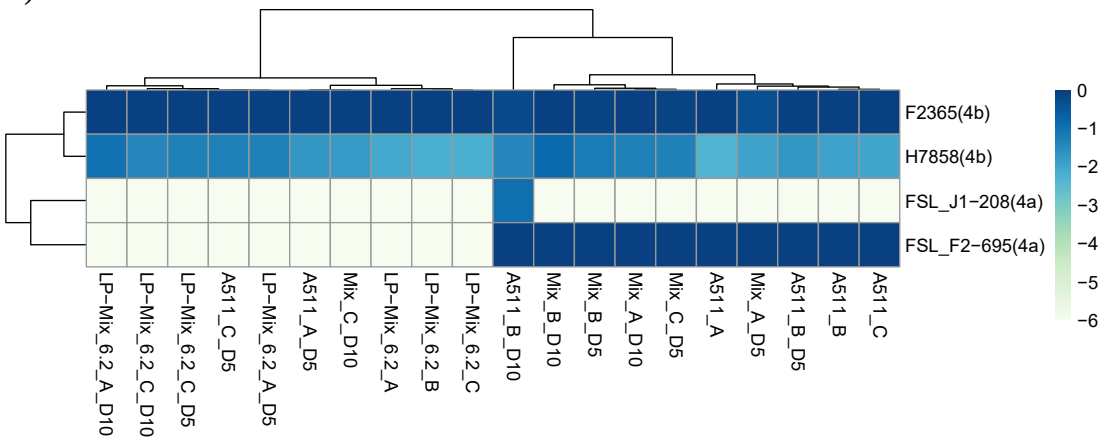

B)

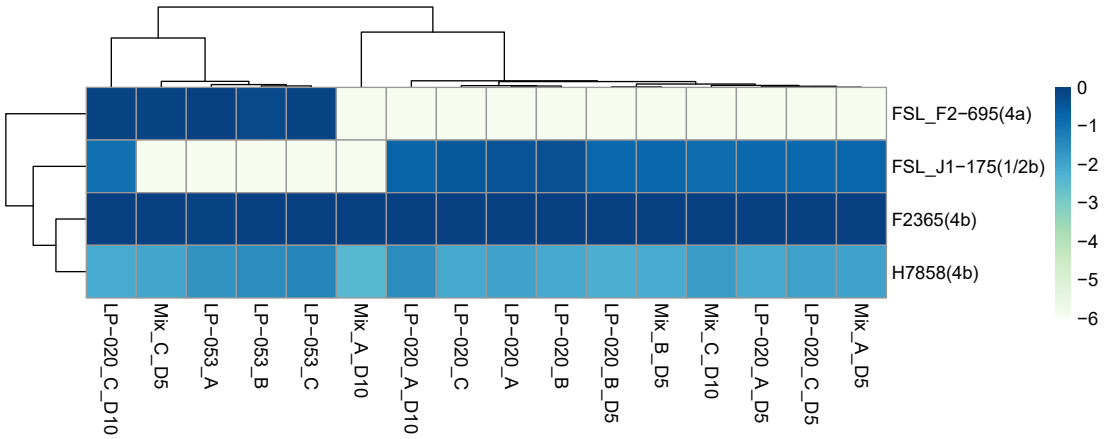

Figure 4. 4 The Efficiency of plaquing assay with purified phages on 6-well plates by double-layer method. Panel (A) represents the efficiency of plaquing (EOP) results of the purified pecentumvirus from the co-evolution against L. monocytogenes H7858,; Panel (B) represents the EOP results of the purified P35-like phages from the co-evolution against L. monocytogenes H7858. Values are the mean of data from two biological replicates.

4.4.4 Temperature-dependent phage resistance test

The test showed that growth and plating media had no significant influence on the A511 titer (Table 4.3). *L. monocytogenes* H7858 shows resistance to A511 when grown at 25°C (Table 4.3), which is consistent with the research on restriction-modification systems (Kim & Kathariou, 2009). A511 is not able to form plaques on *L. monocytogenes* F2365 and *L. monocytogenes* H7858 when incubated at 37°C (Table 4.3), which is consistent with temperature influence on A511 plaquing research (Tokman et al., 2016). A511 can only form plaques on *L. monocytogenes* H7858 with host stains grown at 37°C and infected at 25°C, but still have a ~2-log lower titer compared with the titer of A511 on *L. monocytogenes* F2365 (Table 4.3).

4.4.5 Genome sequencing and analysis of representative mutant strains

All mutant strains and control strains that were used in the EOP assay were selected for DNA extraction, genome sequencing, and analysis, including 17 survivor strains from group 1, 34 survivor strains from group 2, 41 survivor strains from group 3, 12 control strains from the untreated group, and 2 wild type strains.

In group 1, 16 selected survivor strains derived from *L. monocytogenes* 10403S resisted its original treated phage. Compared with control strains, 9 mutations were detected which were not found in the untreated group. For the single phage treatment group, all selected survivor strains have a single mutation. However, for the mixed phage treatment group, all selected survivor strains have at least three mutations.Mutations in LMRG_00542 (lmo1080) or LMRG_00545 (lmo1083) were identified in phage-resistant *L. monocytogenes* 10403S selected by LP-048. Mutations in LMRG_00543 (lmo1081)

Table 4.3 Temperature-dependent phage resistance test

Strain	EOP with host strains grown at[a] :							
	37℃				25℃			
	Infection at 37 ℃		Infection at 25 ℃		Infection at 37 ℃		Infection at 25 ℃	
	LB agar	LB-MOPS	LB agar	LB-MOPS	LB agar	LB-MOPS	LB agar	LB-MOPS
F2365	NA[b]	NA	1	1	NA	NA	1	1
H7858	NA	NA	0.082±0.021	0.014±0.003	NA	NA	NA	NA

[a] EOP values represent the relative value of the average titer compared with the highest average titer under the same experimental conditions.

[b] NA, No activity was observed

were identified in phage-resistant *L. monocytogenes* 10403S selected by A511. When selected by the mixture of LP-048 and A511, although multiple mutations were found, all mutant strains have at least one mutation in LMRG_00542 (lmo1080). Overall, mutations of *L. monocytogenes* 10403S in group 1 were mostly detected in LMRG_00541 (lmo1079), LMRG_00542 (lmo1080), LMRG_00543 (lmo1081), and LMRG_00545 (lmo1083), leading to resistance to LP-048 or A511, which is consistent with previous research (Table 4.4) (T. Denes et al., 2014). LMRG_00541 (lmo1079) encodes a membrane protein YfhO, which is involved in wall teichoic acid (WTA) glycosylation (Denes et al., 2015; Rismondo, Percy, & Gründling, 2018). The deletion of *yfhO* generated a mutant strain that lacks N-Acetylglucosamine (GlcNAc) in its WTA, suggesting YfhO is an essential protein for the modification of WTA with GlcNAc (Eugster et al., 2015). Three frameshift (FS) mutations are detected in *yfhO*, all from samples isolated from the mixed LP-048 and A511 infection (Table 4.4). LMRG_00543 (lmo1081) and LMRG_00545 (lmo1083) encode glucose-1-phosphate thymidylyltransferase and dTDP-glucose 4,6-dehydratase respectively, which are proteins associated with rhamnose biosynthesis (Denes et al., 2015). As the gene products involved in the dTDP-L-Rhamnose biosynthetic pathway, LMRG_00543 (lmo1081) was named as *rmlA* and LMRG_00545 (lmo1083) was named as *rmlB*, depending on the pathway order (Eugster et al., 2015). Three mutations were detected in *rmlA* and all mutations were selected by A511, including two FS mutations and one nonsense (NS) mutation. Four mutations were detected in *rmlB* and all mutations were selected by LP-048, including two radical missense (RMS) mutations and two NS mutations.

Table 4.4 Mutations detected in phage-resistant mutants from the co-evolution of *L. monocytogenes* 10403S and *pecentumvirus*

Gene[a]	EGD-e homolog	Gene product	No. of unique mutations[b]								
			Total	mutation type[c]				Selected by:			
				FS	RMS	CMS	NS	O	LP-048	A511	Mixed
LMRG_00541	lmo1079	YfhO family prot.	3				3				3
LMRG_00542	lmo1080	glycosyltransferase family 2 prot	8	3	1	2	2		5		3
LMRG_00543	lmo1081	glucose-1-phosphate thymidylyltransferase RfbA	3	2			1			3	
LMRG_00545	lmo1083	dTDP-glucose 4,6-dehydratase	4		2		2		4		
LMRG_00890	lmo1438	penicillin-binding prot. 2	1		1						1
LMRG_01388	lmo1579	alanine dehydrogenase	1		1						1
LMRG_01762	lmo2486	DUF4097 family beta strand repeat-containing prot	1	1							1
LMRG_02583	lmo0288	cell wall metabolism sensor histidine kinase WalK	2		2						2
LMRG_02618	lmo0196	septation regulator SpoVG	1					1			1

[a] Only genes of phage-resistant mutants with high alternative allele frequency mutations are listed here.

[b] The number of mutations detected in the phage-resistant mutants are listed here.

[c] Frameshift (FS), radical missense (RMS), conservative missense (CMS), nonsense (NS), others (O).

LMRG_00542 (lmo1080) was named as *rmlT*, due to its location upstream of *rmlA* and is required for the incorporation of L-Rhamnose. Eight mutations were detected in *rmlT*, including five mutations selected by LP-048 and three selected by the mixture of LP-048 and A511, with multiple mutation types (Table 4.5). Mutations in *rmlT*,*rmlA* and *rmlB* resulted in the loss of rhamnose in WTA (Carvalho et al., 2015; Eugster et al., 2015). For example, FSL D4-0114 is a mutant strain that resists the infection of phages by lacking rhamnose in its WTA, due to a nonsense mutation in *rmlT* (Song et al., 2021; Trudelle et al., 2019). Additionally, mutations were also detected in LMRG_01762 (lmo2486) and LMRG_02583 (lmo0288) in the co-evolution experiment between *L. monocytogenes* 10403S and recombinant phage (LP-Mix_6.1 or LP-Mix_6.2) (Tracey Lee Peters et al., 2020). LMRG_01762 (lmo2486) encodes a DUF4097 family beta strand repeat-containing protein, which is identified as a phage shock protein C (PspC) domain-containing protein (Tracey Lee Peters et al., 2020). LMRG_02583 (lmo0288) encodes cell wall metabolism sensor histidine kinase (WalK), which is associated with cell wall metabolism (Watanabe et al., 2012). Interestingly, mutations in LMRG_01762 (lmo2486) and LMRG_02583 (lmo0288) were selected by recombinant phage in previous research and were isolated from the mixed LP-048 and A511 infection in this study, suggesting these mutations may be involved in the resistance to the evolved phages.

In group 2, 18 selected survivor strains derived from *L. monocytogenes* H7858 resist their original treated phage. Compared with control strains, 15 mutations were detected which were not found in the untreated group. Only 6 resistant mutants have a single

Table 4.5 Mutations detected in phage-resistant mutants from the co-evolution of *L. monocytogenes* H7858 and *pecentumvirus*

Gene[a]	Gene product	No. of unique mutations[b]									
		Total	mutation type[c]						Selected by:		
			SS	FS	RMS	CMS	NS	O	A511	LP-Mix_6.2	Mixed
MZN50_01005	ribonuclease J	1	1							1	
MZN50_02735	helix-turn-helix domain-containing prot.	1			1						1
MZN50_02795	UTP--glucose-1-phosphate uridylyltransferase GalU	11			8	2	1		4	1	6
MZN50_02810	glycosyltransferase family 39 prot.	2					2		2		
MZN50_03025	transketolase	2			2						2
MZN50_03525	glycosyltransferase family 39 prot.	1	1								1
MZN50_06720 (rlmH)	23S rRNA (pseudouridine(1915)-N(3))-methyltransferase RlmH	2				2					2
MZN50_08855	DUF6020 family prot.	2		2					2		
MZN50_09730	GW domain-containing glycosaminoglycan-binding prot.	1			1						1
MZN50_10345	phospho-sugar mutase	3			2	1					3
MZN50_12245	ABC transporter permease subunit	1			1				1		
MZN50_12295	ABC transporter permease	1		1							1
MZN50_13560	kinase/pyrophosphorylase	2				2					2
MZN50_14690	methionine adenosyltransferase	1	1						1		
intergenic region (4989 nt upstream of MZN50_07210)	polysaccharide biosynthesis prot.	1						1		1	

[a] Only genes of phage-resistant mutants with high alternative allele frequency mutations are listed here.

[b] The number of mutations detected in the phage-resistant mutants are listed here.

[c] Synonymous substitution (SS),frameshift (FS), radical missense (RMS), conservative missense (CMS), nonsense (NS), others (O).

mutation, and the other 12 resistant mutants have more than one mutation. Six phage-resistant mutants were derived from *L. monocytogenes* H7858 selected by A511. Two resistant mutants have one mutation in MZN50_02810 and one mutation in MZN50_08855, and the other four resistant mutants have at least one mutation in MZN50_02795 (*galU*). Only one resistant mutant was selected by LP-Mix_6.2, detecting three mutations in MZN50_02735, MZN50_02795 (*galU*), and MZN50_06720 (*rlmH*). Treated with the mixture of A511 and LP-Mix_6.2, eight resistant mutants have a mutation in *galU*, regardless of single mutation strains or multiple mutation strains; What's more, there are two resistant mutants which have a single mutation detected in MZN50_12295 (*anrAB*) and MZN50_10345 (lmo2475) respectively. Overall, mutations of *L. monocytogenes* H7858 in group 2 were mostly found in *galU* (Table 4.5). *galU* encodes UTP--glucose-1-phosphate uridylyltransferase (GalU), which is is essential to WTA galactosylation (Kuenemann, Spears, Orndorff, & Fourches, 2018). WTA galactosylation is required for phage binding, and mutations in *galU* contributed to resistance to the reference phage in previous research (Spears et al., 2016). Additionally, *galU* is also believed to be involved in the virulence of *Listeria*, as the attenuation of pathogenicity was observed by the inhibition of *galU* (Kuenemann et al., 2018). Eleven mutations were detected in *galU*, including eight RMS mutations, two conservative missense (CMS) mutations and one NS mutation (Table 4.5). Interestingly, the mutations in *galU* were only detected in the phage-resistant mutants selected by *pecentumvirus*, and not from P35-like phage infections (Table 4.5, Table 4.6). Besides *galU*, a single mutation was also detected in MZN50_12295 (*anrAB*) and MZN50_10345 (lmo2475) in

Table 4.6 Mutations detected in phage-resistant mutants from the co-evolution of *L. monocytogenes* H7858 and P35-like phages

Gene[a]	Gene product	No. of unique mutations[b]								
		Total	mutation type[c]						Selected by:		
			SS	FS	RMS	CMS	NS	O	LP-020	LP-053	Mixed
MZN50_00620	alpha/beta hydrolase	2				2			2		
MZN50_01430 (gcvPB)	aminomethyl-transferring glycine dehydrogenase subunit GcvPB	2			2						2
MZN50_03185	NAD(P)/FAD-dependent oxidoreductase	3	3						3		
MZN50_04245	amino acid permease	2				2					2
MZN50_08845 (pbpD1)	D-alanyl-D-alanine carboxypeptidase PBPD1	2					2				2
MZN50_08850	glycosyltransferase	4				1	3				4
MZN50_08850; MZN50_00005 (lap)	glycosyltransferase & adhesion-mediating acetaldehyde/alcohol dehydrogenase l	2						2			2
MZN50_08855	DUF6020 family prot.	6		5			1		4		2
MZN50_12600	CAP domain-containing prot.	1				1			1		
MZN50_13895	LPXTG cell wall anchor domain-containing prot.	1	1						1		
MZN50_14085 (purD)	phosphoribosylamine--glycine ligase	1	1								1
MZN50_14680 (lapB)	surface-anchored adhesin LapB	1	1								1
intergenic region (3182 nt upstream of MZN50_07145 [lysS])	lysine--tRNA ligase	1						1	1		
intergenic region (3450 nt upstream of MZN50_06920)	alpha-glucosidase	1						1	1		
intergenic region (4112 nt upstream of MZN50_13660)	MATE family efflux transporter	1						1			1
intergenic region (4564 nt upstream of MZN50_02770)	CDP-glycerol glycerophosphotransferase family prot.	2						2	2		

[a] Only genes of phage-resistant mutants with high alternative allele frequency mutations are listed here.

[b] The number of mutations detected in the phage-resistant mutants are listed here.

[c] Synonymous substitution (SS), frameshift (FS), radical missense (RMS), conservative missense (CMS), nonsense (NS), others (O).

phage resistant mutants, which may be involved in phage resistance mechanisms. MZN50_10345 (lmo2475) encodes phospho-sugar mutase, which is an essential enzyme in glycolysis and gluconeogenesis (Levin, Almo, & Satir, 1999). MZN50_12295 (*anrAB*) encodes ATP-binding cassette (ABC) transporter permease (AnrAB) which is a membrane protein (PM Jones & George, 2004).

In group 3, 13 selected survivor strains derived from *L. monocytogenes* H7858 resist its original treated phage. Compared with control strains, 16 mutations were detected which were not found in the untreated group. Most of the resistant mutants have more than one mutation and only two strains have a single mutation. Six phage-resistant mutants were derived from *L. monocytogenes* H7858 selected by LP-020. Four resistant mutants share a mutation in MZN50_08855, and the other two strains share a mutation in the intergenic region (4564 nt upstream of MZN50_02770). No survivor strains resist LP-053, as LP-053 were not able to survive in the co-evolution experiment. Treated with the mixture of LP-020 and LP-053, four resistant mutants share a mutation in MZN50_08850, and one resistant mutant has one mutation in MZN50_04245 (lmo0798) and one mutation in the intergenic region (4112 nt upstream of MZN50_13660). Overall, mutations of *L. monocytogenes* H7858 in group 3 were mostly found in MZN50_08850 and MZN50_08855 (Table 4.6). MZN50_08850 encodes glycosyltransferase and four unique mutations in MZN50_08850 were detected. All mutations in MZN50_08850 were selected by the mixture of LP-020 and LP-053, including one CMS mutation and three NS mutations. MZN50_08855 encodes DUF6020 family protein with unknown function. Six mutations were detected in MZN50_08855, including five FS mutations and one NS

mutation. The mutations in MZN50_08855 were also detected in the phage-resistant mutants selected by *pecentumvirus*. Besides MZN50_08850 and MZN50_08855, a single mutation was also detected in intergenic region (4564 nt upstream of MZN50_02770), MZN50_03185 (lmo1000) and MZN50_14680 (*lapB*) in phage resistant mutants, which may be involved in phage resistance mechanisms. The intergenic region (4564 nt upstream of MZN50_02770) encodes CDP-glycerol glycerophosphotransferase family protein, which is involved in the synthesis of WTA (Pooley, Abellan, & Karamata, 1992). MZN50_03185 (lmo1000) encodes NAD(P)/FAD-dependent oxidoreductase, which is widely involved in the metabolism in the prokaryotes and eukaryotes (Trisolini et al., 2019; Vidal, Kelly, Mordaka, & Heap, 2018). *lapB* encodes surface-anchored adhesin LapB, which only exists in pathogenic *Listeria* species and is required for entry into cells by interacting with a cellular receptor (Reis et al., 2010).

4.5 Discussion

In this study, we conducted a 10 day co-evolution experiment between *L. monocytogenes* and *Listeria* phages, including *L. monocytogenes* 10403S infected with *pecentumvirus*, *L. monocytogenes* H7858 infected with *pecentumvirus*, and *L. monocytogenes* H7858 infected with P35-like phages. We found that i) a diversity of *Listeria* phage lysates and phage-resistant bacterial mutants could be observed under the pressure of co-evolution; ii) the co-evolution arms race may lead to the complete demise of bacteria or phages; iii) the mutant phages obtained from co-evolution can form plaques on *L. monocytogenes* H7858 with restrictions; iv) identification of mutations in phage-resistant mutants that are likely involved in conferring phage resistance; v) mutations in

different genes were identified in phage-resistant *L. monocytogenes* 10403S and *L. monocytogenes* H7858 selected by A511.

4.5.1 A diversity of Listeria phage lysates and phage-resistant bacterial mutants could be observed under the pressure of co-evolution.

The phenotypic testing results showed that most of the mutant strains were unsusceptible to phage infection after co-evolution, which is consistent with previous research (Tracey Lee Peters et al., 2020). However, the phage lysates achieved the ability to overcome some of the resistant mutants after co-evolution. The emergence of phage resistant mutants is one of the most important problems that needs to be solved for the successful application of phage biocontrol in the food production environment (B. K. Chan et al., 2013). Through co-evolution, the resistant strains that may appear can be isolated, and the possible resistance mechanism could be identified (Koskella & Brockhurst, 2014). The phage lysates, especially the lysates from mixed phage treatment groups, that are able to infect a portion of the resistant mutants were also isolated (Koskella & Brockhurst, 2014). If a cocktail that contains phages able to overcome all possible resistance mechanisms were used for biocontrol in the food industry, the re-growth of pathogens and the resultant food contamination could be efficiently avoided (Buckling & Brockhurst, 2012; Oechslin, 2018). The phage lysates with expanded host ranges could be a good source for such a cocktail. Instead of isolating wild type phages from the environment, a co-evolution based approach offers a more targeted method to generate phages capable of infecting specific phage-resistant mutants isolated from the

food production environment. The phages with specific host ranges of interest should be purified from lysates for further research.

4.5.2 The co-evolution arm race may lead to the complete demise of bacteria or phages.

According to the growth curve of each co-evolution group, no re-growth was observed in the RepB of *L. monocytogenes* 10403S treated with A511, and the RepC of *L. monocytogenes* 10403S treated with LP-048 and A511. In addition, no survivors were recovered from these two samples on day 5 and day 10 (Figure 4. 2A). Therefore, all *L. monocytogenes* in these two samples were reduced below the limit of detection in five days by the phage. The growth curve of *L. monocytogenes* H7858 infected with LP-053 has no significant difference with the growth curve of uninfected *L. monocytogenes* H7858, indicating LP-053 shows no inhibitory effect on bacterial growth (Figure 4. 1C). Compared with the mutant strains that were isolated from the LP-053 treatment on day 5, there are more isolates sensitive to both phages and less double-resistant isolates on day 10, which may be due to lack of evolutionary pressure from LP-053. What's more, the lysates obtained from LP-053 treatment and the lysates obtained from the uninfected group shared the same results in the EOP experiment (Figure 4. 3E,Figure 4. 3F). Hence, we assume that LP-053 was not able to survive in the co-evolution arms race. Although the co-evolution arms race can lead to diversity of both bacteria and phages in most conditions, there is still the possibility it can lead to the complete demise of the bacteria or phages. The co-evolution arms race between the bacteria and phages results are also consistent with a stochastic model in previous research (Han & Deem, 2017). The extinction of bacteria or phages may happen under specific conditions (Han & Deem,

2017). However, bacteria could coexist with one phage, resulting in the changes of bacterial population structure (Han & Deem, 2017).

4.5.3 The mutant phages obtained from co-evolution can form plaques on L. monocytogenes H7858 with restrictions.

The result of the EOP assay with phages purified by *L. monocytogenes* H7858 shows that the ability of phages to form plaques on *L. monocytogenes* H7858 and FSL J1-175 may not be observed by spot assay but can be observed when enumerated by the double-layer plating method (Figure 4. 4,Figure S4. 1). Additionally, all the experimental phages that were purified from co-evolution are able to form plaques on *L. monocytogenes* H7858 when enumerated bv double-layer plating (Figure 4. 4,Figure S4. 1).

L. monocytogenes H7858 is classified as an epidemic clone II (EC II) strain that shows resistance to phage infection when grown at a low temperature, due to its type II restriction-modification (RM) system (Kim et al., 2012; Kim & Kathariou, 2009). According to the temperature-dependent phage resistance test, *L. monocytogenes* H7858 is resistant to infection of all experimental strains when grown at 25 °C. For the EOP experiment with purified phages, phage titering by double-layer method shows all experimental phages can form plaques on *L. monocytogenes* H7858, but phage titering by spot assay yields no plaques. Therefore, the titering method also may influence the performance of phages on *L. monocytogenes* H7858. However, purified phages still have a ~2-log reduction titers on *L. monocytogenes* H7858 when grown at 37°C and titered by double-layer method compared with titers on *L. monocytogenes* F2365. In conclusion, the

purified phages obtained from co-evolution can form plaques on *L. monocytogenes* H7858 by double-layer method, and different phage titering methods may influence the plaquing ability of phages. The mechanisms responsible for these differences need further research, which may be important for understanding how these phages might behave in the wild.

4.5.4 Identification of mutations in phage-resistant mutants that are likely involved in conferring phage resistance.

The resistance mechanisms of mutant strains obtained from the co-evolution experiment were studied by genome sequencing and analysis.

In group 1, *L. monocytogenes* 10403S infected with *pecentumvirus*, mutations likely disrupting the function of *yfhO*, *rmlT*, *rmlA*, and *rlmB* are most likely involved in conferring phage resistance. Mutations in *yfhO* lead to the lack of GlcNAc in WTA mutations and mutations in *rmlT*, *rmlA* and *rmlB* lead to the lack of rhamnose in the WTA (Carvalho et al., 2015; Eugster et al., 2015). Rhamnose and GlcNAc are known as important receptors on WTA for phage binding (Denes et al., 2015; Song et al., 2019). Based on the results of genome analysis, all the phage-resistant mutants of *L. monocytogenes* 10403S in this study adopt mechanisms of adsorption inhibition under the pressure of *pecentumvirus*, which is consistent with previous research (Denes et al., 2015).

In group 2, *L. monocytogenes* H7858 infected with *pecentumvirus*, mutations likely disrupting the function of *galU*, *anrAB* and MZN50_10345 (lmo2475) are most likely involved in conferring phage resistance. GalU is identified as an essential membrane

protein to the WTA decoration for phage binding, suggesting the mutation detected in *galU* is related to adsorption inhibition resistance (Kuenemann et al., 2018). *anrAB* encodes ABC transporter permease AnrAB, encoding an ATP-binding protein (AnrA) and a permease (AnrB), which is identified as a multidrug resistance (MDR) transporter for antibiotics (Collins, Curtis, Cotter, Hill, & Ross, 2010). AnrAB is identified as an integral membrane protein, suggesting the mutations in *anrAB* is also associated with the resistance mechanisms by adsorption inhibition (Hollenstein, Dawson, & Locher, 2007). MZN50_10345 (lmo2475) can not be classified without further evidence, as the gene products are widely involved in bacterial metabolism.

In group 3, *L. monocytogenes* H7858 infected with P35-like phages, mutations likely disrupting the function of MZN50_08850, MZN50_08855, the intergenic region (4564 nt upstream of MZN50_02770), MZN50_03185 (lmo1000) and *lapB* are most likely involved in conferring phage resistance. The resistance mechanisms associated with MZN50_08850, MZN50_08855 and MZN50_03185 (lmo1000) can not be classified without further evidence. The mutations that are detected in *lapB* and the intergenic region (4564 nt upstream of MZN50_02770) adopt mechanisms of adsorption inhibition, as the gene products of the intergenic region is involved in the synthesis of WTA and the gene products of *lapB* are cell-surface components. Interestingly, LapB is a surface-anchored adhesin, which is a type of virulence factor. Under the pressure of phages, the phage-resistant mutants developed mutations in genes that encode a virulence factor, this may lead to decreased pathogenicity. The loss of virulence of pathogens is also observed in previous research, when under the selective pressure of phages (Laanto, Bamford,

Laakso, & Sundberg, 2012). Instead of killing most of the pathogens with phages, reducing the virulence of bacteria or pressuring pathogenic strains into nonpathogenic strains by phage infection may be another promising application in the future.

4.5.5 **Mutations in different genes were identified in phage-resistant *L. monocytogenes* 10403S and *L. monocytogenes* H7858 selected by A511.**

Listeria phage A511 was selected as one of the experimental phages for the co-evolution experiment in both group 1 and group 2. However, mutations in totally different genes were identified in phage-resistant mutants derived from *L. monocytogenes* 10403S, compared with phage-resistant mutants derived from *L. monocytogenes* H7858.

In group 1, there are three resistant mutants selected by A511, and all mutant strains have a single mutation in *rmlA*, leading to the loss of rhamnose in WTA (Eugster et al., 2015). In group 2, there are six resistant mutants selected by A511. Four of the mutant strains have at least one mutation in *galU*, which is required for phage binding (Kuenemann et al., 2018; Spears et al., 2016). The other two mutant strains both have two mutations, one mutation in MZN50_02810 and one mutation in MZN50_08855, with unknown functions involved in phage resistance mechanisms.

4.6 Conclusion

In this study, the *Listeria* density dynamic in co-evolution was observed over ten days, showing all experimental phages except LP-053 impact the growth of *L. monocytogenes*. Serotypes of *L. monocytogenes* and species of *Listeria* phages both determine the growth pattern in the process of co-evolution. The co-evolution experiment can be used to predict the phage-resistant mutants that may occur when using phages for

biocontrol and can provide pre-adapted phages to decrease the likelihood of resistance emerging (Borin et al., 2021). All experimental phages and evolved phages in this study require strict temperature conditions to form plaques on *L. monocytogenes* H7858, which may limit the efficiency of phages to control *L. monocytogenes* H7858 in biocontrol applications. What's more, the ability to form plaques on *L. monocytogenes* H7858 is different with different titering methods in the lab, which may lead to different conclusions if not accounted for. The identification of mutations that are responsible for conferring phage resistance shows most phage-resistant mutants in this study resist phage infection through inhibition of adsorption. The genomic analysis of this study provides more information about phage resistance and may be helpful in improving the efficiency of *Listeria* phages for biocontrol applications in the future.

Acknowledgment: I would like to thank Daniel W. Bryan for his contribution to the design of the experiments, his assistance in conducting the experiments, and revising this chapter; Lauren K. Hudson for her help with genomic analysis and interpretation; Tracey L. Peters for her assistance in conducting the experiments; and Thomas G. Denes for his contribution to the design of the experiments and revising this chapter.

5 CONCLUSION

Listeria phages are a promising natural agent for the biocontrol of *Listeria monocytogenes* contamination in the food processing environment. However, the development of phage-resistant mutants is a major challenge of *Listeria* phage applications. This study investigated the interplay between *Listeria monocytogenes* and *Listeria* phages, especially the resistance mechanisms of phage-resistant mutants.

Listeria phage LP-018 was characterized, as LP-018 is the only phage from a collection of 120 phages that can form plaques on mutant strains with no rhamnose in their wall teichoic acids. LP-018 was identified as a new species belonging to *Homburgvirus* by morphological observation and genome analysis. One-step growth curve analysis of LP-018 revealed an eclipse period of ~60-90 min and a burst size of ~2 PFU per infected cell. The inhibition experiment showed LP-018 was able to inhibit the growth of *Listeria monocytogenes* with a high concentration. New LP-018 resistant *Listeria* mutants were isolated, and the results of the adsorption assay suggested the LP-018 resistant mutants resist LP-018 through a mechanism of resistance independent of phage adsorption. The LP-018 mutants were isolated and characterized, identifying a gene in LP-018 that determines the host range.

Then, *Listeria* phages that target *Listeria monocytogenes* serotype 4b strains were selected and characterized, as serotype 4b strains are responsible for the most isolates from clinal cases. Nine phages that show a strong lytic ability against the model serotype 4b *Listeria monocytogenes* F2365 were selected from a collection of 120 phages. All selected phages can be divided into two groups based on the morphological observation, genome analysis, and host range. LP-020, LP-027, and LP-094 were chosen as

representative phages for further characterization through one-step growth curve experiments and growth inhibition experiments. LP-020 shows a strong activity against to all serotype 4 *Listeria monocytogenes* strains in this test, suggesting LP-020 may be particularly useful in biocontrol setting.

Co-evolution experiments between *Listeria* phages, representing two distinct groups *(pecentumvirus* and P35-like), and *L. monocytogenes* (serotype 1/2a and 4b) were conducted, suggesting all experimental phages except LP-053 impact the growth of *L. monocytogenes*. The growth pattern of the host strains in the co-evolution was influenced by both serotypes of *L. monocytogenes* and species of *Listeria* phages. Interestingly, the complete demise of bacteria or phages was observed in some co-evolution groups, showing a no-regrowth curve or the same curve as with the uninfected group. After co-evolution, most isolated survivors were unsusceptible to phage infection, and the phage lysates were able to infect a portion of the resistant mutants, showing an expanded host range. All experimental phages and evolved phages in this study require strict temperature conditions to form plaques on *L. monocytogenes* H7858, which may limit the efficiency of phages to control *L. monocytogenes* H7858 in biocontrol applications. The identification of mutations (i.e. *yfhO*,*rmlT*, *rmlA*) that are responsible for conferring phage resistance shows most phage-resistant mutants in this study resist phage infection through inhibition of adsorption.

LIST OF REFERENCES

(ERS), E. R. S. (Cost Estimates of Foodborne Illnesses). U.S. Department of Agriculture (USDA). Retrieved from http://ers.usda.gov/data-products/cost-estimates-of-foodborne-illnesses.aspx

Aarnisalo, K., Autio, T., Sjöberg, A.-M., Lundén, J., Korkeala, H., & Suihko, M.-L. (2003). Typing of Listeria monocytogenes isolates originating from the food processing industry with automated ribotyping and pulsed-field gel electrophoresis. *Journal of food protection, 66*(2), 249-255.

Abudayyeh, O. O., Gootenberg, J. S., Konermann, S., Joung, J., Slaymaker, I. M., Cox, D. B., . . . Minakhin, L. (2016). C2c2 is a single-component programmable RNA-guided RNA-targeting CRISPR effector. *Science, 353*(6299), aaf5573.

Ackermann, H.-W. (2006). Classification of bacteriophages. *The bacteriophages, 2*, 8-16.

Ackermann, H.-W., Caprioli, T., & Kasatiya, S. S. (1975). A large new Streptococcus bacteriophage. *Canadian journal of microbiology, 21*(4), 571-574.

Ackermann, H.-W., Tremblay, D., & Moineau, S. (2004). Long-term bacteriophage preservation.

Adriaenssens, E., & Brister, J. R. (2017). How to name and classify your phage: an informal guide. *Viruses, 9*(4), 70.

Aliakbar Ahovan, Z., Hashemi, A., De Plano, L. M., Gholipourmalekabadi, M., & Seifalian, A. (2020). Bacteriophage based biosensors: trends, outcomes and challenges. *Nanomaterials, 10*(3), 501.

Alonzo, F., & Freitag, N. E. (2010). *Listeria monocytogenes* PrsA2 is required for virulence factor secretion and bacterial viability within the host cell cytosol. *Infection and immunity, 78*(11), 4944-4957.

Alonzo, F., Port, G. C., Cao, M., & Freitag, N. E. (2009). The posttranslocation chaperone PrsA2 contributes to multiple facets of Listeria monocytogenes pathogenesis. *Infection and immunity, 77*(7), 2612-2623.

Altschul, S. F., Gish, W., Miller, W., Myers, E. W., & Lipman, D. J. (1990). Basic local alignment search tool. *Journal of molecular biology, 215*(3), 403-410.

Anba, J., Bidnenko, E., Hillier, A., Ehrlich, D., & Chopin, M.-C. (1995). Characterization of the lactococcal abiD1 gene coding for phage abortive infection. *Journal of bacteriology, 177*(13), 3818-3823.

Andrews, S. (2010). FastQC. Retrieved from https://www.bioinformatics.babraham.ac.uk/projects/fastqc/

Archambaud, C., Nahori, M.-A., Pizarro-Cerda, J., Cossart, P., & Dussurget, O. (2006). Control of Listeria superoxide dismutase by phosphorylation. *Journal of biological chemistry, 281*(42), 31812-31822.

Ashelford, K. E., Day, M. J., & Fry, J. C. (2003). Elevated abundance of bacteriophage infecting bacteria in soil. *Applied and environmental microbiology, 69*(1), 285-289.

Bae, D., Liu, C., Zhang, T., Jones, M., Peterson, S. N., & Wang, C. (2012). Global gene expression of Listeria monocytogenes to salt stress. *Journal of food protection, 75*(5), 906-912.

Bandyopadhyay, P. K., Studier, F. W., Hamilton, D. L., & Yuan, R. (1985). Inhibition of the type I restriction-modification enzymes EcoB and EcoK by the gene 0.3 protein of bacteriophage T7. *Journal of molecular biology, 182*(4), 567-578.

Bankevich, A., Nurk, S., Antipov, D., Gurevich, A. A., Dvorkin, M., Kulikov, A. S., . . . Prjibelski, A. D. (2012). SPAdes: a new genome assembly algorithm and its applications to single-cell sequencing. *Journal of computational biology, 19*(5), 455-477.

Bansal, M., Nannapaneni, R., Sharma, C. S., & Kiess, A. (2018). Listeria monocytogenes response to sublethal chlorine induced oxidative stress on homologous and heterologous stress adaptation. *Frontiers in microbiology*, 2050.

Barr, J. J. (2017). A bacteriophages journey through the human body. *Immunological Reviews, 279*(1), 106-122.

Barrangou, R., Fremaux, C., Deveau, H., Richards, M., Boyaval, P., Moineau, S., . . . Horvath, P. (2007). CRISPR provides acquired resistance against viruses in prokaryotes. *Science, 315*(5819), 1709-1712.

Batinovic, S., Wassef, F., Knowler, S. A., Rice, D. T., Stanton, C. R., Rose, J., . . . Drummond, G. R. (2019). Bacteriophages in natural and artificial environments. *Pathogens, 8*(3), 100.

Bergholz, T. M., den Bakker, H. C., Fortes, E. D., Boor, K. J., & Wiedmann, M. (2010). Salt stress phenotypes in Listeria monocytogenes vary by genetic lineage and temperature. *Foodborne pathogens and disease, 7*(12), 1537-1549.

Betts, A., Kaltz, O., & Hochberg, M. E. (2014). Contrasted coevolutionary dynamics between a bacterial pathogen and its bacteriophages. *Proceedings of the National Academy of Sciences, 111*(30), 11109-11114.

Beveridge, T. J., & Matias, V. R. (2006). Ultrastructure of gram-positive cell walls. In *Gram-Positive Pathogens, Second Edition* (pp. 3-11): American Society of Microbiology.

Bickle, T. A., & Krüger, D. (1993). Biology of DNA restriction. *Microbiological reviews, 57*(2), 434-450.

Bielmann, R., Habann, M., Eugster, M. R., Lurz, R., Calendar, R., Klumpp, J., & Loessner, M. J. (2015). Receptor binding proteins of Listeria monocytogenes bacteriophages A118 and P35 recognize serovar-specific teichoic acids. *Virology, 477*, 110-118.

Bingham, R., Ekunwe, S. I., Falk, S., Snyder, L., & Kleanthous, C. (2000). The major head protein of bacteriophage T4 binds specifically to elongation factor Tu. *Journal of biological chemistry, 275*(30), 23219-23226.

Bishop-Lilly, K. A., Plaut, R. D., Chen, P. E., Akmal, A., Willner, K. M., Butani, A., . . . Chapman, C. (2012). Whole genome sequencing of phage resistant Bacillus anthracis mutants reveals an essential role for cell surface anchoring protein CsaB in phage AP50c adsorption. *Virology journal, 9*(1), 246.

Bishop, D., & Hinrichs, D. (1987). Adoptive transfer of immunity to Listeria monocytogenes. The influence of in vitro stimulation on lymphocyte subset requirements. *The Journal of Immunology, 139*(6), 2005-2009.

Blower, T. R., Evans, T. J., Przybilski, R., Fineran, P. C., & Salmond, G. P. (2012). Viral evasion of a bacterial suicide system by RNA–based molecular mimicry enables infectious altruism.

Bolger, A. M., Lohse, M., & Usadel, B. (2014). Trimmomatic: a flexible trimmer for Illumina sequence data. *Bioinformatics, 30*(15), 2114-2120.

Bondy-Denomy, J., Pawluk, A., Maxwell, K. L., & Davidson, A. R. (2013). Bacteriophage genes that inactivate the CRISPR/Cas bacterial immune system. *Nature, 493*(7432), 429-432.

Borin, J. M., Avrani, S., Barrick, J. E., Petrie, K. L., & Meyer, J. R. (2021). Coevolutionary phage training leads to greater bacterial suppression and delays the evolution of phage resistance. *Proceedings of the National Academy of Sciences, 118*(23).

Borucki, M. K., & Call, D. R. (2003). Listeria monocytogenes serotype identification by PCR. *Journal of clinical microbiology, 41*(12), 5537-5540.

Brettin, T., Davis, J. J., Disz, T., Edwards, R. A., Gerdes, S., Olsen, G. J., . . . Pusch, G. D. (2015). RASTtk: a modular and extensible implementation of the RAST algorithm for building custom annotation pipelines and annotating batches of genomes. *Scientific reports, 5*, 8365.

Bruttin, A., & Brüssow, H. (2005). Human volunteers receiving Escherichia coli phage T4 orally: a safety test of phage therapy. *Antimicrobial agents and chemotherapy, 49*(7), 2874-2878.

Buckling, A., & Brockhurst, M. (2012). Bacteria–virus coevolution. *Evolutionary systems biology*, 347-370.

Bucur, F. I., Grigore-Gurgu, L., Crauwels, P., Riedel, C. U., & Nicolau, A. I. (2018). Resistance of Listeria monocytogenes to stress conditions encountered in food and food processing environments. *Frontiers in microbiology, 9*, 2700.

Bushnell, B. (2018). BBTools: a suite of fast, multithreaded bioinformatics tools designed for analysis of DNA and RNA sequence data. *Joint Genome Institute.https://jgi. doe. gov/data-and-tools/bbtools*.

Canchaya, C., Proux, C., Fournous, G., Bruttin, A., & Brüssow, H. (2003). Prophage genomics. *Microbiology and molecular biology reviews, 67*(2), 238-276.

Carlton, R., Noordman, W., Biswas, B., De Meester, E., & Loessner, M. J. (2005). Bacteriophage P100 for control of Listeria monocytogenes in foods: genome sequence, bioinformatic analyses, oral toxicity study, and application. *Regulatory Toxicology and Pharmacology, 43*(3), 301-312.

Carlton, R. M. (1999). Phage therapy: past history and future prospects. *Archivum Immunologiae et Therapiae Experimentalis, 47*, 267-274.

Carvalho, F., Atilano, M. L., Pombinho, R., Covas, G., Gallo, R. L., Filipe, S. R., . . . Cabanes, D. (2015). L-Rhamnosylation of Listeria monocytogenes wall teichoic acids promotes resistance to antimicrobial peptides by delaying interaction with the membrane. *PLoS pathogens, 11*(5), e1004919.

Castanon, J. (2007). History of the use of antibiotic as growth promoters in European poultry feeds. *Poultry science, 86*(11), 2466-2471.

Chan, B. K., Abedon, S. T., & Loc-Carrillo, C. (2013). Phage cocktails and the future of phage therapy. *Future microbiology, 8*(6), 769-783.

Chan, Y. C., & Wiedmann, M. (2008). Physiology and genetics of Listeria monocytogenes survival and growth at cold temperatures. *Critical reviews in food science and nutrition, 49*(3), 237-253.

Chassaing, D., & Auvray, F. (2007). The lmo1078 gene encoding a putative UDP-glucose pyrophosphorylase is involved in growth of Listeria monocytogenes at low temperature. *FEMS microbiology letters, 275*(1), 31-37.

Chernomordik, A. (1989). Bacteriophages and their therapeutic-prophylactic use. *Meditsinskaia sestra, 48*(6), 44-47.

Chibeu, A., Agius, L., Gao, A., Sabour, P. M., Kropinski, A. M., & Balamurugan, S. (2013). Efficacy of bacteriophage LISTEX™ P100 combined with chemical antimicrobials in reducing Listeria monocytogenes in cooked turkey and roast beef. *International Journal of Food Microbiology, 167*(2), 208-214.

Cingolani, P., Platts, A., Wang, L. L., Coon, M., Nguyen, T., Wang, L., . . . Ruden, D. M. (2012). A program for annotating and predicting the effects of single nucleotide polymorphisms, SnpEff: SNPs in the genome of Drosophila melanogaster strain w1118; iso-2; iso-3. *Fly, 6*(2), 80-92.

Clark, W. A. (1962). Comparison of several methods for preserving bacteriophages. *Applied microbiology, 10*(5), 466-471.

Coffey, B., Mills, S., Coffey, A., McAuliffe, O., & Ross, R. P. (2010). Phage and their lysins as biocontrol agents for food safety applications. *Annual review of food science and technology, 1*, 449-468.

Collins, B., Curtis, N., Cotter, P. D., Hill, C., & Ross, R. P. (2010). The ABC transporter AnrAB contributes to the innate resistance of Listeria monocytogenes to nisin, bacitracin, and various β-lactam antibiotics. *Antimicrobial agents and chemotherapy, 54*(10), 4416-4423.

Cook, G. M., Robson, J. R., Frampton, R. A., McKenzie, J., Przybilski, R., Fineran, P. C., & Arcus, V. L. (2013). Ribonucleases in bacterial toxin–antitoxin systems. *Biochimica et Biophysica Acta (BBA)-Gene Regulatory Mechanisms, 1829*(6-7), 523-531.

Cooper, C., Denyer, S. P., & Maillard, J. Y. (2014). Stability and purity of a bacteriophage cocktail preparation for nebulizer delivery. *Letters in applied microbiology, 58*(2), 118-122.

Cost Estimates of Foodborne Illnesses. (2021). Retrieved from https://www.ers.usda.gov/data-products/cost-estimates-of-foodborne-illnesses.aspx

Cotter, P. D., Ross, R. P., & Hill, C. (2013). Bacteriocins—a viable alternative to antibiotics? *Nature Reviews Microbiology, 11*(2), 95-105.

CUI, Z.-h., & JI, X.-l. (2020). Advances in Bacteria-Phage Antagonistic Coevolution. *China Biotechnology, 40*(1-2), 140-145.

d'Herelle, M. (1961). Sur un microbe invisible antagoniste des bacilles dysentériques. *Acta Kravsi*.

De Jesus, A. J., & Whiting, R. C. (2003). Thermal inactivation, growth, and survival studies of Listeria monocytogenes strains belonging to three distinct genotypic lineages. *Journal of food protection, 66*(9), 1611-1617.

de Noordhout, C. M., Devleesschauwer, B., Angulo, F. J., Verbeke, G., Haagsma, J., Kirk, M., . . . Speybroeck, N. (2014). The global burden of listeriosis: a systematic review and meta-analysis. *The Lancet Infectious Diseases, 14*(11), 1073-1082.

De Sordi, L., Lourenço, M., & Debarbieux, L. (2019). "I will survive": a tale of bacteriophage-bacteria coevolution in the gut. *Gut microbes, 10*(1), 92-99.

Denes, T., den Bakker, H. C., Tokman, J. I., Guldimann, C., & Wiedmann, M. (2015). Selection and characterization of phage-resistant mutant strains of Listeria monocytogenes reveal host genes linked to phage adsorption. *Appl. Environ. Microbiol., 81*(13), 4295-4305.

Denes, T., Vongkamjan, K., Ackermann, H.-W., Switt, A. I. M., Wiedmann, M., & den Bakker, H. C. (2014). Comparative genomic and morphological analyses of Listeria phages isolated from farm environments. *Appl. Environ. Microbiol., 80*(15), 4616-4625.

Denes, T., & Wiedmann, M. (2014). Environmental responses and phage susceptibility in foodborne pathogens: implications for improving applications in food safety. *Current opinion in biotechnology, 26*, 45-49.

Deveau, H., Barrangou, R., Garneau, J. E., Labonté, J., Fremaux, C., Boyaval, P., . . . Moineau, S. (2008). Phage response to CRISPR-encoded resistance in Streptococcus thermophilus. *Journal of bacteriology, 190*(4), 1390-1400.

Dmitrieva, N. I., Cai, Q., & Burg, M. B. (2004). Cells adapted to high NaCl have many DNA breaks and impaired DNA repair both in cell culture and in vivo. *Proceedings of the National Academy of Sciences, 101*(8), 2317-2322.

Dorscht, J., Klumpp, J., Bielmann, R., Schmelcher, M., Born, Y., Zimmer, M., . . . Loessner, M. J. (2009). Comparative genome analysis of Listeria bacteriophages reveals extensive mosaicism, programmed translational frameshifting, and a novel prophage insertion site. *Journal of bacteriology, 191*(23), 7206-7215.

Dryden, D., Murray, N. E., & Rao, D. (2001). Nucleoside triphosphate-dependent restriction enzymes. *Nucleic acids research, 29*(18), 3728-3741.

Duché, O., Trémoulet, F., Glaser, P., & Labadie, J. (2002). Salt stress proteins induced in Listeria monocytogenes. *Applied and environmental microbiology, 68*(4), 1491-1498.

Durmaz, E., & Klaenhammer, T. R. (2007). Abortive phage resistance mechanism AbiZ speeds the lysis clock to cause premature lysis of phage-infected Lactococcus lactis. In: Am Soc Microbiol.

Dy, R. L., Richter, C., Salmond, G. P., & Fineran, P. C. (2014). Remarkable mechanisms in microbes to resist phage infections. *Annual review of virology, 1*, 307-331.

Emond, E., Holler, B. J., Boucher, I., Vandenbergh, P. A., Vedamuthu, E. R., Kondo, J. K., & Moineau, S. (1997). Phenotypic and genetic characterization of the

bacteriophage abortive infection mechanism AbiK from Lactococcus lactis. *Applied and environmental microbiology, 63*(4), 1274-1283.

Eugster, M. R., Morax, L. S., Hüls, V. J., Huwiler, S. G., Leclercq, A., Lecuit, M., & Loessner, M. J. (2015). Bacteriophage predation promotes serovar diversification in *Listeria monocytogenes*. *Molecular microbiology, 97*(1), 33-46.

Ewels, P., Magnusson, M., Lundin, S., & Käller, M. (2016). MultiQC: summarize analysis results for multiple tools and samples in a single report. *Bioinformatics, 32*(19), 3047-3048.

Fenlon, D. (1985). Wild birds and silage as reservoirs of Listeria in the agricultural environment. *Journal of Applied Bacteriology, 59*(6), 537-543.

Fernandes, S., & São-José, C. (2018). Enzymes and mechanisms employed by tailed bacteriophages to breach the bacterial cell barriers. *Viruses, 10*(8), 396.

Fineran, P. C., Blower, T. R., Foulds, I. J., Humphreys, D. P., Lilley, K. S., & Salmond, G. P. (2009). The phage abortive infection system, ToxIN, functions as a protein–RNA toxin–antitoxin pair. *Proceedings of the National Academy of Sciences, 106*(3), 894-899.

Fister, S., Fuchs, S., Stessl, B., Schoder, D., Wagner, M., & Rossmanith, P. (2016). Screening and characterisation of bacteriophage P100 insensitive Listeria monocytogenes isolates in Austrian dairy plants. *Food Control, 59*, 108-117.

Frank, S. (1992). Models of plant-pathogen coevolution. *Trends in Genetics, 8*(6), 213-219.

Frank, S. A. (1993). Specificity versus detectable polymorphism in host–parasite genetics. *Proceedings of the Royal Society of London. Series B: Biological Sciences, 254*(1341), 191-197.

Fugett, E., Fortes, E., Nnoka, C., & Wiedmann, M. (2006). International Life Sciences Institute North America Listeria monocytogenes strain collection: development of standard Listeria monocytogenes strain sets for research and validation studies. *Journal of food protection, 69*(12), 2929-2938.

Garneau, J. E., Dupuis, M.-È., Villion, M., Romero, D. A., Barrangou, R., Boyaval, P., . . . Moineau, S. (2010). The CRISPR/Cas bacterial immune system cleaves bacteriophage and plasmid DNA. *Nature, 468*(7320), 67-71.

Gayán, E., Serrano, M., Pagán, R., Álvarez, I., & Condón, S. (2015). Environmental and biological factors influencing the UV-C resistance of Listeria monocytogenes. *Food microbiology, 46*, 246-253.

Gomez-Lopez, V. M., Ragaert, P., Debevere, J., & Devlieghere, F. (2007). Pulsed light for food decontamination: a review. *Trends in Food Science & Technology, 18*(9), 464-473.

Góngora-Nieto, M., Sepúlveda, D., Pedrow, P., Barbosa-Cánovas, G., & Swanson, B. (2002). Food processing by pulsed electric fields: Treatment delivery, inactivation level, and regulatory aspects. *LWT-Food Science and Technology, 35*(5), 375-388.

Grau, F. H., & Vanderlinde, P. B. (1990). Growth of Listeria monocytogenes on vacuum-packaged beef. *Journal of food protection, 53*(9), 739-741.

Gray, J. A., Chandry, P. S., Kaur, M., Kocharunchitt, C., Bowman, J. P., & Fox, E. M. (2018). Novel biocontrol methods for Listeria monocytogenes biofilms in food production facilities. *Frontiers in microbiology, 9*, 605.

Guerrero-Ferreira, R. C., Hupfeld, M., Nazarov, S., Taylor, N. M., Shneider, M. M., Obbineni, J. M., . . . Leiman, P. G. (2019). Structure and transformation of bacteriophage A511 baseplate and tail upon infection of Listeria cells. *The EMBO journal, 38*(3), e99455.

Gurevich, A., Saveliev, V., Vyahhi, N., & Tesler, G. (2013). QUAST: quality assessment tool for genome assemblies. *Bioinformatics, 29*(8), 1072-1075.

Guttman, B., Raya, R., & Kutter, E. (2005). Basic phage biology. *Bacteriophages: Biology and applications, 4*, 30-63.

Hagens, S., & Loessner, M. J. (2007). Application of bacteriophages for detection and control of foodborne pathogens. *Applied microbiology and biotechnology, 76*(3), 513-519.

Hain, T., Chatterjee, S. S., Ghai, R., Kuenne, C. T., Billion, A., Steinweg, C., . . . Wehland, J. (2007). Pathogenomics of Listeria spp. *International Journal of Medical Microbiology, 297*(7-8), 541-557.

Halford, S. E., & Marko, J. F. (2004). How do site-specific DNA-binding proteins find their targets? *Nucleic acids research, 32*(10), 3040-3052.

Hamon, Y., & Peron, Y. (1963). *Study of the bacteriocinogenic potency in the genus Listeria. II. Individuality and classification of the bacteriocins in question.* Paper presented at the Annales de l'Institut Pasteur.

Hampton, H. G., Watson, B. N., & Fineran, P. C. (2020). The arms race between bacteria and their phage foes. *Nature, 577*(7790), 327-336.

Han, P., & Deem, M. W. (2017). Non-classical phase diagram for virus bacterial coevolution mediated by clustered regularly interspaced short palindromic repeats. *Journal of The Royal Society Interface, 14*(127), 20160905.

Hanada, K., Shiu, S.-H., & Li, W.-H. (2007). The nonsynonymous/synonymous substitution rate ratio versus the radical/conservative replacement rate ratio in the evolution of mammalian genes. *Molecular biology and evolution, 24*(10), 2235-2241.

Hankin, E. H. (1896). L'action bactericide des eaux de la Jumna et du Gange sur le vibrion du cholera. *Ann Inst Pasteur, 10*(11).

Hasebe, R., Nakao, R., Ohnuma, A., Yamasaki, T., Sawa, H., Takai, S., & Horiuchi, M. (2017). Listeria monocytogenes serotype 4b strains replicate in monocytes/macrophages more than the other serotypes. *Journal of veterinary medical science*, 16-0575.

Hill, D., Sugrue, I., Arendt, E., Hill, C., Stanton, C., & Ross, R. P. (2017). Recent advances in microbial fermentation for dairy and health. *F1000Research, 6*.

Hodgson, D. A. (2000). Generalized transduction of serotype 1/2 and serotype 4b strains of Listeria monocytogenes. *Molecular microbiology, 35*(2), 312-323. Retrieved from https://onlinelibrary.wiley.com/doi/full/10.1046/j.1365-2958.2000.01643.x?sid=nlm%3Apubmed

Hoffman, S., Maculloch, B., & Batz, M. (2015). *Economic burden of major foodborne illnesses acquired in the United States*. Retrieved from

Hollenstein, K., Dawson, R. J., & Locher, K. P. (2007). Structure and mechanism of ABC transporter proteins. *Current opinion in structural biology, 17*(4), 412-418.

Huang, H.-W., Lung, H.-M., Yang, B. B., & Wang, C.-Y. (2014). Responses of microorganisms to high hydrostatic pressure processing. *Food Control, 40*, 250-259.

Huang, Y., Morvay, A. A., Shi, X., Suo, Y., Shi, C., & Knøchel, S. (2018). Comparison of oxidative stress response and biofilm formation of Listeria monocytogenes serotypes 4b and 1/2a. *Food Control, 85*, 416-422.

Hudson, L. K., Peters, T. L., Song, Y., & Denes, T. G. (2019). Complete Genome Sequences and Transmission Electron Micrographs of Listeria Phages of the Genus Homburgvirus. *Microbiology resource announcements, 8*(41), e00825-00819.

Iida, S., Streiff, M. B., Bickle, T. A., & Arber, W. (1987). Two DNA antirestriction systems of bacteriophage P1, darA, and darB: characterization of darA− phages. *Virology, 157*(1), 156-166.

Jacob, F., & Wollman, E. L. (1953). *Induction of phage development in lysogenic bacteria.* Paper presented at the Cold Spring Harbor symposia on quantitative biology.

Jansen, R., Embden, J. D. v., Gaastra, W., & Schouls, L. M. (2002). Identification of genes that are associated with DNA repeats in prokaryotes. *Molecular microbiology, 43*(6), 1565-1575.

Jones, P., Binns, D., Chang, H.-Y., Fraser, M., Li, W., McAnulla, C., . . . Nuka, G. (2014). InterProScan 5: genome-scale protein function classification. *Bioinformatics, 30*(9), 1236-1240.

Jones, P., & George, A. (2004). The ABC transporter structure and mechanism: perspectives on recent research. *Cellular and Molecular Life Sciences CMLS, 61*(6), 682-699.

Jordan, K., & McAuliffe, O. (2018). Listeria monocytogenes in foods. *Advances in food and nutrition research, 86*, 181-213.

Jurczak-Kurek, A., Gąsior, T., Nejman-Faleńczyk, B., Bloch, S., Dydecka, A., Topka, G., . . . Richert, M. (2016). Biodiversity of bacteriophages: morphological and biological properties of a large group of phages isolated from urban sewage. *Scientific reports, 6*(1), 1-17.

Kan, N. C., Lautenberger, J. A., Edgell, M. H., & Hutchison III, C. A. (1979). The nucleotide sequence recognized by the Escherichia coli K12 restriction and modification enzymes. *Journal of molecular biology, 130*(2), 191-209.

Karthikeyan, R., Gayathri, P., Gunasekaran, P., Jagannadham, M. V., & Rajendhran, J. (2019). Comprehensive proteomic analysis and pathogenic role of membrane vesicles of Listeria monocytogenes serotype 4b reveals proteins associated with

virulence and their possible interaction with host. *International Journal of Medical Microbiology, 309*(3-4), 199-212.

Kawacka, I., Olejnik-Schmidt, A., Schmidt, M., & Sip, A. (2020). Effectiveness of phage-based inhibition of listeria monocytogenes in food products and food processing environments. *Microorganisms, 8*(11), 1764.

Kilcher, S., Studer, P., Muessner, C., Klumpp, J., & Loessner, M. J. (2018). Cross-genus rebooting of custom-made, synthetic bacteriophage genomes in L-form bacteria. *Proceedings of the National Academy of Sciences, 115*(3), 567-572.

Kim, J.-W., Dutta, V., Elhanafi, D., Lee, S., Osborne, J. A., & Kathariou, S. (2012). A novel restriction-modification system is responsible for temperature-dependent phage resistance in Listeria monocytogenes ECII. *Applied and environmental microbiology, 78*(6), 1995-2004.

Kim, J.-W., & Kathariou, S. (2009). Temperature-dependent phage resistance of Listeria monocytogenes epidemic clone II. *Applied and environmental microbiology, 75*(8), 2433-2438.

Klumpp, J., Dorscht, J., Lurz, R., Bielmann, R., Wieland, M., Zimmer, M., . . . Loessner, M. J. (2008). The terminally redundant, nonpermuted genome of Listeria bacteriophage A511: a model for the SPO1-like myoviruses of gram-positive bacteria. *Journal of bacteriology, 190*(17), 5753-5765.

Klumpp, J., & Loessner, M. J. (2013). Listeria phages: Genomes, evolution, and application. *Bacteriophage, 3*(3), e26861.

Kolde, R. (2019). Pheatmap: Pretty Heatmaps (version 1.0. 12). *Google Scholar*.

Koskella, B. (2014). Bacteria-phage interactions across time and space: merging local adaptation and time-shift experiments to understand phage evolution. *The American Naturalist, 184*(S1), S9-S21.

Koskella, B., & Brockhurst, M. A. (2014). Bacteria–phage coevolution as a driver of ecological and evolutionary processes in microbial communities. *FEMS microbiology reviews, 38*(5), 916-931.

Kraiss, J. B. R., & Fotin, N. (2008). Listeria regulations in the FDA and USDA: Implications for Dual-Jurisdiction Facilities. *Food Regulation in the United States*, 1-18.

Kramarenko, T., Roasto, M., Meremäe, K., Kuningas, M., Põltsama, P., & Elias, T. (2013). Listeria monocytogenes prevalence and serotype diversity in various foods. *Food Control, 30*(1), 24-29.

Krüger, D., & Bickle, T. A. (1983). Bacteriophage survival: multiple mechanisms for avoiding the deoxyribonucleic acid restriction systems of their hosts. *Microbiological reviews, 47*(3), 345-360.

Krüger, D., Schroeder, C., Santibanez-Koref, M., & Reuter, M. (1989). Avoidance of DNA methylation. *Cell biophysics, 15*(1), 87-95.

Kuenemann, M. A., Spears, P. A., Orndorff, P. E., & Fourches, D. (2018). In silico predicted glucose-1-phosphate uridylyltransferase (GalU) inhibitors block a key pathway required for listeria virulence. *Molecular Informatics, 37*(6-7), 1800004.

Laanto, E., Bamford, J. K., Laakso, J., & Sundberg, L.-R. (2012). Phage-driven loss of virulence in a fish pathogenic bacterium. *PLoS One, 7*(12), e53157.

Labrie, S. J., Samson, J. E., & Moineau, S. (2010). Bacteriophage resistance mechanisms. *Nature Reviews Microbiology, 8*(5), 317-327.

Lado, B. H., & Yousef, A. E. (2002). Alternative food-preservation technologies: efficacy and mechanisms. *Microbes and infection, 4*(4), 433-440.

Lasagabaster, A., Jiménez, E., Lehnherr, T., Miranda-Cadena, K., & Lehnherr, H. (2020). Bacteriophage biocontrol to fight Listeria outbreaks in seafood. *Food and Chemical Toxicology, 145*, 111682.

Lee, S. (2020). Bacteriocins of Listeria monocytogenes and Their Potential as a Virulence Factor. *Toxins, 12*(2), 103.

Leong, D., Alvarez-Ordóñez, A., & Jordan, K. (2014). Monitoring occurrence and persistence of Listeria monocytogenes in foods and food processing environments in the Republic of Ireland. *Frontiers in microbiology, 5*, 436.

Letchumanan, V., Wong, P.-C., Goh, B.-H., Ming, L. C., Pusparajah, P., Wong, S. H., . . . Lee, L.-H. (2018). A review on the characteristics, taxanomy and prevalence of Listeria monocytogenes. *Progress In Microbes & Molecular Biology, 1*(1).

Levin, S., Almo, S. C., & Satir, B. H. (1999). Functional diversity of the phosphoglucomutase superfamily: structural implications. *Protein engineering, 12*(9), 737-746.

Levitz, R., Chapman, D., Amitsur, M., Green, R., Snyder, L., & Kaufmann, G. (1990). The optional E. coli prr locus encodes a latent form of phage T4-induced anticodon nuclease. *The EMBO journal, 9*(5), 1383-1389.

Li, H., Handsaker, B., Wysoker, A., Fennell, T., Ruan, J., Homer, N., . . . Durbin, R. (2009). The sequence alignment/map format and SAMtools. *Bioinformatics, 25*(16), 2078-2079.

Li, X., Koç, C., Kühner, P., Stierhof, Y.-D., Krismer, B., Enright, M. C., . . . Cambillau, C. (2016). An essential role for the baseplate protein Gp45 in phage adsorption to Staphylococcus aureus. *Scientific reports, 6*, 26455.

Liu, D. (2008). *Handbook of Listeria monocytogenes*: CRC press.

Liu, D., Lawrence, M. L., Ainsworth, A. J., & Austin, F. W. (2005). Comparative assessment of acid, alkali and salt tolerance in Listeria monocytogenes virulent and avirulent strains. *FEMS microbiology letters, 243*(2), 373-378.

Liu, Y., Orsi, R. H., Gaballa, A., Wiedmann, M., Boor, K. J., & Guariglia-Oropeza, V. (2019). Systematic review of the Listeria monocytogenes σB regulon supports a role in stress response, virulence and metabolism. *Future microbiology, 14*(9), 801-828.

Loc-Carrillo, C., & Abedon, S. T. (2011). Pros and cons of phage therapy. *Bacteriophage, 1*(2), 111-114. Retrieved from https://www.ncbi.nlm.nih.gov/pmc/articles/PMC3278648/pdf/bact0102_0111.pdf

Loessner, M. J., & Busse, M. (1990). Bacteriophage typing of Listeria species. *Applied and environmental microbiology, 56*(6), 1912-1918.

Lopes-Luz, L., Mendonça, M., Bernardes Fogaça, M., Kipnis, A., Bhunia, A. K., & Bührer-Sékula, S. (2021). Listeria monocytogenes: review of pathogenesis and

virulence determinants-targeted immunological assays. *Critical Reviews in Microbiology*, 1-20.

López-Cuevas, O., Medrano-Félix, J., Castro-Del Campo, N., & Chaidez, C. (2021). Bacteriophage applications for fresh produce food safety. *International journal of environmental health research*, *31*(6), 687-702.

LPSN - List of Prokaryotic names with Standing in Nomenclature. *Genus Listeria*. Retrieved from https://lpsn.dsmz.de/genus/listeria

Macwana, S., & Muriana, P. M. (2012). Spontaneous bacteriocin resistance in Listeria monocytogenes as a susceptibility screen for identifying different mechanisms of resistance and modes of action by bacteriocins of lactic acid bacteria. *Journal of microbiological methods*, *88*(1), 7-13.

Makarova, K. S., Haft, D. H., Barrangou, R., Brouns, S. J., Charpentier, E., Horvath, P., . . . Yakunin, A. F. (2011). Evolution and classification of the CRISPR–Cas systems. *Nature Reviews Microbiology*, *9*(6), 467-477.

Malakar, D., Borah, P., Das, L., & Kumar, N. S. A Comprehensive Review on Molecular Characteristics and Food-Borne Outbreaks of Listeria monocytogenes.

Matereke, L. T., & Okoh, A. I. (2020). Listeria monocytogenes virulence, antimicrobial resistance and environmental persistence: A Review. *Pathogens*, *9*(7), 528.

Matic, I., Radman, M., Taddei, F., Picard, B., Doit, C., Bingen, E., . . . Elion, J. (1997). Highly variable mutation rates in commensal and pathogenic Escherichia coli. *Science*, *277*(5333), 1833-1834.

McNair, K., Bailey, B. A., & Edwards, R. A. (2012). PHACTS, a computational approach to classifying the lifestyle of phages. *Bioinformatics, 28*(5), 614-618.

Mead, P. S., Slutsker, L., Dietz, V., McCaig, L. F., Bresee, J. S., Shapiro, C., . . . Tauxe, R. V. (1999). Food-related illness and death in the United States. *Emerging infectious diseases, 5*(5), 607.

Medvedev, P., & Chikhi, R. (2013). Informed and automated k-mer size selection for genome assembly. *Bioinformatics, 30*(1), 31-37. doi:10.1093/bioinformatics/btt310

Meeske, A. J., Nakandakari-Higa, S., & Marraffini, L. A. (2019). Cas13-induced cellular dormancy prevents the rise of CRISPR-resistant bacteriophage. *Nature, 570*(7760), 241-245.

Mihara, T., Nishimura, Y., Shimizu, Y., Nishiyama, H., Yoshikawa, G., Uehara, H., . . . Ogata, H. (2016). Linking virus genomes with host taxonomy. *Viruses, 8*(3), 66.

Milillo, S. R., Friedly, E. C., Saldivar, J. C., Muthaiyan, A., O'bryan, C., Crandall, P. G., . . . Ricke, S. C. (2012). A review of the ecology, genomics, and stress response of Listeria innocua and Listeria monocytogenes. *Critical reviews in food science and nutrition, 52*(8), 712-725.

Monk, A., Rees, C., Barrow, P., Hagens, S., & Harper, D. (2010). Bacteriophage applications: where are we now? *Letters in applied microbiology, 51*(4), 363-369.

Montañez-Izquierdo, V. Y., Salas-Vázquez, D. I., & Rodríguez-Jerez, J. J. (2012). Use of epifluorescence microscopy to assess the effectiveness of phage P100 in

controlling Listeria monocytogenes biofilms on stainless steel surfaces. *Food Control, 23*(2), 470-477.

Moye, Z., Woolston, J., & Sulakvelidze, A. (2018). Bacteriophage applications for food production and processing. *Viruses, 10*(4), 205.

Nelson, K. E., Fouts, D. E., Mongodin, E. F., Ravel, J., DeBoy, R. T., Kolonay, J. F., . . . Paulsen, I. T. (2004). Whole genome comparisons of serotype 4b and 1/2a strains of the food-borne pathogen Listeria monocytogenes reveal new insights into the core genome components of this species. *Nucleic acids research, 32*(8), 2386-2395.

Nucera, D., Lomonaco, S., Bianchi, D. M., Decastelli, L., Grassi, M. A., Bottero, M. T., & Civera, T. (2010). A five year surveillance report on PFGE types of Listeria monocytogenes isolated in Italy from food and food related environments. *International Journal of Food Microbiology, 140*(2-3), 271-276.

Nyfeldt, A. (1929). Etiologie de la mononucleose infectieuse. *CR Soc. Biol, 101*, 590-591.

Oechslin, F. (2018). Resistance development to bacteriophages occurring during bacteriophage therapy. *Viruses, 10*(7), 351.

Olanya, O. M., Hoshide, A. K., Ijabadeniyi, O. A., Ukuku, D. O., Mukhopadhyay, S., Niemira, B. A., & Ayeni, O. (2019). Cost estimation of listeriosis (Listeria monocytogenes) occurrence in South Africa in 2017 and its food safety implications. *Food Control, 102*, 231-239.

Oliveira, P. H., Touchon, M., & Rocha, E. P. (2014). The interplay of restriction-modification systems with mobile genetic elements and their prokaryotic hosts. *Nucleic acids research, 42*(16), 10618-10631.

Orsi, R. H., den Bakker, H. C., & Wiedmann, M. (2011). Listeria monocytogenes lineages: genomics, evolution, ecology, and phenotypic characteristics. *International Journal of Medical Microbiology, 301*(2), 79-96.

Otsuka, Y., & Yonesaki, T. (2012). Dmd of bacteriophage T4 functions as an antitoxin against Escherichia coli LsoA and RnlA toxins. *Molecular microbiology, 83*(4), 669-681.

Parma, D. H., Snyder, M., Sobolevski, S., Nawroz, M., Brody, E., & Gold, L. (1992). The Rex system of bacteriophage lambda: tolerance and altruistic cell death. *Genes & development, 6*(3), 497-510.

Pecota, D. C., & Wood, T. K. (1996). Exclusion of T4 phage by the hok/sok killer locus from plasmid R1. *Journal of bacteriology, 178*(7), 2044-2050.

Perera, M. N., Abuladze, T., Li, M., Woolston, J., & Sulakvelidze, A. (2015). Bacteriophage cocktail significantly reduces or eliminates Listeria monocytogenes contamination on lettuce, apples, cheese, smoked salmon and frozen foods. *Food microbiology, 52*, 42-48.

Peters, T. L., Hudson, L. K., Bryan, D. W., Song, Y., den Bakker, H. C., Kucerova, Z., & Denes, T. G. (2021). Complete Genome Sequence of a Serotype 7 Listeria monocytogenes Strain, FSL R9-0915. *Microbiology resource announcements, 10*(1), e01158-01120.

Peters, T. L., Hudson, L. K., Song, Y., & Denes, T. G. (2019). Complete Genome Sequences of Two Listeria Phages of the Genus Pecentumvirus. *Microbiology resource announcements, 8*(46).

Peters, T. L., Song, Y., Bryan, D. W., Hudson, L. K., & Denes, T. G. (2020). Mutant and recombinant phages selected from in vitro coevolution conditions overcome phage-resistant Listeria monocytogenes. *Applied and environmental microbiology, 86*(22).

Pieper, U., Brinkmann, T., Krüger, T., Noyer-Weidner, M., & Pingoud, A. (1997). Characterization of the interaction between the restriction endonuclease McrBC from E. coli and its cofactor GTP. *Journal of molecular biology, 272*(2), 190-199.

Piffaretti, J.-C., Kressebuch, H., Aeschbacher, M., Bille, J., Bannerman, E., Musser, J. M., . . . Rocourt, J. (1989). Genetic characterization of clones of the bacterium Listeria monocytogenes causing epidemic disease. *Proceedings of the National Academy of Sciences, 86*(10), 3818-3822.

Pingoud, A., & Jeltsch, A. (2001). Structure and function of type II restriction endonucleases. *Nucleic acids research, 29*(18), 3705-3727.

Pizarro-Cerda, J., & Cossart, P. (2018). Listeria monocytogenes: cell biology of invasion and intracellular growth. *Microbiology spectrum, 6*(6).

Poimenidou, S. V., Chatzithoma, D.-N., Nychas, G.-J., & Skandamis, P. N. (2016). Adaptive response of Listeria monocytogenes to heat, salinity and low pH, after habituation on cherry tomatoes and lettuce leaves. *PLoS One, 11*(10), e0165746.

Pons, J. C., Paez-Espino, D., Riera, G., Ivanova, N., Kyrpides, N. C., & Llabrés, M. (2021). VPF-Class: taxonomic assignment and host prediction of uncultivated viruses based on viral protein families. *Bioinformatics, 37*(13), 1805-1813.

Pontello, M., Guaita, A., Sala, G., Cipolla, M., Gattuso, A., Sonnessa, M., & Gianfranceschi, M. V. (2012). Listeria monocytogenes serotypes in human infections (Italy, 2000-2010). *Annali dell'Istituto superiore di sanità, 48*, 146-150.

Pooley, H., Abellan, F., & Karamata, D. (1992). CDP-glycerol: poly (glycerophosphate) glycerophosphotransferase, which is involved in the synthesis of the major wall teichoic acid in Bacillus subtilis 168, is encoded by tagF (rodC). *Journal of bacteriology, 174*(2), 646-649.

Powell, L. M., Dryden, D. T., Willcock, D. F., Pain, R. H., & Murray, N. E. (1993). DNA recognition by the EcoK methyltransferase: the influence of DNA methylation and the cofactor S-adenosyl-L-methionine. *Journal of molecular biology, 234*(1), 60-71.

Reis, O., Sousa, S., Camejo, A., Villiers, V., Gouin, E., Cossart, P., & Cabanes, D. (2010). LapB, a novel Listeria monocytogenes LPXTG surface adhesin, required for entry into eukaryotic cells and virulence. *The Journal of infectious diseases, 202*(4), 551-562.

Richter, M., Rosselló-Móra, R., Oliver Glöckner, F., & Peplies, J. (2015). JSpeciesWS: a web server for prokaryotic species circumscription based on pairwise genome comparison. *Bioinformatics, 32*(6), 929-931.

Rismondo, J., Percy, M. G., & Gründling, A. (2018). Discovery of genes required for lipoteichoic acid glycosylation predicts two distinct mechanisms for wall teichoic acid glycosylation. *Journal of biological chemistry, 293*(9), 3293-3306.

Roberts, A., Nightingale, K., Jeffers, G., Fortes, E., Kongo, J. M., & Wiedmann, M. (2006). Genetic and phenotypic characterization of Listeria monocytogenes lineage III. *Microbiology, 152*(3), 685-693.

Roberts, R. J., Belfort, M., Bestor, T., Bhagwat, A. S., Bickle, T. A., Bitinaite, J., . . . Dybvig, K. (2003). A nomenclature for restriction enzymes, DNA methyltransferases, homing endonucleases and their genes. *Nucleic acids research, 31*(7), 1805-1812.

Rodríguez-López, P., Rodríguez-Herrera, J. J., Vázquez-Sánchez, D., & Lopez Cabo, M. (2018). Current knowledge on Listeria monocytogenes biofilms in food-related environments: incidence, resistance to biocides, ecology and biocontrol. *Foods, 7*(6), 85.

Safari, F., Sharifi, M., Farajnia, S., Akbari, B., Karimi Baba Ahmadi, M., Negahdaripour, M., & Ghasemi, Y. (2020). The interaction of phages and bacteria: the co-evolutionary arms race. *Critical reviews in biotechnology, 40*(2), 119-137.

Sambrook, J., & Russell, D. W. (2006). Extraction of bacteriophage λ DNA from large-scale cultures using proteinase K and SDS. *Csh Protocols, 2006*(1).

Samson, J. E., Magadán, A. H., Sabri, M., & Moineau, S. (2013). Revenge of the phages: defeating bacterial defences. *Nature Reviews Microbiology, 11*(10), 675-687.

Sauders, B. D., Overdevest, J., Fortes, E., Windham, K., Schukken, Y., Lembo, A., & Wiedmann, M. (2012). Diversity of Listeria species in urban and natural environments. *Appl. Environ. Microbiol., 78*(12), 4420-4433.

Scallan, E., Hoekstra, R. M., Angulo, F. J., Tauxe, R. V., Widdowson, M.-A., Roy, S. L., . . . Griffin, P. M. (2011). Foodborne illness acquired in the United States—major pathogens. *Emerging infectious diseases, 17*(1), 7.

Scanlan, P. D. (2017). Bacteria–bacteriophage coevolution in the human gut: implications for microbial diversity and functionality. *Trends in microbiology, 25*(8), 614-623.

Scanlan, P. D., Buckling, A., & Hall, A. R. (2015). Experimental evolution and bacterial resistance:(co) evolutionary costs and trade-offs as opportunities in phage therapy research. *Bacteriophage, 5*(2), e1050153.

Schlech III, W. F., Lavigne, P. M., Bortolussi, R. A., Allen, A. C., Haldane, E. V., Wort, A. J., . . . Nicholls, E. S. (1983). Epidemic listeriosis—evidence for transmission by food. *New England Journal of Medicine, 308*(4), 203-206.

Schmelcher, M., & Loessner, M. J. (2014). Application of bacteriophages for detection of foodborne pathogens. *Bacteriophage*, *4*(2), e28137.

Schmuki, M. M., Erne, D., Loessner, M. J., & Klumpp, J. (2012). Bacteriophage P70: unique morphology and unrelatedness to other Listeria bacteriophages. *J Virol*, *86*(23), 13099-13102. doi:10.1128/JVI.02350-12

Scholl, D., Cooley, M., Williams, S. R., Gebhart, D., Martin, D., Bates, A., & Mandrell, R. (2009). An engineered R-type pyocin is a highly specific and sensitive

bactericidal agent for the food-borne pathogen Escherichia coli O157: H7. *Antimicrobial agents and chemotherapy*, *53*(7), 3074-3080.

Schultz, E. W. (1945). Listerella infections: a review. *Stanford Med. Bull*, *3*, 135-151.

Seed, K. D., Lazinski, D. W., Calderwood, S. B., & Camilli, A. (2013). A bacteriophage encodes its own CRISPR/Cas adaptive response to evade host innate immunity. *Nature*, *494*(7438), 489-491.

Shamloo, E., Hosseini, H., Moghadam, Z. A., Larsen, M. H., Haslberger, A., & Alebouyeh, M. (2019). Importance of Listeria monocytogenes in food safety: a review of its prevalence, detection, and antibiotic resistance. *Iranian Journal of Veterinary Research*, *20*(4), 241.

Sharma, S., Chatterjee, S., Datta, S., Prasad, R., Dubey, D., Prasad, R. K., & Vairale, M. G. (2017). Bacteriophages and its applications: an overview. *Folia microbiologica*, *62*(1), 17-55.

Shen, Q., Jangam, P. M., Soni, K. A., Nannapaneni, R., Schilling, W., & Silva, J. L. (2014). Low, medium, and high heat tolerant strains of Listeria monocytogenes and increased heat stress resistance after exposure to sublethal heat. *Journal of food protection*, *77*(8), 1298-1307.

Sillankorva, S. M., Oliveira, H., & Azeredo, J. (2012). Bacteriophages and their role in food safety. *International journal of microbiology*, *2012*.

Sinkunas, T., Gasiunas, G., Fremaux, C., Barrangou, R., Horvath, P., & Siksnys, V. (2011). Cas3 is a single-stranded DNA nuclease and ATP-dependent helicase in the CRISPR/Cas immune system. *The EMBO journal*, *30*(7), 1335-1342.

Smith, H. W., & Huggins, M. (1983). Effectiveness of phages in treating experimental Escherichia coli diarrhoea in calves, piglets and lambs. *Microbiology, 129*(8), 2659-2675.

Song, Y., Peters, T. L., Bryan, D. W., Hudson, L. K., & Denes, T. G. (2019). Homburgvirus LP-018 Has a Unique Ability to Infect Phage-Resistant Listeria monocytogenes. *Viruses, 11*(12), 1166.

Song, Y., Peters, T. L., Bryan, D. W., Hudson, L. K., & Denes, T. G. (2021). Characterization of a Novel Group of Listeria Phages That Target Serotype 4b Listeria monocytogenes. *Viruses, 13*(4), 671.

Soni, K. A., & Nannapaneni, R. (2010). Removal of Listeria monocytogenes biofilms with bacteriophage P100. *Journal of food protection, 73*(8), 1519-1524.

Spears, P. A., Havell, E. A., Hamrick, T. S., Goforth, J. B., Levine, A. L., Abraham, S. T., . . . Orndorff, P. E. (2016). Listeria monocytogenes wall teichoic acid decoration in virulence and cell-to-cell spread. *Molecular microbiology, 101*(5), 714-730.

Stewart, F. J., Panne, D., Bickle, T. A., & Raleigh, E. A. (2000). Methyl-specific DNA binding by McrBC, a modification-dependent restriction enzyme. *Journal of molecular biology, 298*(4), 611-622.

Strauch, E., Hammerl, J., & Hertwig, S. (2007). Bacteriophages: new tools for safer food? *Journal für Verbraucherschutz und Lebensmittelsicherheit, 2*(2), 138-143.

Studier, F. W., & Movva, N. (1976). SAMase gene of bacteriophage T3 is responsible for overcoming host restriction. *Journal of virology, 19*(1), 136-145.

Stummeyer, K., Schwarzer, D., Claus, H., Vogel, U., Gerardy-Schahn, R., & Mühlenhoff, M. (2006). Evolution of bacteriophages infecting encapsulated bacteria: lessons from Escherichia coli K1-specific phages. *Molecular microbiology, 60*(5), 1123-1135.

Sullivan, M. J., Petty, N. K., & Beatson, S. A. (2011). Easyfig: a genome comparison visualizer. *Bioinformatics, 27*(7), 1009-1010.

Sumrall, E. T., Keller, A. P., Shen, Y., & Loessner, M. J. (2020). Structure and function of Listeria teichoic acids and their implications. *Molecular microbiology, 113*(3), 627-637.

Sumrall, E. T., Shen, Y., Keller, A. P., Rismondo, J., Pavlou, M., Eugster, M. R., . . . Kilcher, S. (2019). Phage resistance at the cost of virulence: Listeria monocytogenes serovar 4b requires galactosylated teichoic acids for InlB-mediated invasion. *PLoS pathogens, 15*(10), e1008032. Retrieved from https://spiral.imperial.ac.uk:8443/bitstream/10044/1/74039/2/journal.ppat.1008032.pdf

Suo, Y., Huang, Y., Liu, Y., Shi, C., & Shi, X. (2012). The expression of superoxide dismutase (SOD) and a putative ABC transporter permease is inversely correlated during biofilm formation in Listeria monocytogenes 4b G. *PLoS One, 7*(10), e48467.

Suo, Y., Liu, Y., Zhou, X., Huang, Y., Shi, C., Matthews, K., & Shi, X. (2014). Impact of Sod on the Expression of Stress-Related Genes in Listeria monocytogenes 4b G with/without Paraquat Treatment. *Journal of food science, 79*(9), M1745-M1749.

Sutherland, I. W. (1999). Polysaccharases for microbial exopolysaccharides. *Carbohydrate Polymers, 38*(4), 319-328.

Sutherland, I. W., Hughes, K. A., Skillman, L. C., & Tait, K. (2004). The interaction of phage and biofilms. *FEMS microbiology letters, 232*(1), 1-6.

Swaminathan, B., & Gerner-Smidt, P. (2007). The epidemiology of human listeriosis. *Microbes and infection, 9*(10), 1236-1243.

Taylor, H. N., Warner, E. E., Armbrust, M. J., Crowley, V. M., Olsen, K. J., & Jackson, R. N. (2019). Structural basis of Type IV CRISPR RNA biogenesis by a Cas6 endoribonuclease. *RNA biology, 16*(10), 1438-1447.

Tiensuu, T., Andersson, C., Rydén, P., & Johansson, J. (2013). Cycles of light and dark co-ordinate reversible colony differentiation in L isteria monocytogenes. *Molecular microbiology, 87*(4), 909-924.

Tock, M. R., & Dryden, D. T. (2005). The biology of restriction and anti-restriction. *Current opinion in microbiology, 8*(4), 466-472.

Todd, E., & Notermans, S. (2011). Surveillance of listeriosis and its causative pathogen, Listeria monocytogenes. *Food Control, 22*(9), 1484-1490.

Tokman, J. I., Kent, D. J., Wiedmann, M., & Denes, T. (2016). Temperature significantly affects the plaquing and adsorption efficiencies of Listeria phages. *Frontiers in microbiology, 7*, 631.

Torres-Barcelo, C. (2018). Phage Therapy Faces Evolutionary Challenges. *Viruses, 10*(6). doi:10.3390/v10060323

Trisolini, L., Gambacorta, N., Gorgoglione, R., Montaruli, M., Laera, L., Colella, F., . . . Pierri, C. L. (2019). FAD/NADH dependent oxidoreductases: from different amino acid sequences to similar protein shapes for playing an ancient function. *Journal of clinical medicine, 8*(12), 2117.

Trudelle, D. M., Bryan, D. W., Hudson, L. K., & Denes, T. G. (2019). Cross-resistance to phage infection in Listeria monocytogenes serotype 1/2a mutants. *Food microbiology*.

Turner, D., Kropinski, A. M., & Adriaenssens, E. M. (2021). A roadmap for genome-based phage taxonomy. *Viruses, 13*(3), 506.

Turner, I., Garimella, K. V., Iqbal, Z., & McVean, G. (2018). Integrating long-range connectivity information into de Bruijn graphs. *Bioinformatics, 34*(15), 2556-2565.

Twort, F. W. (1961). An investigation on the nature of ultra-microscopic viruses. *Acta Kravsi*.

U.S. Food & Drug Administration GRAS Notice No. 528. Retrieved from https://www.cfsanappsexternal.fda.gov/scripts/fdcc/index.cfm?set=GRASNotices&id=528

Utratna, M., Shaw, I., Starr, E., & O'Byrne, C. P. (2011). Rapid, transient, and proportional activation of σB in response to osmotic stress in Listeria monocytogenes. *Applied and environmental microbiology, 77*(21), 7841-7845.

Veesler, D., Spinelli, S., Mahony, J., Lichière, J., Blangy, S., Bricogne, G., . . . van Sinderen, D. (2012). Structure of the phage TP901-1 1.8 MDa baseplate suggests

an alternative host adhesion mechanism. *Proceedings of the National Academy of Sciences*, *109*(23), 8954-8958.

Vengarai Jagannathan, B., Kitchens, S., Vijayakumar, P. P., Price, S., & Morgan, M. (2020). Potential for bacteriophage cocktail to complement commercial sanitizer use on produce against Escherichia coli O157: H7. *Microorganisms*, *8*(9), 1316.

Vidal, L. S., Kelly, C. L., Mordaka, P. M., & Heap, J. T. (2018). Review of NAD (P) H-dependent oxidoreductases: Properties, engineering and application. *Biochimica et Biophysica Acta (BBA)-Proteins and Proteomics*, *1866*(2), 327-347.

Vines, A., Reeves, M., Hunter, S., & Swaminathan, B. (1992). Restriction fragment length polymorphism in four virulence-associated genes of Listeria monocytogenes. *Research in microbiology*, *143*(3), 281-294.

Vivant, A.-L., Garmyn, D., & Piveteau, P. (2013). Listeria monocytogenes, a down-to-earth pathogen. *Frontiers in cellular and infection microbiology*, *3*, 87.

Vongkamjan, K., Switt, A. M., den Bakker, H. C., Fortes, E. D., & Wiedmann, M. (2012). Silage collected from dairy farms harbors an abundance of listeriaphages with considerable host range and genome size diversity. *Appl. Environ. Microbiol.*, *78*(24), 8666-8675.

Watanabe, T., Igarashi, M., Okajima, T., Ishii, E., Kino, H., Hatano, M., . . . Okamoto, S. (2012). Isolation and characterization of signermycin B, an antibiotic that targets the dimerization domain of histidine kinase WalK. *Antimicrobial agents and chemotherapy*, *56*(7), 3657-3663.

Webb, J., King, G., Ternent, D., Titheradge, A., & Murray, N. (1996). Restriction by EcoKI is enhanced by co-operative interactions between target sequences and is dependent on DEAD box motifs. *The EMBO journal, 15*(8), 2003-2009.

Wick, R. R., Judd, L. M., Gorrie, C. L., & Holt, K. E. (2017). Completing bacterial genome assemblies with multiplex MinION sequencing. *Microbial genomics, 3*(10).

Zemansky, J., Kline, B. C., Woodward, J. J., Leber, J. H., Marquis, H., & Portnoy, D. A. (2009). Development of a mariner-based transposon and identification of Listeria monocytogenes determinants, including the peptidyl-prolyl isomerase PrsA2, that contribute to its hemolytic phenotype. *Journal of bacteriology, 191*(12), 3950-3964.

Zetsche, B., Gootenberg, J. S., Abudayyeh, O. O., Slaymaker, I. M., Makarova, K. S., Essletzbichler, P., . . . Regev, A. (2015). Cpf1 is a single RNA-guided endonuclease of a class 2 CRISPR-Cas system. *Cell, 163*(3), 759-771.

Zink, R., Loessner, M., Glas, I., & Scherer, S. (1994). Supplementary Listeria-typing with defective Listeria phage particles (monocins). *Letters in applied microbiology, 19*(2), 99-101.

Zink, R., Loessner, M. J., & Scherer, S. (1995). Charaterization of cryptic prophages (monocins) in Listeria and sequence analysis of a holin/endolysin gene. *Microbiology, 141*(10), 2577-2584.

APPENDIX

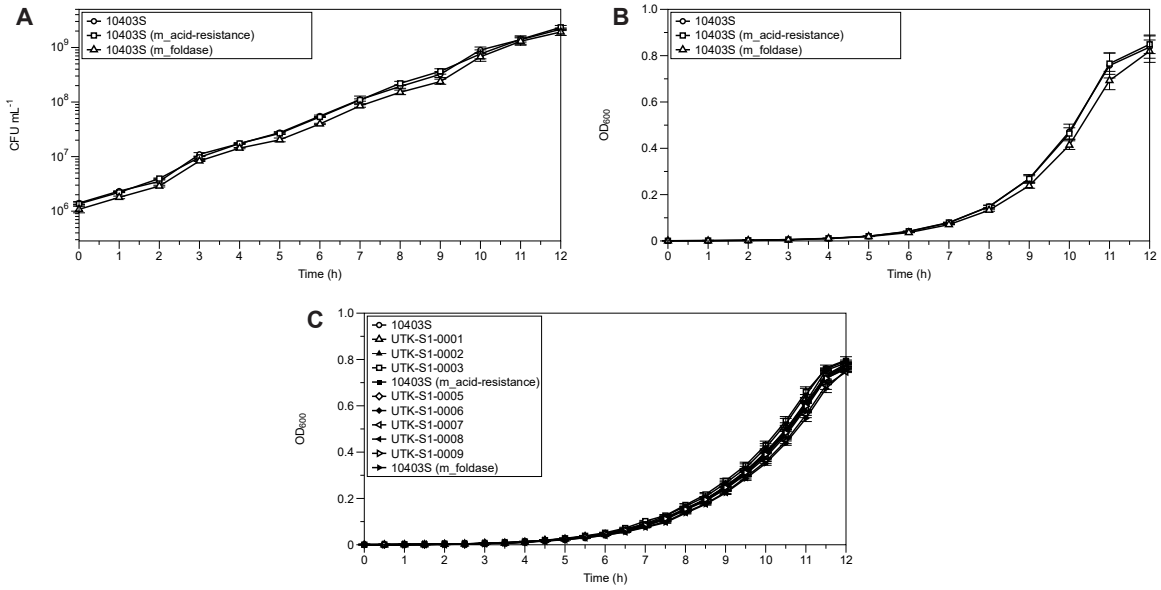

Figure S2. 1 Growth curve of 10403S, 10403S (m_acid-resistance) and 10403S (m_foldase) at 25°C. LB-MOPS was inoculated 1:100 with an overnight culture, grown to an OD600 of 0.1 then diluted 1:100 and measured by (A) CFU mL^{-1} or (B) OD600 for 12 hours (data for A and B were collected from the same experiment). (C) Growth curve of 10403S and LP-018 resistant 10403S mutants at 25°C. LB-MOPS was inoculated 1:100 with an overnight culture, grown to an OD_{600} of 0.1 then diluted 1:100 and measured by OD_{600} for 12 hours. Data are mean values of three biological replicates and error bars represent standard error.

Table S2. 1 Additional phage-resistant mutant strains of *Listeria monocytogenes*

Strain*	Description
***Listeria monocytogenes* mutant strains**	
UTK S1-0001	10403S mutant; frameshift mutation in *LMRG_01613* (encodes foldase PrsA2 precursor)
UTK S1-0002	10403S mutant; frameshift mutation in *LMRG_01613* (encodes foldase PrsA2 precursor)
UTK S1-0003	10403S mutant; nonsense mutation in *LMRG_00278* (encodes acid-resistance family protein HdeD), missense mutation in *LMRG_01441* (encodes a preprotein translocase subunit YajC)
UTK S1-0005	10403S mutant; frameshift mutation in *LMRG_00278* (encodes acid-resistance family protein HdeD)
UTK S1-0006	10403S mutant; frameshift mutation in *LMRG_00278* (encodes acid-resistance family protein HdeD)
UTK S1-0007	10403S mutant; nonsense mutation in *LMRG_01613* (encodes foldase PrsA2 precursor)
UTK S1-0008	10403S mutant; frameshift mutation in *LMRG_01613* (encodes foldase PrsA2 precursor)
UTK S1-0009	10403S mutant; nonsense mutation in *LMRG_01613* (encodes foldase PrsA2 precursor)

*All strains sourced from this study

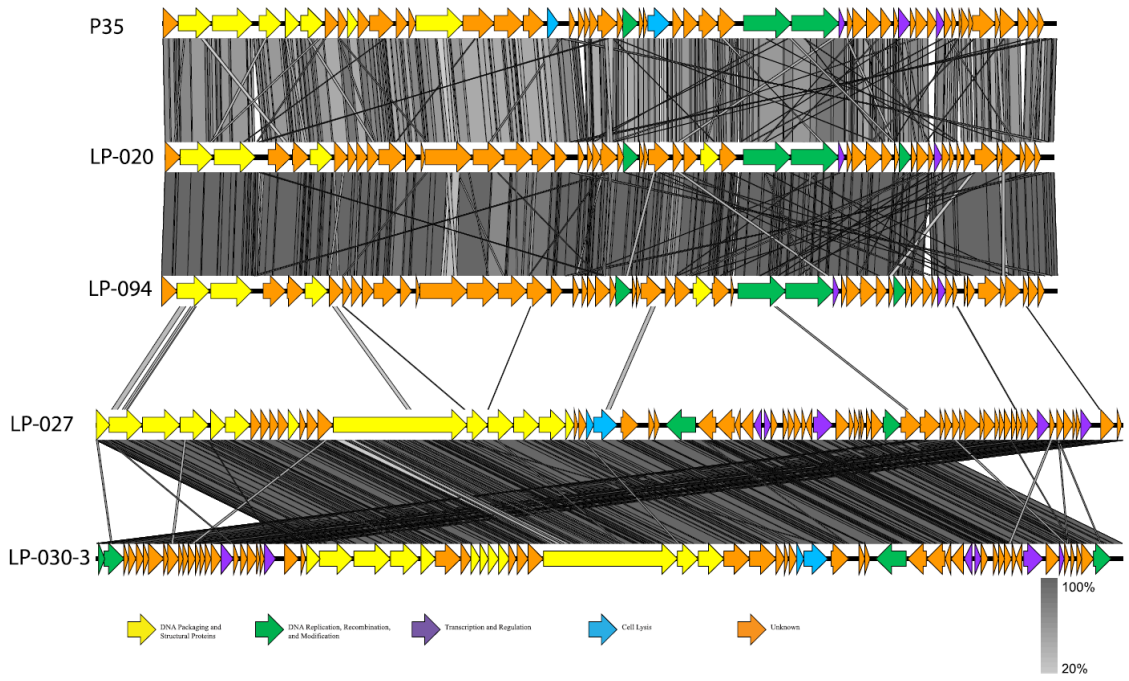

Figure S3. 1 Linear tBLASTx comparrisons of representative P35-like and LP-30-3-like *Listeria* phages. Genes are represented by arrows and are colored based on putative function (see key at bottom). The shaded region between genomes represents amino acid similarity, with darker gray representing higher similarity and lighter gray indicating lower similarity (see scale at bottom right)

Table S3. 1 Phage lifestyle prediction

Phage	Predicted Class	Prediction Confidence	Averaged Probability	Standard Deviation
LP-024	Temperate	Confident	0.592	0.038
LP-027	Temperate	Confident	0.589	0.032
LP-020	Lytic	Non-Confident	0.507	0.03
LP-021	Temperate	Non-Confident	0.512	0.036
LP-053	Temperate	Non-Confident	0.512	0.057
LP-054	Temperate	Non-Confident	0.514	0.045
LP-057	Lytic	Non-Confident	0.507	0.024
LP-085	Temperate	Non-Confident	0.531	0.035
LP-094	Temperate	Non-Confident	0.511	0.039

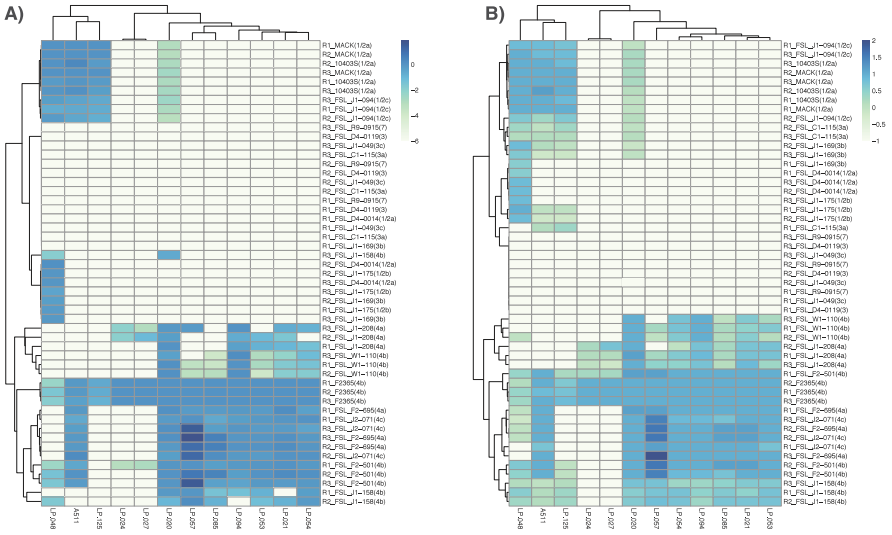

Figure S3. 2 Host range analysis of *Listeria* phages against a panel of *Listeria monocytogenes* strains that represent different serotypes. Panel A) represent the clustered efficiency of plaquing (EOP) results of three individual replicates where values represent the log transformed efficiencies of plaquing of each phage against each bacterial strain compared to the phage propagation host strain. Panel B) values represent the clustered efficiency of activity (EOA) results of three individual replicates where values represent the greatest dilution factor where inhibitory phage activity was observed against each strain relative to the phage propagation host strain

Figure S4. 1 The Efficiency of plaquing assay with purified phages on representative mutant strains. Panel (A) and Panel (B) represent efficiency of activity (EOA) heatmap results and efficiency of plaquing (EOP) heatmap results with the purified phages from the co-evolution between *L. monocytogenes* H7858 and *pecentumvirus*. Panel (C) and Panel (D) represent EOA heatmap results and EOP heatmap results with the phage lysates from the co-evolution between *L. monocytogenes* H7858 and P35-like phages. Experimental strains were selected based on the phenotypic testing results. Values are the mean of data from two biological replicates.

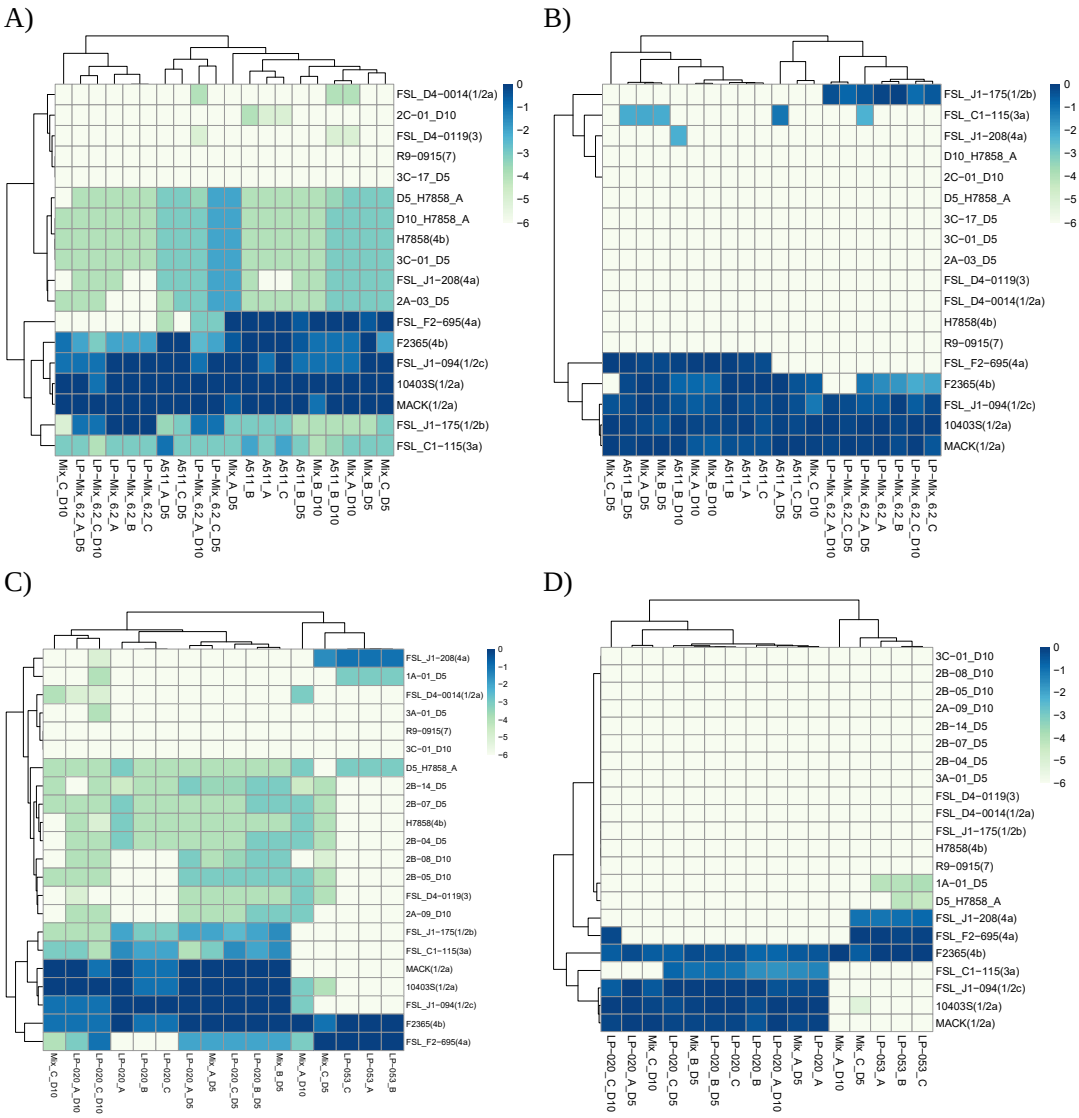
A)
FSL_D4−0014(1/2a)
2C−01_D10
FSL_D4−0119(3)
R9−0915(7)
3C−17_D5
D5_H7858_A
D10_H7858_A
H7858(4b)
3C−01_D5
FSL_J1−208(4a)
2A−03_D5
FSL_F2−695(4a)
F2365(4b)
FSL_J1−094(1/2c)
10403S(1/2a)
MACK(1/2a)
FSL_J1−175(1/2b)
FSL_C1−115(3a)
Mix_C_D10
LP−Mix_6.2_A_D5
LP−Mix_6.2_C_D10
LP−Mix_6.2_A
LP−Mix_6.2_B
LP−Mix_6.2_C
A511_A_D5
A511_C_D5
LP−Mix_6.2_A_D10
LP−Mix_6.2_C_D5
Mix_A_D5
A511_B
A511_A
A511_C
A511_B_D5
A511_B_D10
Mix_A_D10
Mix_B_D5
Mix_C_D5
0
−1
−2
−3
−4
−5
−6
B)
FSL_J1−175(1/2b)
FSL_C1−115(3a)
FSL_J1−208(4a)
D10_H7858_A
2C−01_D10
D5_H7858_A
3C−17_D5
3C−01_D5
2A−03_D5
FSL_D4−0119(3)
FSL_D4−0014(1/2a)
H7858(4b)
R9−0915(7)
FSL_F2−695(4a)
F2365(4b)
FSL_J1−094(1/2c)
10403S(1/2a)
MACK(1/2a)
Mix_C_D5
A511_B_D5
Mix_A_D5
Mix_B_D5
A511_B_D10
Mix_A_D10
Mix_B_D10
A511_B
A511_A
A511_C
A511_A_D5
A511_C_D5
Mix_C_D10
LP−Mix_6.2_C_D5
LP−Mix_6.2_A_D10
LP−Mix_6.2_A_D5
LP−Mix_6.2_A
LP−Mix_6.2_B
LP−Mix_6.2_C_D10
LP−Mix_6.2_C
0
−1
−2
−3
−4
−5
−6
C)
FSL_J1−208(4a)
1A−01_D5
FSL_D4−0014(1/2a)
3A−01_D5
R9−0915(7)
3C−01_D10
D5_H7858_A
2B−14_D5
2B−07_D5
H7858(4b)
2B−04_D5
2B−08_D10
2B−05_D10
FSL_D4−0119(3)
2A−09_D10
FSL_J1−175(1/2b)
FSL_C1−115(3a)
MACK(1/2a)
10403S(1/2a)
FSL_J1−094(1/2c)
F2365(4b)
FSL_F2−695(4a)
Mix_C_D10
LP−020_A_D10
LP−020_C_D10
LP−020_A
LP−020_B
LP−020_C
LP−020_A_D5
Mix_A_D5
LP−020_C_D5
LP−020_B_D5
Mix_B_D5
Mix_A_D10
Mix_C_D5
LP−053_C
LP−053_A
LP−053_B
0
−1
−2
−3
−4
−5
−6
D)
3C−01_D10
2B−08_D10
2B−05_D10
2A−09_D10
2B−14_D5
2B−07_D5
2B−04_D5
3A−01_D5
FSL_D4−0119(3)
FSL_D4−0014(1/2a)
FSL_J1−175(1/2b)
H7858(4b)
R9−0915(7)
1A−01_D5
D5_H7858_A
FSL_J1−208(4a)
FSL_F2−695(4a)
F2365(4b)
FSL_C1−115(3a)
FSL_J1−094(1/2c)
10403S(1/2a)
MACK(1/2a)
LP−020_C_D10
LP−020_A_D5
Mix_C_D10
Mix_B_D5
LP−020_C_D5
LP−020_B_D5
LP−020_C
LP−020_B
LP−020_A_D10
Mix_A_D5
LP−020_A
Mix_A_D10
Mix_C_D5
LP−053_A
LP−053_B
LP−053_C
0
−1
−2
−3
−4
−5
−6

VITA

Yaxiong Song was born on October 7th, 1990 in Tangshan City, Hebei Province, China. He got his bachelor's degree from the Dalian University of Technology in 2013, majoring in Bioengineering. After his graduation, he continued his study at the Dalian University of Technology as a master student, achieving his master's degree in 2016, majoring in biochemical engineering. In the spring of 2018, he joined the Thomas Denes' lab, Department of Food Science, the University of Tennessee, to study *Listeria* phages for his doctoral degree.